

- **THEME: PRECISION DISTURBANCES**
- **FEEDBACK LOOPS IN MICROMACHINING**
- **METROLOGY CHALLENGES IN ADDITIVE MANUFACTURING**
- **A LIGHT-GUIDED ACTUATOR – MOTION CONTROL THROUGH CHEMISTRY**

# DSPE

YOUR PRECISION PORTAL

## 2020 CONFERENCE ON PRECISION MECHATRONICS

8 & 9 September

De Ruwenberg - Sint Michielsgestel

PROGRAM ONLINE  
**Registration  
is open!**

LECTURES | POSTERS AND DEMONSTRATIONS | SHARING IDEAS AND EXPERIENCES

## MEET YOUR PEERS IN PRECISION MECHATRONICS

This year's theme, **Uncovering the Essence**, is the challenge that each of us is working on, either directly or indirectly, for example by investigating the fundamentals of particle contamination or developing improved control schemes. Ultimately, precision engineering and mechatronics, i.e. the equipment it produces, is an important enabler for uncovering the essence of comprehensive phenomena such as climate change, life or even the cosmos.

All this would be impossible without electron microscopes, satellites, healthcare devices and semiconductor equipment for manufacturing the required computing power. Therefore, traditional core topics have been supplemented with sessions on adjacent application areas. Areas of interest range from disruptive technologies and design principles to picometer stability and energy efficiency.

With three guest speakers, 21 oral presentations, many posters/demos and a social event, there will be plenty of room for networking and food for thought and discussion about the essence and its (precision) details.

### EARLY BIRD BONUS!

If you register before May 15, 2020, you will receive the book **The Green Illusion (Dutch)**

Conference  
partner:



#### CONFERENCE CONTRIBUTION:



ASML



PI



UNIVERSITEIT  
TWENTE.



TNO



PHILIPS



Canon



Program & latest COVID-19 related information: [www.dspe-conference.nl](http://www.dspe-conference.nl)

## PUBLICATION INFORMATION

## Objective

Professional journal on precision engineering and the official organ of DSPE, the Dutch Society for Precision Engineering. Mikroniek provides current information about scientific, technical and business developments in the fields of precision engineering, mechatronics and optics. The journal is read by researchers and professionals in charge of the development and realisation of advanced precision machinery.



## Publisher

DSPE  
Annemarie Schrauwen  
High Tech Campus 1, 5656 AE Eindhoven  
PO Box 80036, 5600 JW Eindhoven  
info@dspe.nl, www.dspe.nl

## Editorial board

Prof.dr.ir. Just Herder (chairman, Delft University of Technology, University of Twente),  
Servaas Bank (VDL ETG), B.Sc.,  
ir.ing. Bert Brals (Sioux Mechatronics),  
Maarten Dekker, M.Sc. (Philips),  
Otte Haitisma, M.Sc. (Demcon),  
dr.ir. Jan de Jong (University of Twente),  
ing. Ronald Lamers, M.Sc. (Thermo Fisher Scientific),  
Erik Manders, M.Sc. (Philips Innovation Services),  
dr.ir. Pieter Nuij (MaDyCon),  
dr.ir. Gerrit Oosterhuis (VDL ETG),  
Maurice Teuwen, M.Sc. (Janssen Precision Engineering)

## Editor

Hans van Eerden, hans.vaneerden@dspe.nl

## Advertising canvasser

Gerrit Kulsdom, Sales & Services  
+31 (0)229 – 211 211, gerrit@salesandservices.nl

## Design and realisation

Drukkerij Snep, Eindhoven  
+31 (0)40 – 251 99 29, info@snep.nl

## Subscription

Mikroniek is for DSPE members only.  
DSPE membership is open to institutes, companies, self-employed professionals and private persons, and starts at € 80.00 (excl. VAT) per year.

Mikroniek appears six times a year.

© Nothing from this publication may be reproduced or copied without the express permission of the publisher.

ISSN 0026-3699



The cover illustration (featuring two examples of the impact of a particle in lithography) is courtesy of ASML. Read the article on page 16 ff.

## IN THIS ISSUE

## THEME: PRECISION DISTURBANCES

05

**Polymer damper technology for improved system dynamics**

An effective, passive damping method based on polymer damping offers low-cost damper development and first-time-right damper design.

10

**A hybrid design approach to discontinuous constrained layer dampers**

Combining existing equations and an estimate to compensate for discontinuities yields an accurate estimate of the damping in a complex CLD geometry.

16

**Collaborating for cleanliness from A to Z**

Report of the CLEAN2020 theme day.

18

**Reliable capturing of motion-related frequencies**

Using FFT for signal analysis comes with particular requirements and constraints on the data record to be captured, which are quite often ignored.

22

**Machine metrology for optimal performance**

Fast and accurate method for dynamic 3D measurement of the thermal stability of 5-axis machine tools.

26

**Advantages of substrate-mastered scales**

Effective thermal error compensation for laser cutting machines.

28

**Viscoelastic (over)constraining**

Design of a flexure mechanism employing a custom-synthesised elastomer compound for increased dynamic performance.

33

**Research – A light-guided actuator**

Motion control through chemistry, using liquid crystalline polymers, bearing the promise of light-driven robots that can walk and transport low-weight cargos.

36

**Manufacturing technology – The art of micromachining**

Reith Laser addresses the laser processing feedback loops.

40

**Metrology – First measurement technology, then standards**

Overcoming measurement bottlenecks in additive manufacturing.

05



33



## FEATURES

## 04 EDITORIAL

Hans Krikhaar, president of DSPE and professor at Fontys University of Applied Sciences, on precision disturbances and the current terrifying disturbance threatening the world at large; the coronavirus.

## 15 TAPPING INTO A NEW DSPE MEMBER'S EXPERTISE

Pfeiffer Vacuum – specialist in vacuum generation and leak testing.

## 42 ECP2 COURSE CALENDAR

Overview of European Certified Precision Engineering courses.

## 43 NEWS

Including: Integrated solution for deburring, cleaning and drying.

## 50 UPCOMING EVENTS

Including: Euspen's 20th International Conference as a virtual event.



## DISTURBING

This issue of Mikroniek features the theme of precision disturbances. The performance of high-tech precision systems suffers from vibrations, thermal loads and other detrimental influences. The measurement of position, speed, acceleration, temperature, etc., is required to monitor these disturbances. Subsequently, dynamics, thermomechanics, electromagnetic compatibility, etc. are the disciplines to control them. Measurement and control of precision disturbances are serious issues in our high-tech community.

At the moment, however, a far more terrifying disturbance is threatening the world at large. The spread of the coronavirus has taken us by surprise and the casualties are very high. Everyone's primary concern is naturally to mitigate the spread of the virus, keep the healthcare system going and save as many patients' lives as possible. High-tech systems such as ventilation modules and other medical equipment can make crucial contributions to defeating the corona pandemic.

In response, many companies are making serious efforts to increase the output of their systems production or provide quick-fix remedies. Here, our systems engineering expertise plays a crucial role, for example when developing a 'low-tech' ventilation system within weeks – several of these initiatives started last month. Upcoming technologies, such as additive manufacturing, help to provide immediate solutions in the development of new products or the refurbishment of systems that were declared end-of-life, but now have been recalled for duty. This crisis calls for smart manufacturing.

So, on the one hand, there is a lot of crisis-related activity going on in the high-tech industry. On the other hand, supply chains have collapsed and factories have already shut down – for the long term this will change our perspective on business continuity and 'precision', i.e. just-in-time, supply. Public life has also come to a standstill in our community. Some events have already been rescheduled, such as the DSPE Knowledge Day on Engineering for Particle Contamination Control. Other events have gone online, notably the prestigious euspen Conference, of which the 20th edition in early June was designated to be a landmark event at CERN, the largest particle physics laboratory in the world.

As with all crises, this one unleashes positive effects as well. Communication is only intensifying, for private and professional purposes alike, via the internet and modern communication devices, facilitated by the precision-engineering-driven progress in the semiconductor and photonics industries. It is amazing to experience how these days the quality of our modern way of communicating can be sustained all over the world.

Where sustainability and the circular economy are concerned, this crisis, as devastating as it is in terms of public health, may turn out to the advantage of environmental health. The temporary reduction of energy consumption and material usage may become lasting, when we will learn the lessons of remote collaboration, reuse and refurbishment. Engineering can play a vital role here by developing smart systems, while taking into account – as a matter of good precision engineering practice – the precision disturbances featured in this Mikroniek issue.

Taking care of each other and taking care of our beautiful blue planet should be higher on our 'to do' list, both now and post-corona. I hope the corona crisis will be contained as soon as possible and that you all stay well or will recover soon.

Hans Krikhaar  
*President of DSPE and professor of Smart Manufacturing & Integrated Systems Engineering  
at Fontys University of Applied Sciences*  
[hans.krikhaar@dspe.nl](mailto:hans.krikhaar@dspe.nl)



# EXTENSIVE MODELLING FOR EFFECTIVE DAMPING

Modern, high-end mechatronic systems require superb dynamic system properties to meet the requirements. For decades, design for high stiffness and high eigenfrequencies was the route to achieve these properties. It is often impossible to gain much more by further optimising the shape of the structure or the material properties. However, it appears that damping is an effective design parameter to be optimised in order to improve the dynamic system properties even further. MI-Partners has developed an effective, passive damping method based on polymer damping. This method offers low-cost damper development and first-time-right damper design.

PIETER WULLMS AND THEO RUIJL

## Introduction

The requirements concerning the dynamic position stability of high-end mechatronic systems are becoming increasingly tighter. This applies to moving systems, such as stages, as well as to static systems, such as force and metrology frames. An effective and robust way to improve the system dynamics is by applying damping. This can be done in either an active or in a passive manner.

In several applications, passive damping is preferred more than active, with the main reasons being robustness, applicability, performance and cost. Viscoelastic damping, a method to provide passive damping, can be achieved very efficiently by means of polymers. The amount of damping per volume of material is high [1, 2], the material is robust and can be shaped efficiently, which produces design freedom to tailor damping elements for specific applications [3, 4].

Viscoelastic materials are applied in various applications to achieve damping, however in many of these applications the precise performance is less critical and the design has often been realised by trial and error. In high-end applications, the complexity and requirements are such that extensive modelling is necessary and predictability of the final performance is essential for an efficient and successful development of the entire system.

## Viscoelastic behaviour

For viscoelastic materials that exhibit damping, the stress and strain are not in phase. The strain lags behind the stress by a certain phase angle  $\delta$ . For dynamic modelling in the frequency domain, it is convenient to describe the linear viscoelastic behaviour in complex notation. Consider the complex time-dependent strain as:

$$\varepsilon^*(t) = \varepsilon_0 e^{j\omega t} \quad (1)$$

Here,  $\varepsilon_0$  depicts the amplitude of the sinusoidal variation of the strain and  $\omega$  the frequency. A linear viscoelastic response will give the corresponding stress:

$$\sigma^*(t) = \sigma_0 e^{j(\omega t + \delta)} \quad (2)$$

It is common in the polymer technology domain to describe the linear viscoelastic relation between stress and strain by means of the complex modulus as:

$$E^* = \sigma^* / \varepsilon^* \quad (3)$$

Substituting (1) and (2) into (3) and applying Euler's exponential relationship yields:

$$E^* = (\sigma_0 / \varepsilon_0) \cdot e^{j\delta} = (\sigma_0 / \varepsilon_0) \cdot [\cos(\delta) + j\sin(\delta)] \quad (4)$$

In general, the ratio between  $\sigma_0$  and  $\varepsilon_0$  as well as the phase angle  $\delta$  are frequency- and temperature-dependent [1]. As such we can define two, in general frequency- and temperature-dependent functions, the storage modulus  $E'$  and the loss modulus  $E''$ , and rewrite (4) into:

$$E^* = (\sigma_0 / \varepsilon_0) \cdot [\cos(\delta) + j\sin(\delta)] = E' + jE'' \quad (5)$$

The ratio between the loss modulus and the storage modulus is called the loss factor  $\eta$ , or  $\tan(\delta)$ :

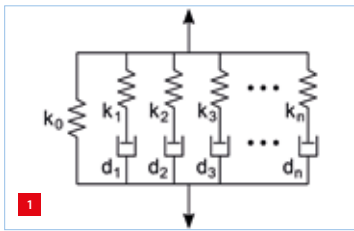
$$\eta = E'' / E' = \tan(\delta) \quad (6)$$

A polymer typically shows an enormous change in stiffness (i.e.  $|E^*|$ ) at the so-called glass transition temperature  $T_g$ . The loss-factor  $\eta$  has its maximum around this temperature.

## AUTHORS' NOTE

Pieter Wullms (senior mechatronic system designer) and Theo A.M. Ruijl (CTO / senior mechatronics system architect) both work with MI-Partners, located in Veldhoven (NL).

p.wullms@mi-partners.nl  
www.mi-partners.nl



Model of frequency-dependent viscoelastic stiffness  $k^*(\omega)$  by means of the Multiple Standard Model.

$$k^* = k' + jk'' = k_0 + \sum_{i=1}^n \frac{jk_i d_i \omega}{j d_i \omega + k_i}$$

$$= \left( k_0 + \sum_{i=1}^n \frac{k_i d_i^2 \omega^2}{d_i^2 \omega^2 + k_i^2} \right) + j \left( \sum_{i=1}^n \frac{k_i^2 d_i \omega}{d_i^2 \omega^2 + k_i^2} \right)$$

### Viscoelastic model

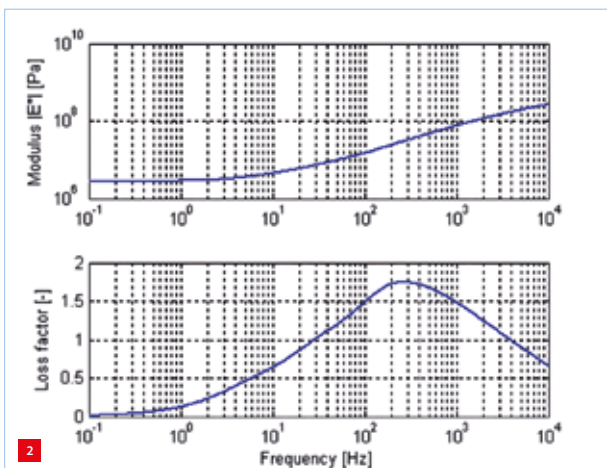
A useful and common way to describe the viscoelastic stiffness of polymers, required to model the effect of damping on a system, is by means of combinations of elastic elements (ideal elastic springs) and viscous elements (ideal viscous dampers). Figure 1 shows a so-called Multiple Standard Model or Maxwell model.

This model can be used to describe the complex dynamic modulus in a general sense, i.e. with Young's modulus  $E^*$  and shear modulus  $G^*$ , or the dynamic stiffness of a physical damper  $k^*$ . A fit of the Multiple Standard Model of the polymer developed by MI-Partners is shown in Figure 2. It shows the high damping (loss factor of max 1.7) in a frequency range very common for mechanical systems.

### Material characterisation

In general, for high-end dynamic systems an accurate material description over a large frequency range is necessary to predict the effect of damping properly and design the dampers correctly. This requires accurate measurements of the complex frequency-dependent modulus (Young's and shear modulus) as a function of frequency and temperature.

To measure the dynamic modulus of viscoelastic materials, DMTA (dynamic mechanical thermal analysis) is commonly used [1]. The dynamic stiffness of a sample is



Modulus plot at 25 °C of the polymer developed by MI-Partners, fitted by the Multiple Standard Model with  $n = 10$ .

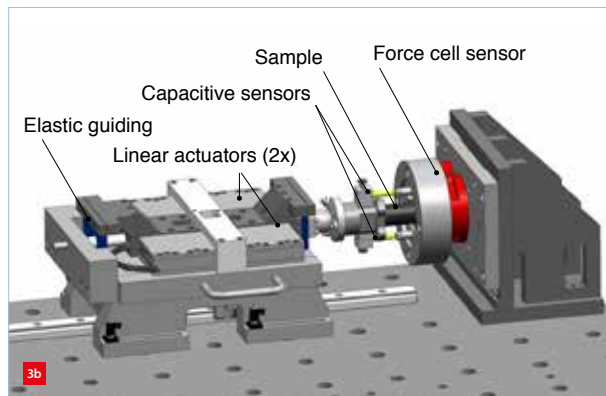
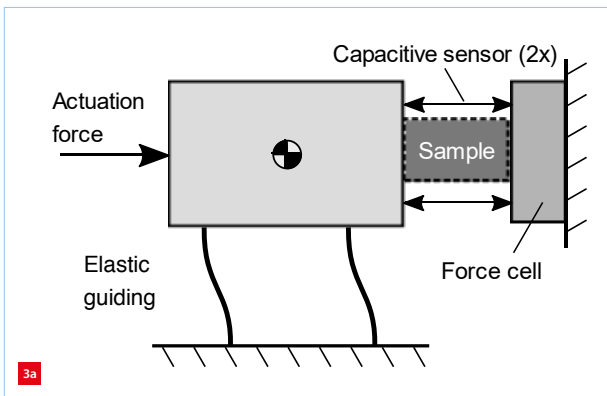
measured over a limited frequency range (typically up to 100 Hz) at various temperatures (0 to 120 °C). For a polymer, qualitatively the effect of frequency is the inverse of the effect of temperature; the higher the frequency, the stiffer the polymer, versus the higher the temperature, the weaker the polymer. This temperature-to-frequency behaviour is described by the Williams-Landel-Ferry (WLF) relation.

In the DMTA, the WLF relation is used to interchange frequency and temperature to simulate the material's response over a large frequency range (typically 6 to 10 orders) by measuring over a limited frequency range, but at different temperatures.

For the present applications, the result of such a DMTA is found to be insufficiently accurate, caused for example by errors due to the limited validity of the WLF relation over a larger frequency range. Furthermore, the sheet samples are clamped in the set-up. Such fixation becomes doubtful at a higher stiffness of the sample (e.g. higher frequencies or lower temperatures), resulting in measurement errors. The applied strain levels are relatively high, typically  $> 0.5\%$ , whereas in the present applications strain levels are typically  $< 0.01\%$ . Furthermore, such an apparatus is only feasible to handle predefined samples and is not able to characterise arbitrary entire damper modules.

To overcome the limitations of the DMTA apparatus, two dedicated dynamic measurement set-ups have been built at MI-Partners. They are placed in a temperature-controlled enclosure, which can also be used to change the temperature during evaluation (typically 15 to 40 °C). The Damper Test Rig (DTR) has a generic interface which allows different samples up to 300 mm x 300 mm x 100 mm to be measured up to a frequency of 400 Hz (Figure 3). The DTR interface allows a proper mounting of the sample, either by bolting a damper with metal interfaces to the set-up or gluing the polymer material sample to the test set-up, to ensure a proper interface.

The DTR generates a force by means of a direct-drive linear motor. The applied force is measured by a load cell, positioned at the static end of the sample, and the deformation of the sample is measured by two symmetrically positioned capacitive sensors. The dynamic Young's modulus can be determined from the measured stiffness  $k^*(\omega, T)$  by taking the sample geometry into account.



The Damper Test Rig (DTR) for material and damper characterisation up to 400 Hz.

(a) Principle.

(b) Overview.

The High-Frequency Damper Test Rig (HF-DTR) is depicted in Figure 4. To enable characterisation in the range of 50 Hz to 5 kHz, this set-up has been equipped with accelerometers to determine the deformation of the sample and a piezo force cell to measure the force exerted on the sample.

The force is applied by a modal exciter. To minimise errors due to surrounding dynamics (e.g. supporting table) a reaction mass is used. Both the modal exciter and the reaction mass are supported at 5 Hz to create a low-pass filter to and from the surrounding. To minimise rocking of the reaction mass and as such transversal acceleration and via cross-talk inside the sensors (accelerometers and force cell) measuring errors, the modal exciter and sample under test are properly aligned with the centre of gravity of the reaction mass.

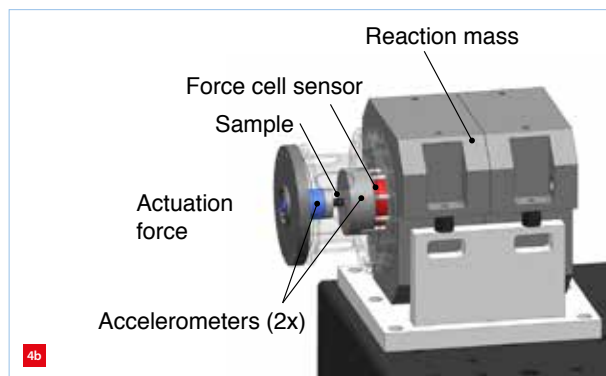
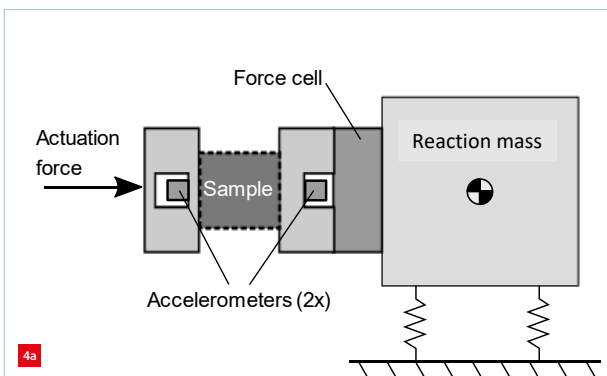
The extreme frequency range up to 5 kHz imposes strict requirements on the sample and sample fixation. Hence the HF-DTR is limited in accepting sample geometry and size. To obtain a measuring range up to 5 kHz, the first internal mode in the measurement direction has been designed above 9 kHz. Furthermore, corrections are necessary to compensate for sensor dynamics (1) and the test set-up dynamics (2) to reach an uncertainty below 1% and 1°.

The sensor dynamics correction (1) mainly includes the low-pass filtering of the accelerometer (provided by the sensor supplier). The correction of the set-up dynamics (2) involves compliancy in the interfaces, inertia effects and the influence of the internal mode at 9 kHz toward lower frequencies. Based on a 1-DoF dynamic lump-mass model (DoF = degree of freedom), the influences on  $k^*$  are predicted and corrected (model-based).

The test set-up has been verified by the measurement of an elastic reference sample, without damping and constant stiffness over the frequency range. This sample was statically calibrated in an external set-up. Figure 5 shows the error of the dynamic measurement of this elastic reference sample on the HF-DTR set-up with and without any compensation.

### Damper design methodology

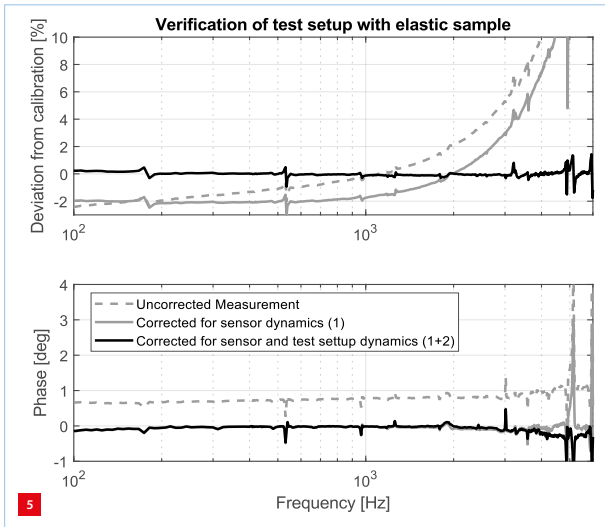
From the characterisation of the polymers it appears that the damping in shear ( $G$ -modulus) and tension loading (Young's modulus  $E$ ) are the same. In addition, the applied material displays linear behaviour, even up to considerable larger strain levels than applicable in the present applications. Note that this does not hold in general for every polymer. Hence, the material can be treated as



The High-Frequency Damper Test Rig (HF-DTR) for material and damper characterisation in the range of 50 to 5,000 Hz.

(a) Principle.

(b) Overview.



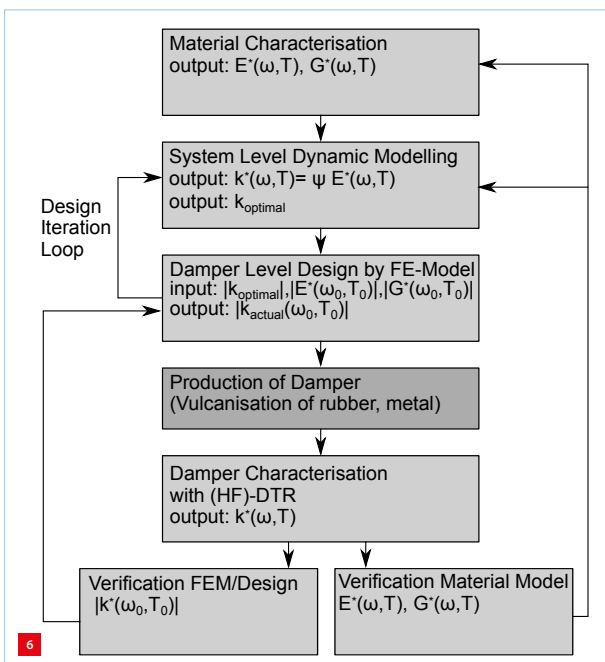
Verification of HF-DTR set-up with an elastic reference sample, and the effect of the sensor and test set-up dynamics compensation.

homogenous isotropic linear viscoelastic. As such, the dynamic stiffness of an arbitrary specimen is given by:

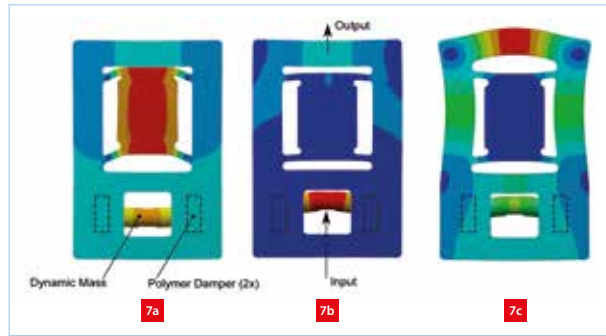
$$k^*(\omega, T) = \psi E^*(\omega, T) \quad (7)$$

Here, the constant  $\psi$  is determined by the actual damper geometry (geometric stiffness constant  $[\text{m}^{-1}]$ ).

The diagram in Figure 6 shows the entire design sequence. The system dynamics are modelled (e.g. a state-space model). As such, complex systems can be evaluated containing all kind of dynamic characteristics, including feedback loops. The viscoelastic generalised Maxwell models are added in Matlab. The damped dynamic system is then evaluated and the properties of the viscoelastic part



Damper design methodology.



Dummy stage with comparable dynamics in three modes, input force  $F_{in}$  and output displacement  $X_{out}$ . (a) Mode 1: ~1,150 Hz. (b) Mode 2: ~2,050 Hz. (c) Mode 3: ~2,650 Hz.

can be optimised. This process results in an optimal design target stiffness  $k^*_{\text{optimal}}$  for the damper.

The damper can accordingly be designed to the corresponding stiffness by means of finite-element analyses using a homogenous isotropic linear elastic model by applying  $(|E^*(\omega_0, T_0)|, |G^*(\omega_0, T_0)|)$ . Finally, the iteratively obtained actual geometry with  $k^*_{\text{actual}}$  is evaluated again in the dynamic system model in Matlab. After finishing the complete design including interfacing, the damper can be produced in close cooperation with an external partner. The last step is to verify the damper properties, e.g. the geometry and dynamic stiffness, which can be measured in the test set-ups (DTR or HF-DTR).

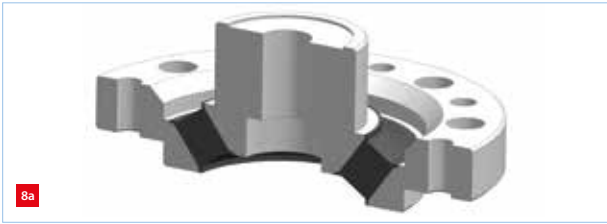
This complete design and realisation sequence, from material characterisation to design verification, can be realised within an uncertainty of about 15% with regard to stiffness and damping. The variations include batch variations of the polymer, modelling and measurement inaccuracies. This small uncertainty allows for predictable and successful application of damping in high-end applications.

### Polymer damper in a positioning stage

For highly dynamic stages, as for example used in fast-tool servos for mass production of optical components, the servo bandwidth is typically limited by internal mechanical resonances. In this case, in order to increase the controller bandwidth to improve the dynamic system performance, a dedicated damper was designed to dampen these internal resonances.

To test and verify the damping principle on a system level, a dummy stage was made with corresponding dynamics. The first three dominant modes of the dummy stage are shown in Figure 7. The polymer damper (Figure 8) is positioned in the suspension (left and right) of the mass (dynamic mass). The damper assembly (polymer damper with dynamic mass) acts as an additional dynamic mass, which becomes part of the entire dynamic system at several critical modes. The 'eigenfrequency' of the dynamic mass in combination with the suspension is designed near the dominant modes.





Polymer damper (vulcanised rubber-metal parts) suspending the dynamic mass.

(a) Design.

(b) Realisation.



The polymer damper dissipates energy in every mode where the dynamic mass is interacting and the viscoelastic material is deforming. The result is a broad (frequency band) and robust damping principle. In the actual system, no additional mass was added, but the weight of an existing sub-module was used to act as the dynamic mass. The corresponding damped and undamped bode plots from force input to displacement output (see Figure 7) are shown in Figure 9. The first dominant internal modes are in the range of 1.6 to 2.7 kHz and appear as highly undamped resonance peaks in the transfer function, thereby limiting the controller bandwidth. The bode plot shows the measured and simulated responses, which are in good agreement. The deviation at the first three damped resonances is within 2 dB, which shows the high predictability of this methodology.

The polymer damper is able to suppress these dominant modes by 30 dB and more. It appears that the controller bandwidth could be increased by roughly 35%. Furthermore, as the transfer function becomes 'smoother', an enormous increase in system robustness is achieved. This case shows the high potency of applying viscoelastic damping in a high-end mechatronic system.

## Summary and conclusion

It has been shown that polymer damping technology can be applied in high-end dynamic positioning systems to improve servo bandwidth and system robustness. A polymer material with high damping and reproducibility has been developed and the dynamic properties (storage

and loss moduli) have been accurately characterised with two dedicated dynamic measurement rigs.

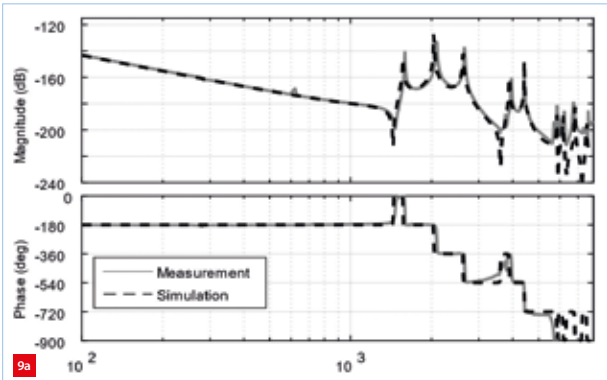
Finally, a design methodology has been developed, including dynamic system modelling and finite-element models of the polymer, resulting in a systematic design approach. It has been shown that the application at system level has such high predictability that this technology can be used in the development of high-end mechatronic systems, high-precision measurement equipment and high-accuracy production equipment; see Figure 10. Other industries can benefit as well.



Examples of realised dampers.

## REFERENCES

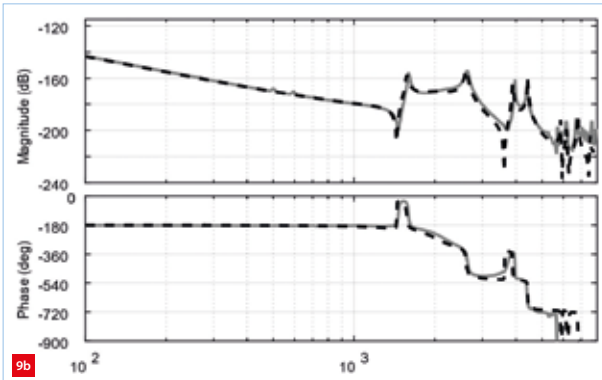
- [1] Corsaro, R.D., and Sperling, L.H., "Sound and Vibration Damping with Polymers", *Proceedings 197th National Meeting of the ACS, ACS Symposium Series*, S. 5-22, 1989.
- [2] Jones, D.L.G., *Handbook of Viscoelastic Vibration Damping*, John Wiley & Sons, Chichester, 2001.
- [3] Rivin, E., *Passive Vibration Isolation*, ASME Press, New York, 2003.
- [4] Gent, A.N., *Engineering with Rubber - How to Design Rubber Components*, Hanser, München, 2001.



Measurement and simulation of the dummy system.

(a) Without damping.

(b) With damping.



# BALANCING COMPLEXITY AND DYNAMIC PERFORMANCE

In the conceptual design phase of many high-end mechatronic applications, damping already has to be included to enable the evaluation of different concepts for meeting the dynamics requirements. Without knowing the full geometrical complexity yet, estimates of damping values have to be made as input for dynamic model calculations. For constrained layer dampers, which can reduce vibration levels in planar structures by applying viscoelastic material, analytical equations exist, but these only apply to oversimplified geometries. For calculating modal damping values for discontinuous surfaces, NTS has developed a hybrid method based on the existing equations and supplemented with an additional estimate to compensate for the discontinuities. This leads to an accurate estimate of the damping in a more complex geometry.

KEES VERBAAN, MARTIJN DUIVEN, PIETER NUIJ AND DAVID RIJLAARSDAM

## Introduction

In current positioning systems, especially in fast and accurate processing equipment and inspection equipment in the semiconductor industry, move and settle times are becoming ever shorter to continuously increase throughput. In addition, jitter values during standstill have to be low to achieve good positioning performance and process quality. In a classical design approach, the derived system requirements set the boundaries for the module requirements in terms of bandwidths of the control loops and, derived from these values, the natural frequencies of the mechanical (sub)assemblies and the natural frequencies of the vibration isolation system. Structural damping of the mechanical parts is assumed to be low ( $< 0.5\%$ ), which is correct for a high-end mechatronic device without artificial damping.

The implication of a thin horizontal stage will be that it has a low stiffness in the vertical direction and, therefore, will show low natural frequencies. These properties lead to, respectively:

- 1) A relatively high transmissibility for vibrations in the vertical direction over the whole frequency range.
- 2) Combined with low modal damping, which is a function of the material damping, large displacement amplification factors (Q-factors) at the resonance frequencies.

In addition, a drawback arises from the fact that if stage natural frequencies decrease, they will shift to a frequency region in which the vibration isolation system with air mounts is less effective. A larger part of the floor vibrational content will be transmitted into vertical displacement of the motion stage. A typical design of such a stage is shown in Figure 1.



*Motion stage with a large span-thickness ratio. The natural frequencies and modal damping are typically low for this design due to the geometrical design and material selection.*

## AUTHORS' NOTE

Kees Verbaan (system architect) and Martijn Duiven (mechanical lead engineer) work with NTS Development & Engineering, Eindhoven (NL), Pieter Nuij is the owner of MaDyCon, Ospeldijk (NL), and David Rijlaarsdam is manager quality and business improvement at Additive Industries, Eindhoven.

kees.verbaan@nts-group.nl  
www.nts-group.nl  
www.madycon.nl  
www.additiveindustries.nl

At present, mechanical designs are made on the cutting edge of technological possibilities, and even if exotic materials with a high specific stiffness are applied, the limited material stiffness becomes a limiting factor on the performance. As an additional parameter to improve machine performance, passive damping is increasingly applied [1]. For lightly damped structures, the natural frequencies are a function of the material properties and the geometry. For typical motion stages the minimal span is determined by the object size of the object to be processed. Challenges in performance arise at the point where the span-thickness ratio becomes substantially larger than 10 (which represents a relatively thin stage) due to other functional and/or volume constraints.

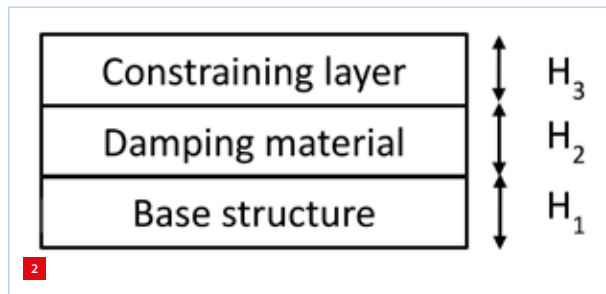
Several methods are available to overcome these challenges and to improve the dynamic performance of such a thin stage, such as applying materials with a larger specific stiffness and design of geometrically complex mechanical structures to maximise the modal stiffness and minimise the modal mass. These solutions typically result from the classical design approach, which aims for distributing mass with isotropic mass and stiffness properties in the most efficient manner. To further improve the dynamic behaviour, a more integral design approach includes the design of passive damping. This leads to an integral approach in which all three mechanical system properties are balanced: (modal) mass, damping and stiffness.

A complication of calculations with damping as compared to undamped calculations is that:

- 1) The type of analysis changes from real into complex in the sense that complex numbers are needed as input to describe the material behaviour and, therefore, will be present in the solution (in the previous article see page 5; the section on viscoelastic behaviour).
- 2) Moreover, adding artificial dampers to a mechanical system leads to different damping values for the different modes [2]. The cause is twofold: firstly, the damper placement/location on the mechanical structure, and secondly, the frequency-dependent damping ratio of a linear viscoelastic (LVE) damping material. This in contradiction to material damping for metals, which is typically low and manifests itself equally for all modes.

These implications require a type of analysis that takes these phenomena into account while calculating the damping. A number of approaches exist to calculate the modal damping values. The four most frequently used types are listed below:

- 1) Analytical approach: equations for the different damping solutions can be used to estimate damping values. The accuracy is limited and the calculations usually estimate the damping for a single mode. An advantage, on the other hand, is that it can be used in an early design phase to judge the sense of damping for a certain system with limited effort.
- 2) Determine the undamped modes with the finite-element method (FEM) and import the results into a mathematical post-processing software package like Matlab. In this case, the full complexity from 3D CAD is transferred to the processing software. Damping as well as control loops can be influenced and can be optimised – together – with mathematical optimisation techniques if required. This method allows for full flexibility but is more complex (time-consuming) to perform. This type of analysis is typically applied in the feasibility phase of a machine design, where the different parameters have to be balanced for optimal performance.



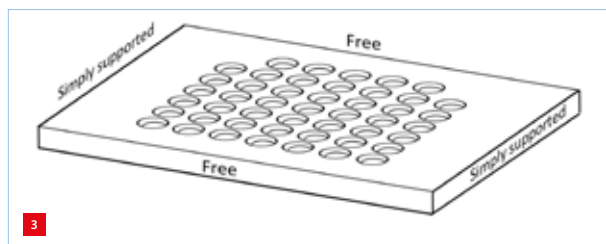
*Schematic of a constrained layer damper.*

- 3) Complex eigenvalue analysis in FEM. These solvers calculate the complex eigenvalues of a mechanical structure, which are the natural frequencies and mode shapes with damping values added. Full geometrical complexity is included, which makes it a valuable method to check the results of approaches 1 and 2.
- 4) Fully harmonic solution in FEM. This analysis provides frequency response functions (FRFs) from a certain (force) input to a certain (position/velocity/acceleration) output including the damping variation for the different modes. This method is also well suited to check the calculations from approaches 1 and 2.

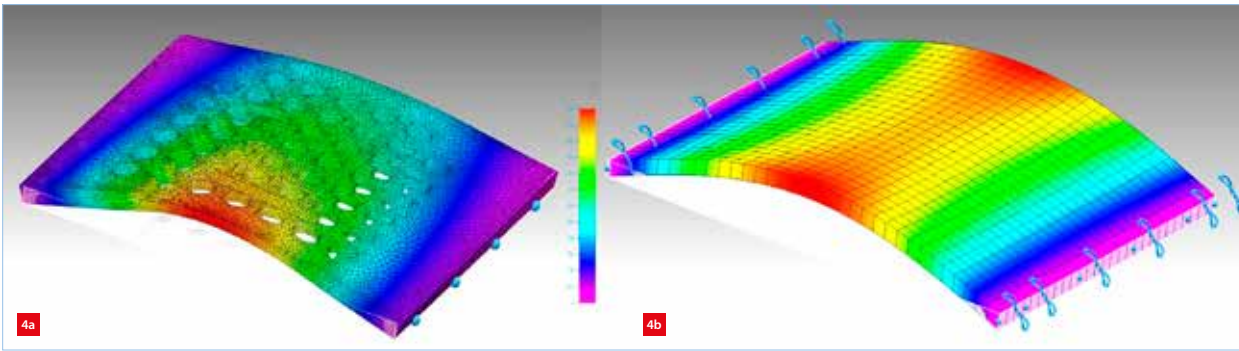
### Discontinuous constrained layer damper design

Although all four approaches listed above are interesting, and NTS Development & Engineering has dedicated tooling available to perform these analyses, this article describes a specific design approach for the application of a constrained layer damper (CLD) (Figure 2) on the discontinuous surface of a stage (Figure 3). This is in fact an extension of the first analytical approach, but is driven by the ongoing need for performance improvement and the related need for accurate performance estimates in an early stage of machine concept design.

As an example, a motion stage with a span-thickness-ratio of 23 was used, which implies a relatively thin geometry. A CLD with limited thickness has been designed to improve the dynamic performance at the first dominant resonance frequency. Parameters are the material mechanical properties and the dimensions of the three plates; the base structure H1 (stage), the constrained layer H2 (damping layer) and the constraining layer H3. The main displacement contribution of the corresponding mode shape acts in the vertical direction.



*Schematic drawing of the stage with the boundary conditions.*



FEM results for the first mode of the motion stage; the colour scale indicates the local magnitude of the mode shape, from small (purple) to large (red).

(a) With a discontinuous surface.

(b) With a continuous surface.

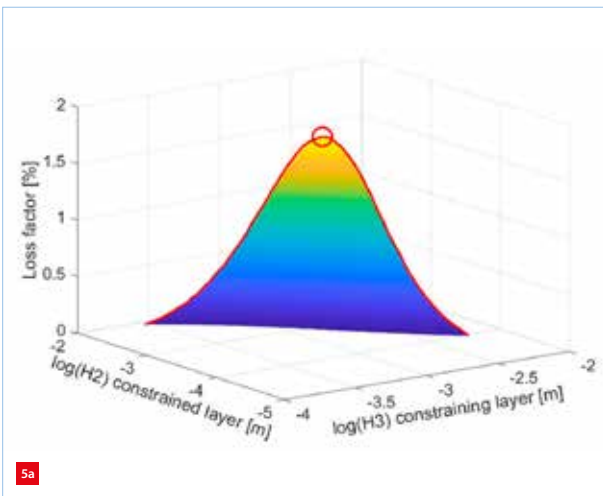
As starting point in the design process, a rubber type was selected which exhibits good damping properties, i.e. a large loss factor in the frequency range of that resonance under operational temperatures. For small strain values these types of materials can be classified as LVE materials [3] whose behaviour can be expressed as a complex stiffness value as a function of frequency (in the previous article see page 6; the section on the viscoelastic model). This complex stiffness consists of a real part (storage modulus) and an imaginary part (loss modulus), which represent the ability of the material to, respectively, store and dissipate energy per vibration cycle.

The geometrical design part of the stage with CLD starts with computing the undamped characteristics of the discontinuous stage design with correct boundary conditions (see Figure 3). FEM is applied to perform a modal analysis. This type of analysis provides a high-quality answer for the natural frequencies and mode shapes of complex geometries, including stress and strain distributions. Figure 4a shows the mode shape of the first mode.

The second step is the approximation of these modal results by analytical equations [4] for a continuous surface (Figure 4b) in order to be able to estimate variations in modal damping outside the FEM environment and enable optimisation algorithms to be applied. Equations based on the theory for continuous CLD layers, known as the RKU equations [5], are applied to provide estimates for the modal damping of the stage with a CLD layer added. The materials' real and complex parts of the Young's modulus have to be used in this equation to calculate the modal damping factor of the complex structure at the resonance frequency.

### Damping optimisation

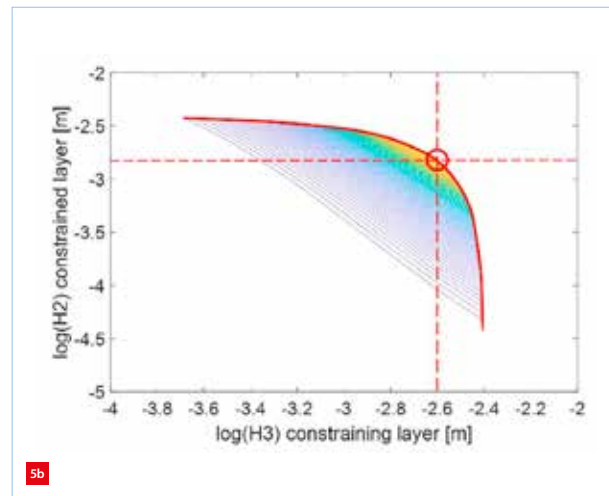
The RKU equations allow for calculation of the modal damping value of a continuous plate with a CLD layer applied. Parameters in the equation are the material mechanical properties and the dimensions of the three plates;  $H_1$ ,  $H_2$  and  $H_3$ . An optimisation algorithm is applied to find the maximum modal damping as a function of the overall thickness given the boundary conditions. This is visualised in Figure 5.



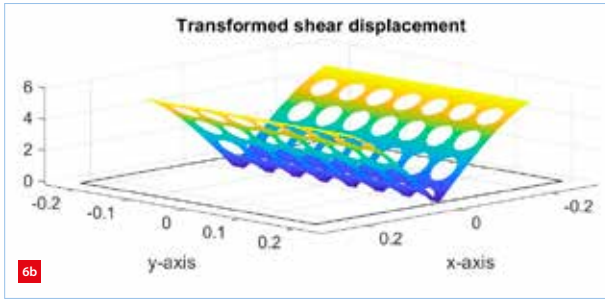
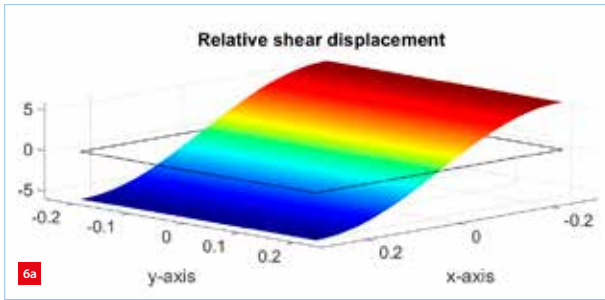
Modal damping (loss factor) of the stage with a continuous CLD layer, as a function of the constrained layer thickness ( $H_2$ ) and the constraining layer thickness ( $H_3$ ). The maximum CLD thickness (4 mm) with respect to the overall stage thickness limits the achievable modal damping in this case. The optimum damping value is indicated in both figures and amounts to 3.2%.

(a) Graph

(b) Contour plot.

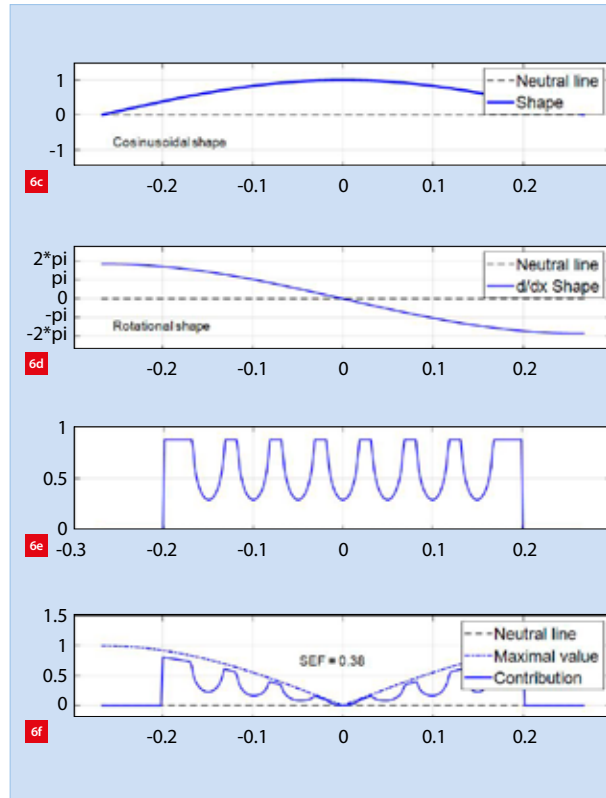






Calculation of the shear efficiency factor (SEF) value.

- (a) The shear displacement for the continuous full-size layer.
- (b) The absolute shear for the reduced-size discontinuous layer.
- (c) The first mode shape of the supported/free constrained stage.
- (d) The shear displacement.
- (e) The surface effectiveness of the discontinuous stage.
- (f) The shear contribution as a function of the x-direction of the CLD.



A minimal modal damping value was set as a constraint to reduce the parameter space and to improve convergence in the optimisation process. The resulting value is an approximation for the modal damping of a continuous plate equipped with a CLD and amounted to 3.2%. This value has to be compensated for the discontinuities in the CLD layer. This compensation factor is called shear efficiency factor (SEF), which expresses the damping effectiveness of the discontinuous CLD layer with respect to the full-size continuous layer. The basis for this estimate lies in the relative shear displacement in the constrained layer that is introduced by the constraining layer with respect to the base layer. This strain deformation can be calculated as a function of the mode shape and as a function of the spatial coordinates of the base layer.

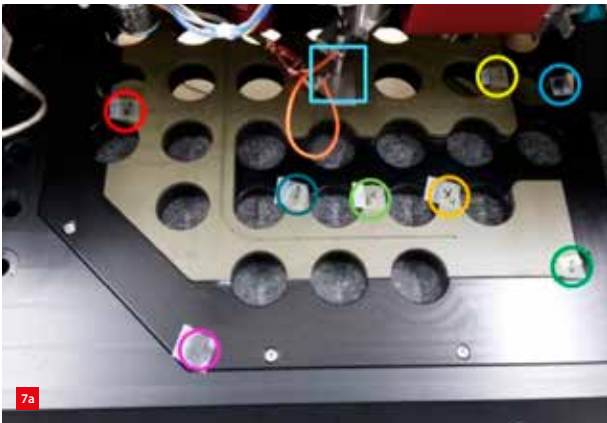
The SEF is defined as the ratio of the integrated shear displacement over the discontinuous CLD surface with respect to the integrated shear displacement over the continuous layer. This factor expresses the effectiveness by taking the relative shear displacements into account as well as the effective CLD area. The SEF ranges from 0 when the discontinuous CLD area equals zero (only holes), to 1 for a full-size and continuous CLD (no holes). For this specific stage, the analytically determined SEF value amounted to 0.38. The overall modal damping value can be calculated by multiplying the SEF with the modal value obtained from the optimisation. Assumptions in this approach are 1) the mode shape is sinusoidal [4]; and 2) the neutral line during

bending remains at the same height for the stage without and with CLD.

Figure 6 visualises the calculation of the SEF value by deriving the relative shear displacement in the continuous constrained layer (a-d) from the mode shape (c) and subsequently multiplying by the relative effectiveness (e). The relative effectiveness is the quotient of the surface area of the discontinuous layer as a function of the x-direction over the corresponding surface area of the continuous layer. Multiplying the absolute value of the shear displacement with the relative effectiveness (both functions of the x-direction) results in the effective average shear contribution (f). The application of this approach on the motion stage with holes as described in this paper resulted in a theoretical modal damping value of  $0.38 \cdot 3.2\% = 1.22\%$  at the first resonance frequency around 100 Hz.

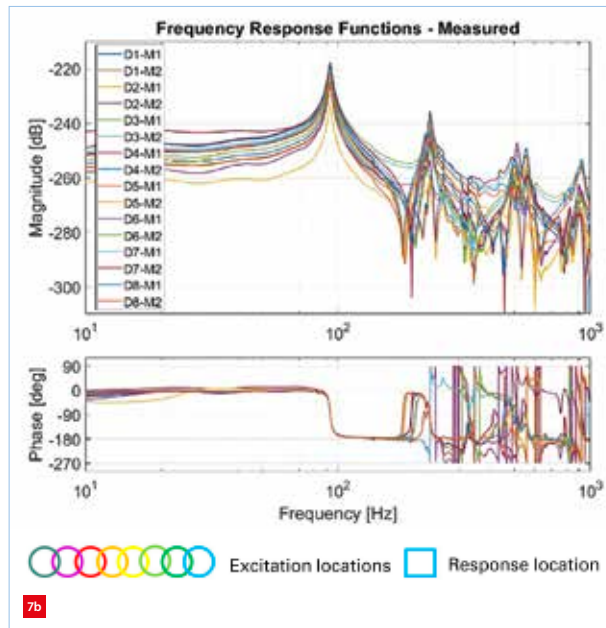
### Experimental validation

The experimental validation has been performed by applying experimental modal analysis (Figure 7) on the motion stage to measure the modal damping of the first five flexible vertical modes (in-plane modes could not be observed in this modal analysis; they will have higher frequencies). The stage was excited by an impulse hammer in eight positions (see Figure 7a) and stage displacement was measured by a fixed capacitive probe, both connected to a data acquisition system. The resulting frequency response functions from force to displacement are displayed in Figure 7b.



Experimental validation.

(a) The discontinuous stage with the locations of excitation and the (response) location of the displacement sensor.  
(b) The corresponding frequency response functions.



The modal damping was estimated at the first resonance frequency and was compensated for the numerical damping introduced by the exponential weighting function, which was applied to the displacement signal of the capacitive probe. An exponential weighting function is used to reduce spectral leakage in impact excitation measurements by adding numerical damping to the response signal. The amount of additional damping must be accounted for in the FRF estimates.

This approach resulted in an accurate modal damping value for the first flexible mode of the stage, being 1.19% at a frequency of 97.7 Hz. This shows a damping increase of approximately nine times, compared to the modal damping value of 0.13% of the undamped stage. The vibration spectra of the motion stage with CLD have been measured with the capacitive probe and a comparison has been made to the vibrational content of the motion stage without CLD (see Figure 8a). The time traces of both cases are presented in Figure 8b. From these measurements it can be calculated that the rms amplitude has been reduced by a factor of three with respect to an undamped stage.

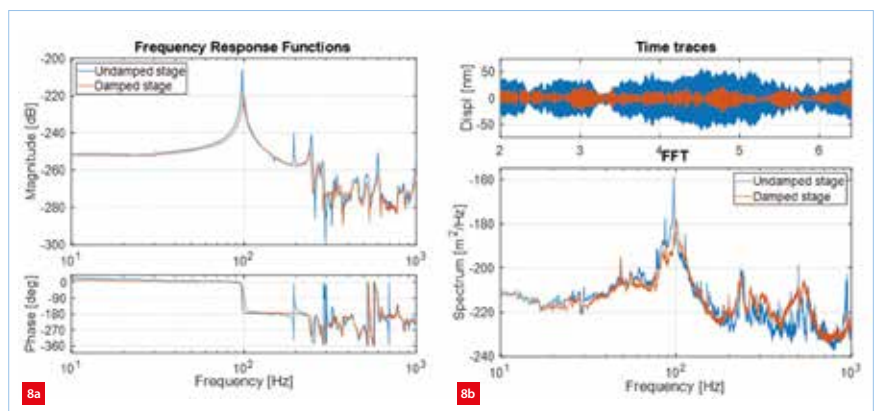
## Conclusion

The hybrid design approach as described, with a combination of undamped modal analysis by means of FEM and analytical estimates for the added damping, provides a realistic value for the overall modal damping value for a plate-like mechanical structure with a discontinuous constrained layer damper applied. The accuracy of the calculated damping is within 5% for the example shown. This analytical approach, combining results from

undamped FEM analysis with analytical estimates, facilitates optimisation and is a very powerful tool in an early design phase. If critical for the final performance, the performance can be validated with a fully harmonic calculation or damped eigenmode calculation in FEM.

## REFERENCES

- [1] Van der Meulen, S., "Enabling overlay/focus improvement via passive damping in ASML motion stages", *DSPE Conference on Precision Mechatronics*, 2016.
- [2] Den Hartog, J.P., *Mechanical vibrations*, Courier Corporation, 1985.
- [3] Macosko, C.W., and Larson, R.G., *Rheology: principles, measurements, and applications*, John Wiley & Sons, 1994.
- [4] Blevins, R.D., *Formulas for natural frequency and mode shape*, Krieger Publishing Company, 1979.
- [5] Jones, D.I., *Handbook of viscoelastic vibration damping*, John Wiley & Sons, 2001.



Vibrational content of the stage.

(a) The measured undamped and damped frequency response functions.  
(b) Time traces of the vertical stage displacement without and with CLD (top), and the corresponding vibration spectra of the stage (bottom).

## Pfeiffer Vacuum – specialist in vacuum generation and leak testing

**Pfeiffer Vacuum provides innovative and custom vacuum solutions worldwide, building on technological perfection, competent advice and reliable service. Since 130 years, the company has been setting standards in vacuum technology. With the invention of the turbopump, Pfeiffer Vacuum paved the way for further development within the vacuum industry and they continue to be one of the technology and world market leaders in this field. Pfeiffer Vacuum Benelux is located in Culemborg (NL).**

Customers' requirements are typically highly complex. The vacuum solutions are permanently optimised through close cooperation with customers from various industries and continuous development work.

### Generating vacuum

One vacuum is not like another – it's the specific requirement that is important every time. Whether low, medium, high or ultrahigh vacuum is required for a specific application, Pfeiffer Vacuum offers a wide range of backing pumps, hybrid and magnetically levitated turbopumps, chambers and components.

Rotary vane pumps suit all applications in the low- and medium-vacuum range. They are sturdy and have a long life, whether they are used as backing pumps to generate the backing pressure called for by turbopumps, or as a single stand-alone pump. Oil lubrication ensures an extremely long lifetime, even in continuous operation. Through its compactness, a diaphragm pump is ideal for integration in increasingly small analytical systems and turbopumping stations. Beginning with a pumping speed of 0.25 m<sup>3</sup> per hour, customers can choose from a wide selection of pumps. The strongest of these vacuum pumps manages a pumping speed of max. 4.3 m<sup>3</sup>/h.

Numerous applications in research and industry, in fact, need a vacuum with an extremely low absolute pressure (high vacuum). Turbopumps have established themselves globally



as the technological standard. High-speed rotors with up to 90,000 rpm generate the pressure conditions required for application. This allows a vacuum of up to 10<sup>-11</sup> mbar to be generated in the high- and ultrahigh-vacuum range.

### Leak detection

Leak testing is crucial for the reliability of production processes. As important as it is, it is challenging to determine the perfect leak test process for a particular application. The process begins with the definition of the required tightness, i.e. leak rate. Within their leak testing equipment Pfeiffer Vacuum is presenting helium leak detection as well as the Micro-Flow technology from their subsidiary ATC.



### Measurement and analysis

Analog and digital total vacuum or pressure measurement instruments are used to measure and control the total pressure in a vacuum system. Pfeiffer Vacuum offers different lines of total pressure gauges. Furthermore, they supply an extensive range of analysers for gas determination in a vacuum process. From the mass spectrometer to the complex analysis system for gas analysis in the ultrahigh-vacuum range right up to atmospheric pressure. The basis is always the quadrupole mass spectrometer whose field axis technology ensures high sensitivity.

#### INFORMATION

[WWW.PFEIFFER-VACUUM.COM](http://WWW.PFEIFFER-VACUUM.COM)



# COLLABORATING FOR CLEANLINESS FROM A TO Z

The CLEAN2020 theme day, organised by Mikrocentrum in collaboration with VCCN, provided an expert's view on cleanliness. Speakers from academia and industry presented new developments and standards, discussed product and process optimisation, reviewed quality control and inspection procedures, and shared best-practice applications. Topics ranged from ASML's new standards for cleanliness to Zeiss' policy regarding part cleanliness for lithography applications within the complete supply chain.

On 28 January 2020, the CLEAN2020 theme day, a full house (Figure 1) at Mikrocentrum in Veldhoven (NL), was opened by Philip van Beek of VCCN (Dutch Contamination Control Society). He reflected on the future of cleanliness; its importance will continue to increase and cleaning and cleanroom technologies will keep on evolving. "Smart cleanrooms will be the road towards 2030; combined with a better control of critical cleaning procedures this will help the industry to further improve cleanliness", Van Beek stated.

## ASML

Dirk Trienekens, cleanliness expert at ASML, in turn stressed the importance of cleanliness. In some cases, contamination is only cosmetic and, in the end, will not influence the performance of ASML machines. It is however not easy to assess whether contamination is strictly cosmetic or will affect functionality. The wrong type of contamination in the wrong area of the machine can have devastating effects on the output, as Trienekens illustrated for the impact of particles on the lithography process (Figure 2).

To address the requirements for cleanliness, ASML has had a cleanliness GSA (Generic Standard of ASML) in place for years, but its supply chain has been struggling with this GSA, Trienekens declared. The resulting lack of awareness and understanding causes issues in the field: high rework levels and dirty products. Adding to the problem, ASML

now needs to raise the bar for their new systems. To secure system performance, which can suffer from defectivity (mainly due to particles) and optics lifetime degradation (primarily due to molecular contamination), ASML has to be more stringent when it comes to cleanliness. Therefore, a new set of cleanliness requirements for suppliers has been defined and laid down in a new cleanliness GSA framework.

To promote stricter adherence, ASML focused on creating more awareness of the importance of cleanliness, defined a clearer document structure and reduced the amount of text. The new ASML standards also refer to ISO standards where possible. Implementation of the new GSA has been started in consultation with the supply chain. Trienekens also acknowledged VCCN guideline no. 12, "Product/part cleanliness with respect to particles and chemicals (including outgassing rate in vacuum)", of which the definition is in progress.

Trienekens discussed the new GSA and the new way of working associated with it, briefly zooming in on the approach for the most critical (grade-1) parts, where simply performing a cleaning action after manufacturing will no longer suffice. The new approach for grade-1 parts requires suppliers and ASML to work together to proactively determine and eliminate risks with respect to contamination in the production process, Trienekens concluded.

## TNO

Freek Molkenboer, systems engineer at TNO, talked about molecular surface cleanliness. Cleanliness should already be addressed during the design phase for a new product or system. Surface cleanliness requirements have to be defined realistically, to prevent either products being insufficiently cleaned or unnecessary cleaning costs being incurred. Molkenboer illustrated his thesis with the case of TNO's EBL2 research facility, which is used for investigating the lifetime of parts that are subjected to EUV radiation (Figure 3). At the heart of this facility, it is an ultraclean vacuum system.

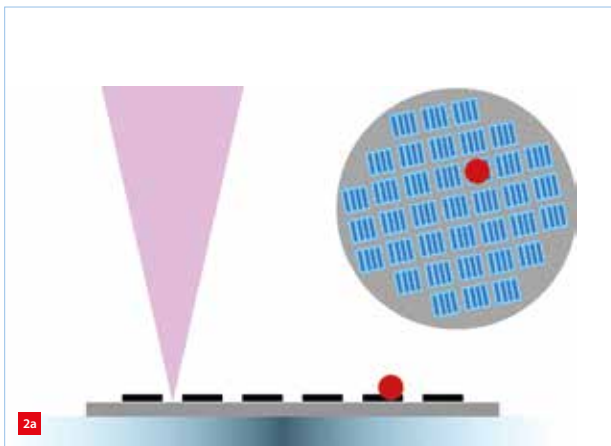
### EDITORIAL NOTE

The input by Philip van Beek, board member of VCCN, is acknowledged.



The CLEAN2020 event attracted over 300 visitors.

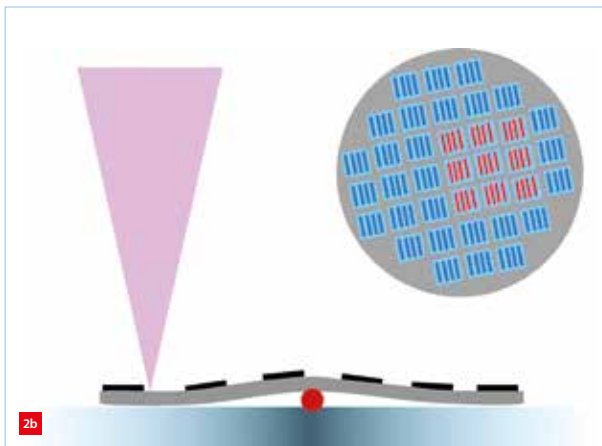




Impact of a particle in lithography. (Images: ASML)

(a) Frontside of the wafer: an unfunctional die.

(b) Backside of the wafer: overlay errors, focus errors and, in extreme cases, wafer damage.



To ensure that the EBL2 facility had the correct cleanliness at the right location, the design was started by defining a contamination budget considering the route of samples through the system, addressed production challenges (such as clean assembly and prevention of cross-contamination by the tools used) and concluded with the validation, including measurement of the outgassing within the system.

Following the ASML speaker, Molkenboer, member of the VCCN working group on guideline no. 12 (in which both OEMs and suppliers are represented), also talked about this guideline. He highlighted that it covers the complete design process according to the well-known systems engineering V-model, from user requirements & concept of operations, down to parts fabrication and assembly, and up again to system demonstration & validation. The guideline addresses surface cleanliness specification, the full production phase (machining, cleaning, assembly and packaging) and measurement methods.

## Zeiss

Further contributions included practical contamination control and cleaning approaches, innovations in inspection, and flexible mobile solutions. Robert Meier, head of Cleaning Process Technology Mechanics High-NA at Zeiss Semiconductor Manufacturing Technology,

concluded the day by presenting how the company achieves cleanliness throughout the supply chain in the context of manufacturing complex optics for semiconductor lithography systems.

Crucial in this respect are the highly specialised EUV cleaning processes, including the installation of specific machinery and dedicated cleanliness processes. The presentation focused on organic contamination and the presence of critical elements at atomic level and their influence on optical lifetime in the EUV systems (Figure 4). According to Meier, a key success factor was the standardisation of the related processes and metrology procedures throughout the complete supply chain.

The take-home message, according to chairman of the day Philip van Beek, was that customers and suppliers have to work together on the basis of understanding one another's problems. Only a joint effort can provide the solutions that the high-tech industry requires.

### INFORMATION

[WWW.MIKROCENTRUM.NL/EVENEMENTEN/THEMABUJENKOMSTEN/CLEAN-EVENT](http://WWW.MIKROCENTRUM.NL/EVENEMENTEN/THEMABUJENKOMSTEN/CLEAN-EVENT)  
[WWW.VCCN.NL](http://WWW.VCCN.NL)



The design of EBL2, TNO's research facility for investigating the lifetime of parts that are subjected to EUV radiation, was based on its cleanliness requirements. (Photo: TNO)



Alignment of EUV optics under clean conditions at Zeiss Semiconductor Manufacturing Technology. (Photo: Zeiss)

# PREVENTING FFT FROM FALLING SHORT

Using Fast Fourier Transform for signal analysis comes with particular requirements and constraints on the data record to be captured, which are quite often not adhered to or are even totally ignored. One example is the determination of specific, e.g. mains-related, frequency components. Oversampling, longer records and high analogue-digital conversion resolution help to enhance the spectral level accuracy but yield a very high number of spectral lines. Here, model order reduction can be achieved by full synchronisation between the record length and the periodic interval, in which the lowest common multiple periods occur.

MART COENEN

## Introduction

The basic concept of Fast Fourier Transform (FFT) was introduced in 1807 and was further developed in the late 1950s when signal discretisation became popular, e.g. as a follow-up to the Fourier series [1]. With today's measurement capabilities, using high-end oscilloscopes to capture time-repetitive signals with mega-sample record length and sub-nanosecond sampling rates, new options have arisen for translating time-periodic signals into their equivalence in the frequency domain. Sub-nanosecond sampling and mega-sample records result in a mega number of spectral lines, typically defined as Power Spectral Density (PSD). To obey the 'true' mathematical FFT-IFFT (inverse FFT) relation between time and frequency domain, all spectral lines (amplitude and phase) resulting from spectral leakage are required for the time signal reconstruction and manipulation.

Many techniques have been developed to address the non-synchronous sampling versus the 'real' length of the periodic signal to assure that the length of the record  $T_{\text{datablock}}$  equals an integer amount of basic periods of the periodic signal  $T_{\text{signal}}$ , being 'zero-ed' by using all kinds of non-rectangular, windowing filter techniques: Hamming, Kaiser, Blackmann-Harris, etc. Adding leading or trailing 'zero amplitude samples' is applied to extend a record's length such that it contains  $2^N$  samples. These 'zero' additions allow for fast(er) Discrete Fourier Transform (DFT), without adding energy, i.e. info, to the original signal.

Referring to the Fourier fundamentals [1], the solution can be found in the oversampled time signal itself, by analysing the time data for its periodic zero-crossings to determine the exact signal's period, i.e. the period of its lowest common multiple. It subsequently entails resampling the fixed equidistantly sampled data record, typically a broken

number of samples for the real zero-crossing, into a  $2^N$  record of new samples, where  $2^N$  is the smallest number larger than the broken number of samples. Signal energy and integrity are not affected and only 'real' spectral lines, i.e. harmonics, result. By using the first few hundred harmonics of the 'real' periodic signal (which could also be the lowest common multiple of several frequencies), rather than the brute-force given mega number, the original time signal can be represented with high fidelity [2].

## FFT constraints

When analogue periodic signals need to be analysed on their signal content using FFT, there are a few simple constraints to be considered:

- In general, FFT does not provide true absolute frequencies but results in frequency bins with a certain amplitude, i.e. energy, together with optimally calculated phase information for that amplitude in each frequency bin.
- The record length determines the lowest frequency (aside from the DC component), i.e. the frequency resolution. All frequency bins have equal bandwidth, which is the inverse of the time duration of the record length. Additional weighting functions can be used to reduce or extend the bandwidth [3].
- The sampling frequency (divided by 2; according to the Nyquist theorem) determines the highest central frequency of the spectral bins.
- The vertical resolution determines the dynamic range. The dynamic range of an FFT is determined by the quantisation noise which depends on the smallest step size of the amplitude quantisation used [3-6]. Oversampling the recurring signal helps to increase the dynamic range as well as extending the record length to multiples of the lowest common multiple periods of the targeted signal.

### AUTHOR'S NOTE

Mart Coenen is the owner of private consulting company EMCmcc, located in Breda (NL). EMCmcc offers electro-magnetic compatibility (EMC), electrical safety, signal integrity and power integrity design consultancy as well as (pre-)compliance measurement services.

[mart.coenen@emcmcc.nl](mailto:mart.coenen@emcmcc.nl)  
[www.emcmcc.nl](http://www.emcmcc.nl)

- Non-true-periodic sample records lead to spectral leakage in the frequency domain [2, 7, 8]. This deficiency can be partly resolved by applying windowing filters.

### Motion-related signals

When looking at modern motion-related system signals, there are a few signal components to be considered. If a modern AC-mains-driven motion drive is employed, the following fundamental frequencies occur:

- The mains frequency itself: 50 Hz  $\pm$  2%; single-phase bridge-rectified: 100 Hz; 3-phase bridge-rectified it will be 150 Hz; and when even 6-pulse rectification is used: 300 Hz.
- Power Factor Correction (PFC), used to ensure compliance with the power quality requirements, covering the first 50 harmonics of the mains frequency. Typically, a PFC controller runs at several tens of kHz.
- The motion frequency, a motion profile necessary to generate the motion required. With most modern motion systems, the speed, acceleration and jerk (= time derivative of the acceleration) profiles (VAJ) are known in advance.
- The pulse-width modulation (PWM) frequency of the motion drive system, typically 10 to 1,000 times higher than the maximum motion frequency required. With today's motion systems, the PWM frequency is derived from a DSP (digital signal processor) clock frequency and is fixed. The higher the PWM frequency ratio with respect to the motion frequencies, the more phase margin is available in the motion control system.

For energy-recovering motion systems, the retrieved motion energy can be transferred back to the supply system. In this case, the mains rectifier, as well as the PFC circuitry, are all confined in one control system. In this case, the mains frequency remains dominant and the PFC frequency is often coupled to the PWM frequency of the motion drive stage and as such to the quartz-crystal-based DSP clock of the motion system.

For the mains frequency, it is still the case that it will vary slightly over time but not instantaneously [9]. Furthermore, over 24 hours, the number of mains cycles is nearly fixed to ensure correct indication of timers and clocks using synchronous motors, i.e. time indication systems counting mains periods as a reference.

The motion frequency is restricted to a few kHz at the most as it will be limited by the mechanical inertia of the motion system used. If a motion system with 3,000 rpm (= 50 Hz) is used, a PWM frequency of  $> 1$  kHz is used; a typical ratio (PWM versus motion frequencies) is in the order of 20. As low PWM frequencies are audible, typical PWM frequencies involving motion are chosen higher than 16 kHz, i.e. a ratio

of over 300. High(er) PWM frequencies cause switching losses in the motion drive stage and are only used with very high-speed switching elements (MOSFET, SiC, GaN).

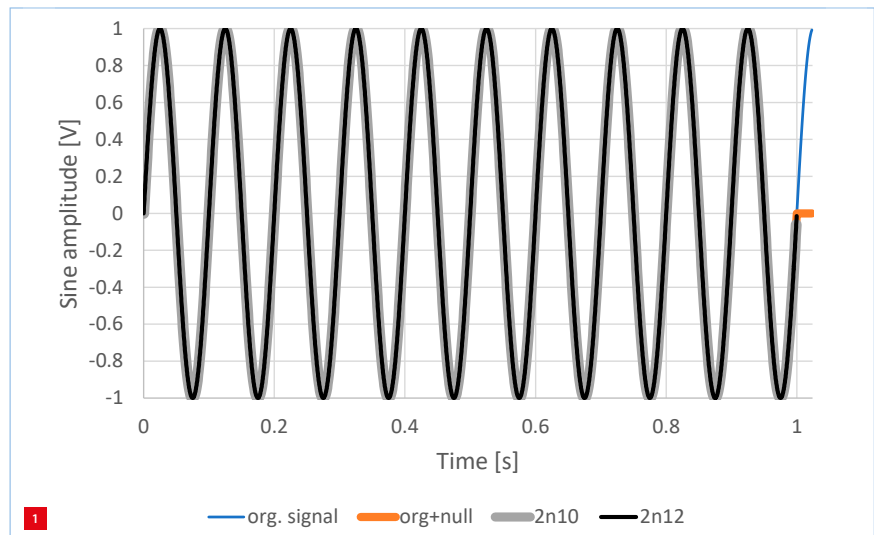
Considering the frequency components described above, the frequency spectrum will contain all harmonics and inter-modulation harmonics of the motion signals; these can all be forecasted. While knowing these predictable frequencies, the mother-child principle [4] can be used to separate uncommon signals with high resolution. [The mother-child principle metaphorically refers to measuring the heartbeats (of mother and unborn child) on the mother's belly as well as on the mother's wrist (of mother only). By synchronous subtraction, the mother's heartbeat can be fully separated from the child's.] This principle can also be used to detect wear-out/bearing corrosion (causing additional signals) when the spectrum is 'clean', as (additional) spectral lines that will appear or change can be easily detected.

### Case study

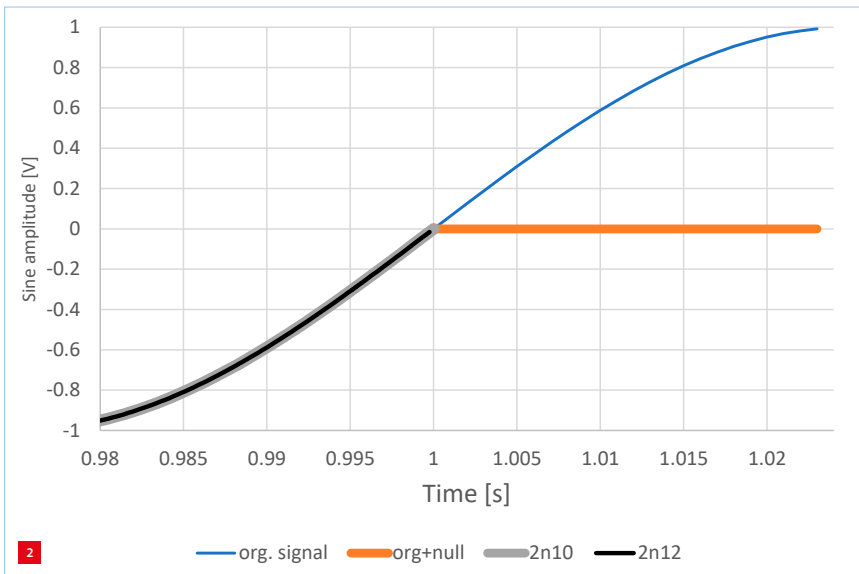
With either Matlab, Python, Octave or MS Excel (with the inclusion of the analysis package), FFT analysis can be carried out. For the sake of simplicity, a sinewave signal of 10 Hz, amplitude 1, is calculated in a time frame of about 1 second. For the FFT analysis, no windowing filter is applied, i.e. a rectangular window is used. To enable Excel to perform Discrete Fourier Transform (DFT), a time record with  $2^N$  samples needs to be taken. In the first two examples, 1,024 ( $2^{10}$ ) samples are taken for the record length.

A total of four cases concerning a 10 Hz signal are analysed:

1. Time record: 1.024 sec., 1,024 samples (org. signal; blue).
2. Time record: 1.024 sec., 1,000 samples followed by 'nulls' to complete the 1,024 samples (org + null; orange).
3. Time record: 1.000 sec., 1,024 samples ( $2n10$ ; grey).
4. Time record: 1.000 sec., 4,096 samples ( $2n12$ ; black).



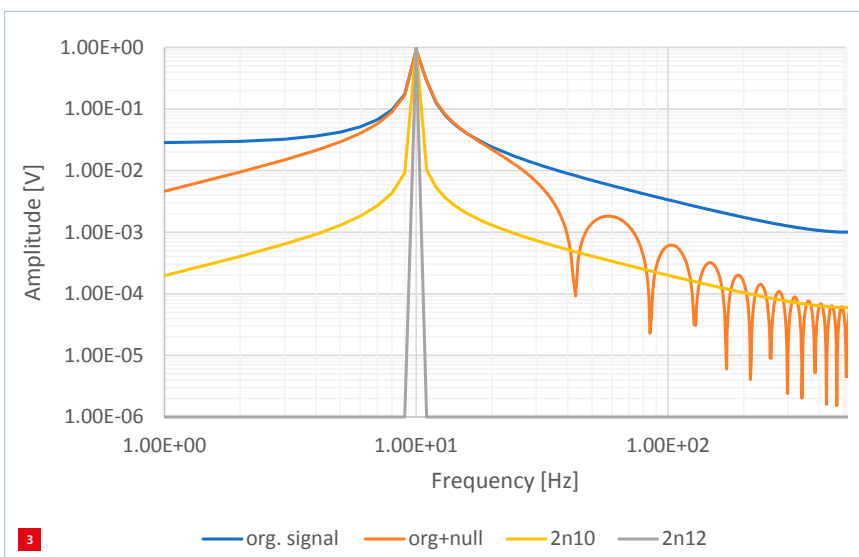
Time domain plot of the four signal cases.



End-of-record time domain plot of the four signal cases.

Initially, until 10 periods, no differences can be found other than at the end of the record. The first record is, compared to the time signal, too long by 24 samples. The second record is exactly 1,000 samples long and followed by trailing (24) zeros to complete the 1,024 samples.

The third record equals the first one, but now with the 10 periods represented by 1,024 samples. The 1,000 samples have been resampled to 1,024 samples over a 1-second interval record. The fourth record equals the third one but now resampled to 4,096 samples. As can be seen from the zoomed-in 'end of the record', Figure 2, the differences at the end of the record are quite significant. The main difference between the 1,024 and 4,096 samples is in the last value of the record of  $2^N$  samples ( $N$  is 10 and 12, respectively), whereas sample no. 1 and sample no.  $2^N+1$  are equal in amplitude.



DC-less FFT results at 10 Hz for cases 1 to 4 as shown in Figures 1 and 2. (Note the change in colour coding in cases 3 and 4 as compared to the previous figures.)

Each of the four records can be FFT-analysed in a straightforward manner with significantly different findings; see Figure 3. The first two cases, based on their discontinuity, require the entire spectrum to represent the time signal in the frequency domain. Here, this amounts to 512 spectral lines with complex value (i.e. absolute amplitude and phase) plus a DC component (which has been omitted by using log-log scales). All frequency bins have 1 Hz bandwidth, due to the 1-s record length.

Resampling the periodic signal back to a  $2^N$ -record length, cases 3 and 4, helps to reduce spectral leakage. In the fourth case, the entire signal as entered in the time domain can be given by a single spectral line in the frequency domain, similar to the formal Fourier series theory, i.e. taking the exact synchronous  $2^N$  samples with the periodicity of the time signal yields model order reduction by a factor of 512 as compared to the brute-force FFT method. When multi-million time samples are taken and set into the frequency domain, model order reduction will extend (far) beyond a factor of 1,000.

## Conclusions

Using FFT for signal analysis results in particular requirements and constraints on the data record to be captured, which are quite often not adhered to or even totally ignored. In particular, the determination of specific frequency components, e.g. 50 Hz  $\pm$  2%, requires longer signal records, i.e. a 1-s record results in 1 Hz frequency resolution. Shorter measurements result in even worse spectral resolution, though the amplitude can be derived quite accurately.

Oversampling, with a factor of more than 20 with respect to the signal intended to be captured, longer records (e.g. up to 64 M samples) and high analogue-digital conversion resolutions (16 bits) help to enhance the spectral level accuracy, i.e. dynamic range, but also lead to spectral density results with a very high number of spectral lines (due to 'Nyquist').

Full synchronisation between the record length and the periodic interval, in which the lowest common multiple periods occur, is a necessity to enable model order reduction. The most significant lowest common multiple period should be found, and this period often includes a fractional sample period. This period should be resampled to  $2^N$  samples to enable DFT at the highest computational speed and high resolution with minimum energy dispersion to non-existing frequency components.

## Acknowledgement

The subject of spectral analysis and signal energy dispersion has been 'under the hood' for more than 40 years [8] and



has been reinvestigated while participating in the European H-2020 ESCEL I-Mech project [10] (grant agreement ID: 737453), now involved with 'active EMI noise-cancellation' [7] (EMI is electromagnetic interference).

Based on the many years of experience in various motion applications, a new training course, "EMC for Motion Systems", has been defined, in collaboration with DSPE (a society where many motion-related issues come together) and High Tech Institute (HTI). The lectures will be presented by TU Eindhoven, Philips Healthcare, Analog Devices and EMCMCC representatives and will include demos and hands-on sessions. The first edition of the 3-day seminar was scheduled for 6-8 April in Eindhoven. Due to the corona crisis, the training course has been postponed until November 2020.

#### REFERENCES

- [1] G.P. Tolstov (translated from Russian by R.A. Silverman), *Fourier series*, Dover Publications, 2017.
- [2] M.J. Coenen, T.A.K. Gierstberg, A. van Roermund, A.P. de Koning, and T.J. Coenen, "Time-domain surface scan method", *Proceedings of the 2012 Asia-Pacific Symposium on Electromagnetic Compatibility (APEMC)*, Singapore, 2012.
- [3] P. Nuij, and D. Rijlaarsdam, "The transformation from time to frequency domain", *Mikroniek*, vol. 54 (2), pp. 8-13, 2014.
- [4] A.W.M. van der Enden, and N.A.M. Verhoeckx, *Digitale signaalbewerking* (Dutch), Delta Press, 2002.
- [5] A.V. Oppenheim, and R.W. Schaffer, *Discrete-time signal processing*, Prentice Hall, 1999.
- [6] H.L. Hirsch, *Statistical Signal Characterization*, Artech House, 1992.
- [7] M. Coenen, and J. Deb, "Active EMI Noise Cancellation", *2018 International Symposium on Electromagnetic Compatibility - EMC Europe*, Amsterdam, 2018.
- [8] M.J. Coenen, "Digitale frekwentievermenigvuldiger" (Dutch), B.Sc. thesis, HTS (University of Applied Sciences) Breda, 1979.
- [9] [www.mainsfrequency.com](http://www.mainsfrequency.com)
- [10] M. Čech, A.-J. Beltman, and K. Ozols, "I-MECH - Smart System Integration for Mechatronic Applications", *IEEE International Conference on Emerging Technologies and Factory Automation (ETFA)*, no. 8869465, pp. 843-850, 2019.



## The future is closer than you think

You want your company to stand out, but how? You'll need specialists who can share their thoughts at every level. With creativity, dedication, and lots of knowhow, NTS helps its customers find the ultimate solution to every problem.

We specialize in developing, manufacturing, and assembling (opto-)mechatronic systems, mechanical modules, and critical components. Our expertise? Precision and maneuverability.

From the initial design to the prototype, all the way to assembly – our comprehensive support helps customers realize their ideal product faster. NTS excels in solving complex issues. Leave it to us to design and create an application that's exactly what our customer was looking for. With our versatile knowledge and wealth of experience, we help accelerate technological innovations.

The technology of the future?  
With NTS, it's at your fingertips.

[nts-group.nl/career](https://nts-group.nl/career)



Our (opto-)mechatronic systems and mechanical modules contribute to future technologies

**Accelerating the future**

# MACHINE METROLOGY FOR OPTIMAL PERFORMANCE

The machining time for complex workpieces such as turbine blades, impellers, medical protheses and complex machine frames, as manufactured on 5-axis machine tools, can be very long, typically many hours. The machine's thermal stability is critical for meeting geometrical tolerances and must remain below a certain value. This article presents a fast and accurate method for the dynamic 3D measurement of thermal stability and features a case study describing the use of a non-contact wireless probe.

GUIDO FLORUSSEN, HENNY SPAAN AND THERESA SPAAN-BURKE



Set-up of a classic thermal distortion test using three capacitance sensors.

A machine tool contains many heat sources and the spindle is commonly the largest. Spindle power can be 40 kW or even more. Linear motors can also heat up significantly and these are found in fast moving machine tools. Other heat sources are hydraulic pumps, friction in gears and drive

trains, electronics, and the cutting process – the environmental air temperature is also of concern; conditioned workshops are rare but do exist.

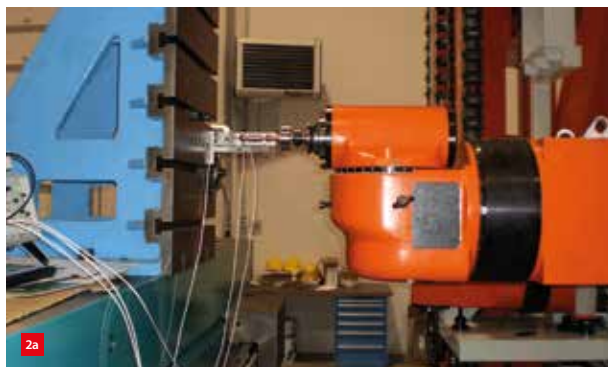
Machine tools are available in many sizes and configurations and their thermal stability can vary largely: from 'poor' to 'nearly perfect'. Thermal machine behaviour can be improved by using:

- smart design (i.e. low-expansion materials, symmetry);
- temperature control of vital machine components (e.g. the spindle unit, hydrostatic axes);
- air conditioning in the workshop;
- correction models employing integrated temperature sensors (e.g. analytical, empirical or hybrid machine thermal error models).

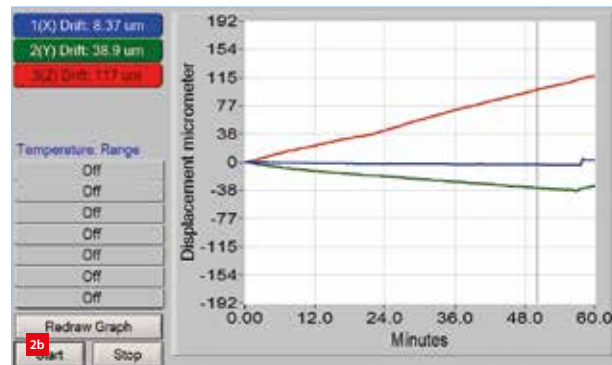
Temperature control can be very effective, but requires a large amount of energy.

## Classic thermal test

In ISO 230-3, "Test code for machine tools – Part 3: Determination of thermal effects", [1] advised tests are described. To measure the thermal stability of a machine



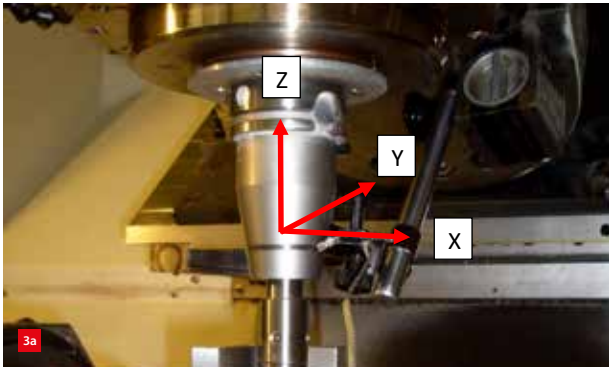
Thermal distortion test on a 'poor' example of a large machine tool.  
(a) Set-up, showing dual masterball and probe nest; X-as is perpendicular to drawing plane, Y-axis is vertical, Z-axis runs into the spindle.  
(b) Thermal distortion (displacement between spindle and table) in X (blue line), Y (green) and Z (red) versus time.  
Drift (within one hour) in X, Y and Z is 8.37, 38.9 and 117  $\mu\text{m}$ , respectively.



## AUTHORS' NOTE

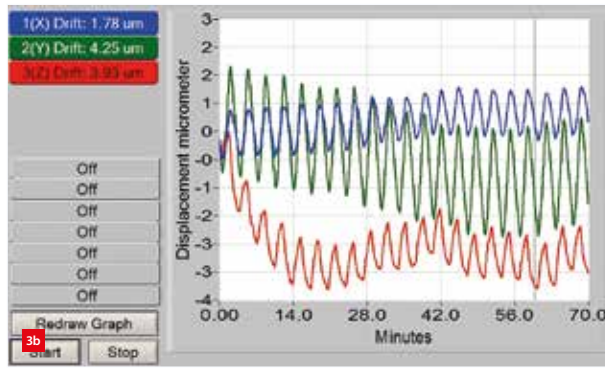
Guido Florussen (senior metrology specialist), Henny Spaan (owner) and Theresa Spaan-Burke (innovation director) all work with IBS Precision Engineering, located in Eindhoven (NL).

burke@ibspe.com  
www.ibspe.com



Thermal distortion test for a milling machine with active cooling.

(a) Set-up, showing orientation of the X-, Y- and Z-axis.



(b) Result (displacement between spindle and table) for 70 minutes, with spindle rotating at 10,000 rpm. Thermal drift is less than 4.25 μm.

tool, a high-precision masterball (roundness error < 25 nm) is placed in the spindle and three capacitance sensors are placed in a probe-nest, mounted rigidly on the machine's workpiece table (Figure 1). The spindle is commanded to execute a constant spindle speed (or a spectrum with variations in speed and interval duration) and the relative displacement of the masterball is recorded in X-, Y- and Z-direction. When five sensors are used in combination with a dual masterball or cylinder, the tilt error around X and Y can also be measured. This ISO test assumes that the dominant heat source is the spindle and ignores heat from the cutting process. During finishing, where the precision is required, cutting depths and forces are typically small. When applying such a test, it is best to simulate the machine's normal operation conditions as well as possible.

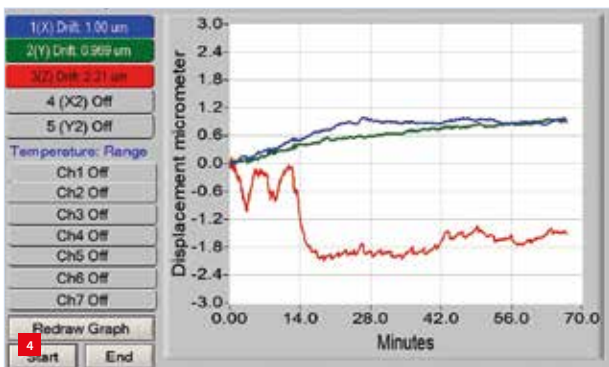
Figure 2 shows a 'poor' example of a large machine tool: the spindle is rotating at its maximum speed of 2,500 rpm and the relative displacement between spindle and table is measured. In this example the thermally induced drift is largest in Z-direction and exceeds 100 μm in less than one hour. This test had even to be stopped to avoid contact between the masterball and the sensor. No thermal correction methods have been used in this machine tool. Figure 3 displays the measured drift of a milling machine used for cutting turbine blades where the spindle is running

at 10,000 rpm for 70 minutes. This machine cools its spindle within 1 °C (wave period is about 3.5 minute) and shows a good thermal stability, with a drift of less than 4.25 μm. The periodic impact of the cooling is clearly visible.

Figure 4 presents an even better example. This can be classified as representative of 'best-in-class' machines on the market. Here a milling machine, used for manufacturing 'smooth-surface moulds', is commanded to execute 42,000 rpm and the measured thermal distortions are recorded. The measured displacement is less than 2.2 μm in Z-direction, and in X- and Y-direction the thermally induced drift is even less than 1 μm. Machines with such good stability are rare and very expensive (> 1 M€) and typically employ multiple thermal correction techniques combined.

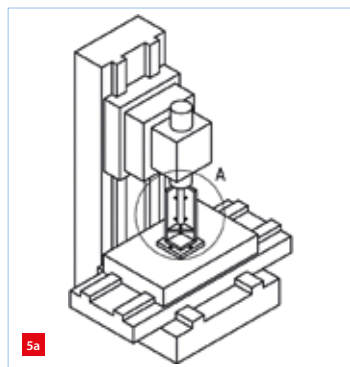
In the tests above, only the spindle is active and the axes do not move. In ISO 10791-10, "Test conditions for machining centres – Part 10: Evaluation of thermal distortions", [2] additional tests are implemented to include moving axes, see Figure 5.

The ISO 230 series covers the test conditions for accuracy measurement of (conventional) machine tools where the ISO 10791 series apply to machining centres, which can execute multiple machining operations; 5-axis machine tools would typically class as machining centres. The approach to thermal tests is the same in both standards.



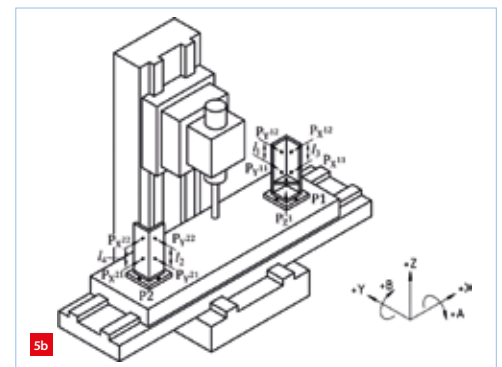
Thermal distortion test result (displacement between spindle and table) for a 'best-in-class' milling machine at 42,000 rpm.

Drift in X (blue), Y (green) and Z (red) is shown over 70 minutes.



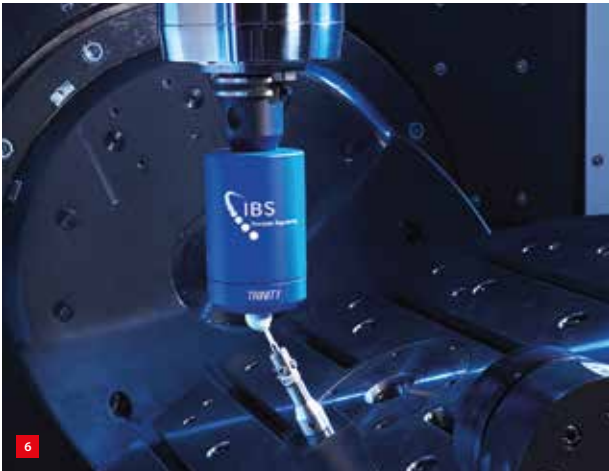
Schematic drawings of ISO 10791-10.

(a) Classic test set-up.



(b) New set-up for which a linear axis is moved between P1 and P2 for a period of time.



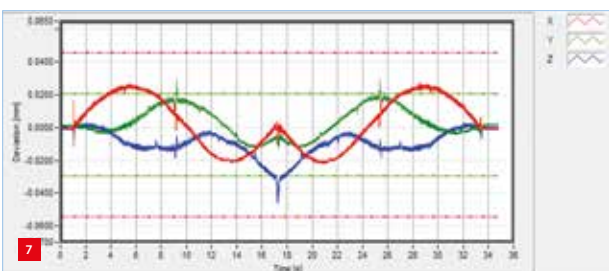


Rotary Inspector set-up: 3D probe in spindle, masterball on the table.

### Using the Rotary Inspector

5-Axis machine tools incorporate linear X-, Y- and Z-drives combined with two rotary tables to allow rotation about two of these axes. Classic thermal distortion tests cannot determine changes in pivot line position and squareness of the rotary axes, relevant for all 5-axis machine tools. IBS Precision Engineering has developed a measurement system dedicated for 5-axis machine tools named Rotary Inspector. The measurement system consists of a Trinity wireless measuring head, comprising three displacement sensors for non-contact measurement, and a precision masterball. The measuring head (probe) is mounted in the spindle and the masterball is placed in a fixed position on the table (Figure 6).

A measurement protocol is implemented which contains three kinematic tests, in line with the ISO 10791-6 requirements for total machine tool accuracy [3]. The machine is first commanded to rotate the first rotary axis (e.g. B-axis) while two linear axes follow (i.e. X and Z), then the same for the second rotary axis (e.g. C-axis) while X and Y follow, and finally all five axes are activated. For this last 5-axis test, the C-axis rotates twice as fast as the B-axis, as prescribed in ISO 10791-6. These tests are executed in approximately 1 minute; where the speed is usually chosen to replicate typical speeds applied during machine operation for production. The kinematic tests capture a snapshot of the machine's accuracy.



Displacement (deviation) in X, Y and Z between Trinity measuring head (representing cutting tool) and masterball (representing workpiece) during synchronised 5-axis motion of linear axes and rotation table (see Table 1).

**Table 1**

Pivot line position and squareness errors of machine A and B rotation axes derived from 3-axis tests.

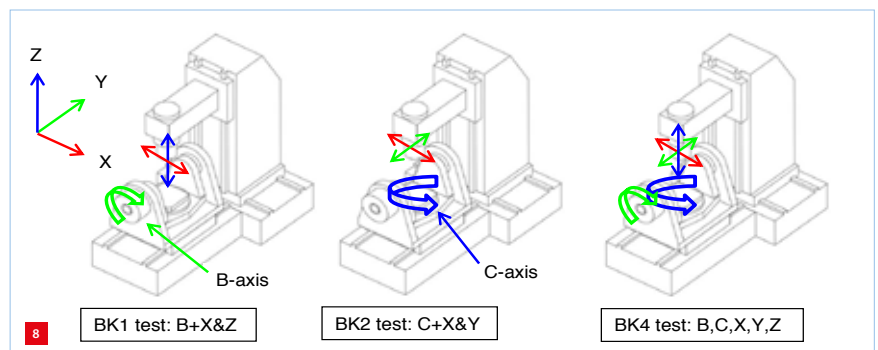
BK1 test (A-axis)		BK2 test (B-axis)	
Pivot line position error	Value (mm)	Pivot line position error	Value (m)
YOA	-0.0037	XOB	-0.0023
ZOA	-0.0157	ZOB	-0.0159
Pivot line squareness error	Value (°)	Pivot line squareness error	Value (°)
COA	0.0002	COB	0.0006
BOA	0.0005	AOB	0.0001

Figure 7 and Table 1 present the results of an example measurement. The 5-axis test result (Figure 7) shows the amplitude of the X-, Y- and Z-direction displacement between the masterball and the probe during the test motion. Where the position of the masterball is determined by the rotary axes and that of the probe by the linear axes. As the masterball represents the contact point of the work-piece and the probe the end of the cutting tool, the smaller these deviations are, the better the machine's precision.

The pivot line position error (or displacement) and the pivot line squareness error of each rotary axis (Table 1) are derived from the 3-axis tests. For the A-axis, the position error of its pivot line in Y-direction is denoted by YOA and in Z-direction by ZOA. The squareness error of the pivot line of the A-axis is described by COA (i.e. rotation around Z-axis) and BOA represents the other squareness error (i.e. rotation around Y-axis). For the B-axis, these parameters are XOB (i.e. pivot line position error in X-direction) and ZOB (i.e. pivot line position error in Z-direction), whereas COB (i.e. rotation around Z-axis) and AOB (i.e. rotation around X-axis) represent the squareness errors of the pivot line. Errors can be corrected directly in the kinematic chain; the results of the 5-axis test can thus be improved.

### Case study DMU machine

The Rotary Inspector system was mounted on a 5-axis machine tool having a B- and a C-axis present at the table. The machine was commanded to continuously execute the corresponding NC file in a loop, moving all axes, see



Schematics of kinematic tests on a 5-axis machine tool with B- and C-axis at the table (see Table 2).



**Table 2**

Programmed motions to heat up a 5-axis machine tool, set in a loop (see Figure 8).

Test name	B-axis angle	C-axis angle	Linear axes
BK1 test	0° > 90° > 0°	0° (idle)	X and Z follow, Y idle
BK2 test	0° (idle)	0° > 360° > 0°	X and Y follow, Z idle
BK4 test	0° > 90°	0° > 180°	X, Y and Z follow
	90° > 0°	180° > 360°	X, Y and Z follow
	0° > 90°	360° > 180°	X, Y and Z follow
	90° > 0°	180° > 0°	X, Y and Z follow

**Table 3**

Pivot line position error of the B-axis during heat-up.

B-axis	XOB		ZOB	
Time $t$ (min)	Value [mm]	Change [ $\mu$ m]	Value [mm]	Change [ $\mu$ m]
0	-0.0177	-	-0.0298	-
5	-0.0186	-0.9	-0.0309	-1.1
30	-0.0227	-4.1	-0.0410	-10.1
<b>Cumulative</b>		<b>-5.0</b>		<b>-11.2</b>

**Table 4**

Pivot line squareness error of B-axis during heat-up.

B-axis	AOB		COB	
Time $t$ (min)	Value [°]	Change [°]	Value [°]	Change [°]
0	-0.0073	-	-0.0091	-
5	-0.0071	0.0002	-0.0091	-
30	-0.0071	-	-0.0100	-0.0009
<b>Cumulative</b>		<b>0.0002</b>		<b>-0.0009</b>

Figure 8 and Table 1. Feed rate was set to 1,500 mm/min. In Table 3 the results are compared between 'cold start', and after 5 and 30 minutes of 'heat-up by moving axes'. During the 30 minutes heat-up the B-axis has moved  $-5.0 \mu\text{m}$  in X-direction and  $-11.2 \mu\text{m}$  in Z-direction. The squareness of the B-axis pivot line to the linear axis was also determined, see Table 4. The rotation of the B-axis pivot line can be neglected as this is less than 1 millidegree.

The Rotary Inspector measurement data obtained can also be analysed using Rotary Analyzer software, showing best-fit

circles in the XZ-plane for the B-axis (see Figure 9a) and in the XY-plane for the C-axis (see Figure 9b). As the machine was commanded to execute a relative circle with 0.2 mm radius (between a rotary axis and the circular path of two linear axes), measurement data is distributed on a circle.

A perfect machine would show a concentric circle with 0.2 mm radius. Any deviations are representative of errors in the alignment of the rotary axis path to the linear axes or vice versa. The B-axis was measured with the BK1 test (see Table 2 and Figure 8); the measurement was performed twice, at  $t = 0$  and  $t = 30$  min. The C-axis was measured with the BK2 test (also at  $t = 0$  and  $t = 30$  min). Due to the drift of the total machine, the centre point of both the B- and C-axis in Figure 9 has moved. This has resulted in a different circular path as shown in both graphs; blue is the circular path for  $t = 0$  (cold machine) and red is the path for  $t = 30$  min (warm machine).

With the thermal errors measured, these can be automatically compensated. Such automation has been implemented at IBS for Siemens and Heidenhain machine controllers. With Siemens, for example, errors are corrected using the Siemens VCS (Volumetric Compensation System) application. For the Taiwanese market, a compensation module has been implemented that links to their smart machine platform, Productivity 4.0.

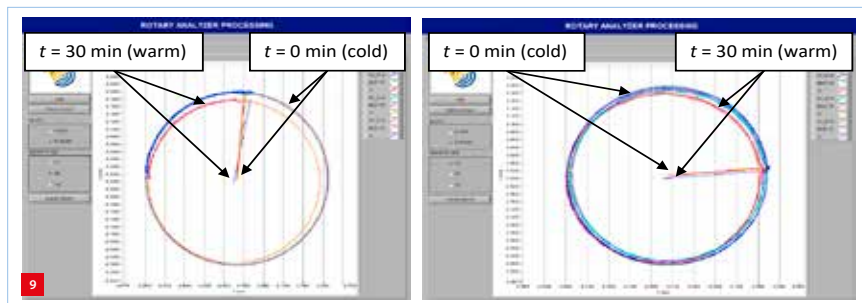
## Summary

Thermal tests are considered as rather expensive because of the considerable machine down time. The thermal stability of 5-axis machine tools can vary a lot; from a few micrometres to more than one hundred micrometres. Besides the spindle also the machine's axes are moved in the latest standardised thermal machine tool tests to heat-up a machine. Measures to control and limit the machine's thermal distortion are applied more and more in industry and this trend is expected to continue in the next decade as it improves the machine's accuracy and stability significantly.

When calibrating a machine tool, its thermal behaviour should be considered for best accuracy. This means that heat-up cycles should be applied when testing a machine tool, representing its normal use better. Upon implementation of the fast and accurate 3D thermal test procedure presented in this article, high-precision machines should be able to achieve sub-micron thermal stability whereas the large, general-purpose machines may be expected to have a thermal stability in the order of  $20 \mu\text{m}$ .

## REFERENCES

- [1] ISO 230-3, "Test code for machine tools – Part 3: Determination of thermal effects", second edition, 2007.
- [2] ISO 10791-10, "Test conditions for machining centres – Part 10: Evaluation of thermal distortions", first edition, 2007.
- [3] ISO 10791-6, "Test conditions for machining centres – Part 6: Accuracy of speeds and interpolations", second edition, 2014.



Analysis results for the DMU machine.

- (a) B-axis (XZ-plane).  
(b) C-axis (XY-plane).

# ADVANTAGES OF SUBSTRATE-MASTERED SCALES

**In precision laser machining processes, local air temperature fluctuations can cause a part to fall out of tolerance. A remedy is to provide linear encoder systems with mastered scales mounted on a substrate material with relatively high thermal mass, to enable effective thermal error compensation. Advantages of mastered scales include simplification of thermal compensation regimes, elimination of scale disturbance error and the potential for reduction of non-repeatable measurement errors.**

A linear encoder consists of a position measurement readhead device paired with a scale (an accurately marked ruler). The readhead measures position by optically sensing the regularly-spaced scale markings and outputs this information as an analogue or digital signal. The signal is subsequently converted into a position reading by a digital readout or motion controller. Linear encoder scales can be many meters long and are, therefore, sensitive to thermal changes.

The thermal behaviour of the encoder scale is an important consideration when selecting any encoder system. Encoder scales can effectively be either thermally independent of the substrate (floating) or thermally dependent on the substrate (mastered). Floating scale expands and contracts according to the thermal characteristics of the scale material, whereas mastered scale expands and contracts at the same rate as the underlying substrate.

A useful measure of the performance of a floating scale is disturbance, which is the difference in length between a theoretical perfectly floating scale and the actual scale. This positional error of the end of the scale is caused by the mounting method partially coupling the expansion of the scale with the expansion of the substrate. Disturbance is not usually significant for short scale lengths but can increase substantially for longer scale lengths.

## Selection considerations

There are a number of applications where mastered scales are favoured [1]. These include:

- When the co-ordinate system of the machine rather than absolute position is desired, such as when moving to a workpiece that is located at a fixed position on the bed of the machine.

- When the CTE (coefficient of thermal expansion) of the workpiece closely matches the CTE of the machine substrate and the two are kept at the same temperature, the expansions of the scale and workpiece are closely matched. Therefore, any length change of the substrate, at a given temperature, is automatically compensated by an equivalent length change of the scale.
- When the machine axis is long, the uncertainties associated with mastered scale do not increase with length whereas with floating scale they do significantly increase with length.
- If the substrate has low thermal conductivity and a high thermal mass (for example, a thick piece of granite), short-term fluctuations in air temperature will cause minimal substrate temperature change and low expansion of the substrate and therefore it may be acceptable to ignore these short-term temperature changes. However, it is important to note that longer-term changes in temperature must still be considered. These may be harder to measure appropriately as it is the average substrate temperature that is important. Therefore, more direct length measurements, such as periodically comparing against a known standard, may be more appropriate.

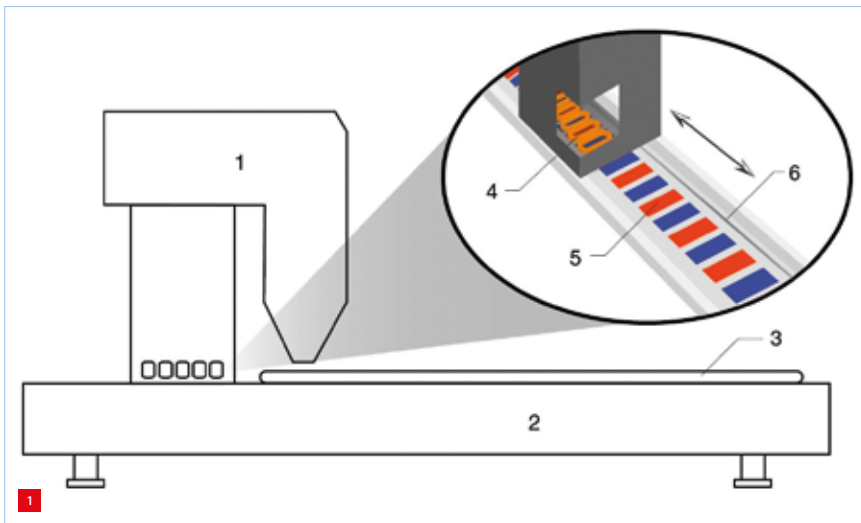
## Laser cutting

CNC laser cutting machines are commonly used to cut sheet or plate metals including stainless steel, carbon steel, copper and aluminium. Commercial laser cutting machines typically cut metal with thicknesses of 1 to 20 mm using a fibre laser source with power in the 1 to 10 kW range. These machines comprise a CNC motion system with linear motors on the X- and Y-axes, a beam collimator and a cutting head, as shown in Figure 1. The laser cutting head also includes focusing optics and an assist gas nozzle that aids the cutting process.

### EDITORIAL NOTE

This article was based on a press release by Renishaw, a global, high-precision metrology and healthcare technology group.

[www.renishaw.com](http://www.renishaw.com)



Elevation view of a laser cutting machine.  
 (1) Laser cutting head and gantry shoulder.  
 (2) Machine bed.  
 (3) Metal plate blank.  
 (4) Motor drive coils.  
 (5) Permanent magnet stator.  
 (6) Encoder scale.

Sheet metal is loaded onto a large machine bed (e.g. 3.2 m x 20 m). Each sheet is supported by rows of metal teeth that support the workpiece and allow the scrap metal to fall away. The laser head is attached to a carriage that moves along a gantry (X-axis) and both shoulders of the gantry are driven along the Y-axis by two linear motors. Dynamic Z-axis control with a linear induction motor is typically required for precise beam focusing. Linear encoders are installed on the X-, Y- and Z-axes and provide position feedback to the CNC controller.

Heat build-up during precision laser cutting is highly localised, and the heat dissipates quickly such that the average workpiece temperature is approximately equal to the air temperature.

### Application example

Laser metal cutting is an industrial process that takes place in a factory where the air temperature is likely to fluctuate over time (for example, due to an air conditioning cycle). Air temperature changes cause expansion/contraction of the encoder scale, which combines with scale disturbance to generate a significant positioning error. This could lead to an out-of-tolerance finished part which needs to be reworked or scrapped.

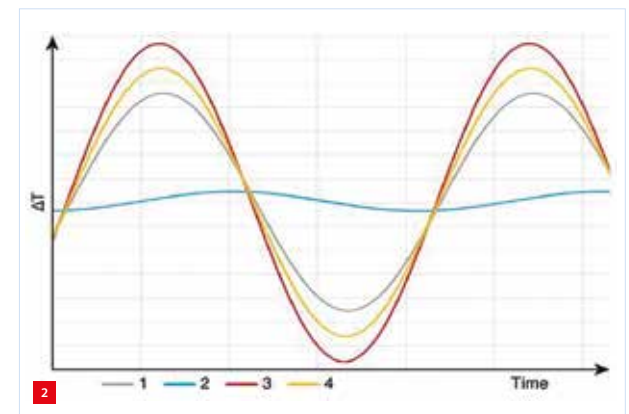
A fibre laser cutting machine is used to cut, using the same cutting path, a series of plate steel blanks (2 m x 2 m x 2 mm) arranged in rows along the machine's longitudinal axis. Air temperature fluctuations make direct temperature compensation challenging, particularly for a 20 m axis, as shown in Figure 2. In this case, the machine's longitudinal and gantry axes have significant thermal mass and maintain a near constant average temperature, and therefore size, throughout the cutting process.

An enhanced metrology solution would be to use a linear encoder with a substrate-mastered scale for motion control in the plane of the machine bed, along both the X- and Y-axes. Thermal expansion of the encoder scale and the machine axis would then be closely matched, which removes the need for active compensation of the scale. Laser position accuracy is further improved because scale disturbance is not significant for this system.

The effect of long-term air temperature changes on the workpiece could be compensated by machining a calibration part at regular intervals to provide a coarse offset correction. This correction remains valid for a long time due to the high thermal mass of the machine substrate, which maintains a relatively constant average temperature and ensures dimensional stability of the scale throughout the cutting process.

### REFERENCE

[1] [www.renishaw.com/en/optical-encoders-white-papers--10133](http://www.renishaw.com/en/optical-encoders-white-papers--10133)



Thermal environment of an encoder scale mounted on a large machine axis.  
 (1) Temperature of the encoder scale.  
 (2) Bulk temperature of the machine axis.  
 (3) Fluctuating ambient air temperature.  
 (4) Measured (e.g. with a thermocouple) scale temperature.

# VISCOELASTIC (OVER)CONSTRAINING

Flexure mechanisms are commonly designed to be exactly constrained to promote deterministic behaviour, yet at the expense of limitations on parasitic eigenfrequencies and support stiffness. This article presents the use of viscoelastic material for providing additional stiffness in a certain frequency range without the indeterminism commonly associated with overconstraining. This design principle of dynamically stiffened exact-constraint design is exemplified by a parallel leafspring mechanism, employing a custom-synthesised elastomer compound to compensate for unintended misalignments, without significant internal stress build-up, while improving the dynamic performance.

SVEN KLEIN AVINK, MARIJN NIJENHUIS, WILMA DIERKES, JACQUES NOORDERMEER AND DANNIS BROUWER

## Introduction

To ensure deterministic behaviour, flexure mechanisms are typically designed to be exactly constrained [1-4]. This mitigates the problems of overconstrained designs: if very tight tolerances are not met, misalignment errors and temperature gradients can lead to internal forces that compromise system behaviour, repeatability and predictability. While generally avoided, overconstrained flexure mechanisms can offer better dynamic performance (i.e. higher parasitic eigenfrequencies).

To exploit these benefits and simultaneously avoid the problems of overconstrained designs, a new class of flexure mechanisms is investigated in which overconstraints are applied by means of viscoelastic material. Since the effective stiffness of the viscoelastic material is frequency-dependent, the design can be tuned in such a way that the overconstraint is only present in a designed frequency range.

As a consequence, static loads, e.g. due to misalignment errors, for which the exactly constrained behaviour is desired, will hardly affect the mechanism. For dynamic loads, for which the overconstrained behaviour is desired, the effective stiffness and the first parasitic eigenfrequency will be higher, improving aspects such as control bandwidth and tracking error.

In the literature, various publications on the merits and problems of overconstrained flexure mechanisms can be found. The effects of misalignments on stiffness, eigenfrequency and buckling have been investigated for a single-overconstraint parallel flexure mechanism, a single-overconstraint cross-hinge mechanism, and a triple-overconstraint four-bar mechanism [5-7].

The potential of overconstrained mechanisms for higher performance has been investigated as an alternative design paradigm, referred to as elastic averaging [8]. The use of viscoelastic material for providing passive damping in mechatronics systems has been investigated [9-10]. To the authors' knowledge, there are no earlier publications on the use of viscoelastic material for applying constraints in flexure mechanisms in order to mitigate problems normally associated with overconstrained designs.

In this article, a single-overconstraint parallel flexure mechanism is used as a case study to demonstrate the concept, without delving into practical applications. The formulation of a custom-synthesised elastomer is detailed. It has been designed for the purpose of improving the (high-frequency) dynamic performance and decreasing the sensitivity to (low-frequency) misalignment errors. Measurements on a dedicated demonstrator set-up with controllable misalignment show how these performance attributes vary for the exactly constrained, the conventionally overconstrained, and the viscoelastically constrained case (also referred to as the dynamically stiffened case). Simulations with a numerical model corroborate the measurements.

## Methodology

### Description of mechanism

A parallel flexure mechanism, consisting of two nominally identical and parallel leafsprings with a connecting shuttle, serves as the case study. This mechanism is considered to have one degree of freedom (DoF), a translation of the shuttle in the  $x$ -direction of Figure 1, on account of the low stiffness in that direction. Motion of the shuttle in all other directions is associated with a much higher stiffness and considered to be constrained.

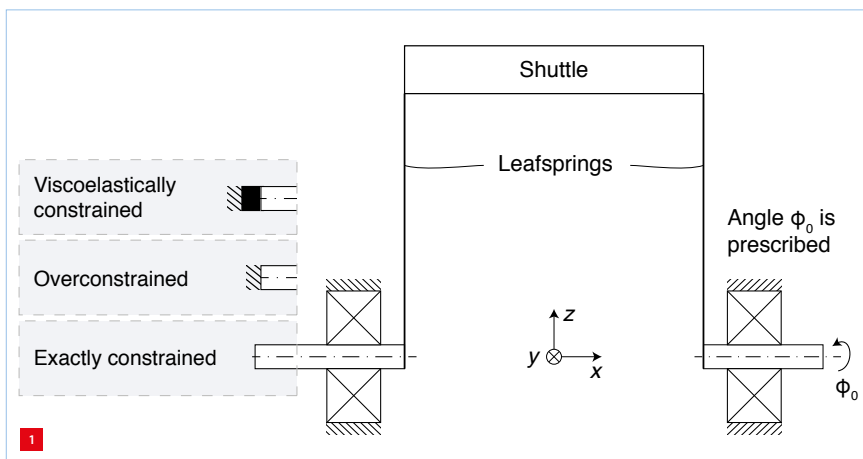
## AUTHORS' NOTE

Sven Klein Avink, recipient of the Wim van der Hoek Award 2019, graduated in the chair of Precision Engineering of the Faculty of Engineering Technology at the University of Twente, Enschede (NL). Currently, he is a project engineer at MCA linear motion robotics in Varsseveld (NL).

Marijn Nijenhuis (assistant professor) and Dannis Brouwer (professor) are members of the chair of Precision Engineering. Wilma Dierkes (associate professor) and Jacques Noordermeer (professor) are in the chair of Elastomer Technology and Engineering at the same faculty.

svenkleinavink@hotmail.com  
www.utwente.nl/en/et/ms3/  
research-chairs





Schematic front view of a parallel flexure mechanism in three configurations. A controllable misalignment fixes angle  $\phi_0$  in three configurations.  
 (1) Exactly constrained, with the additional flexure hinge (on the left) removing the overconstraint.  
 (2) Overconstrained, with both leafsprings clamped at the base.  
 (3) Viscoelastically constrained, with a custom elastomer placed in parallel to the left hinge.

In the conventionally overconstrained case, both leafsprings are clamped at the base. In this way, both leafsprings constrain the rotation of the shuttle around its longitudinal axis (the rotational  $x$ -axis), leading to indeterministic behaviour, since a small misalignment angle at the base (indicated by  $\phi_0$ ) can induce large internal loads that affect stiffness and eigenfrequency.

In the exactly constrained case, this is remedied by the use of an additional flexure hinge, which removes the redundant constraint. Only one leafspring now constrains the longitudinal rotational motion of the shuttle around the  $x$ -axis, meaning that a misalignment angle at the base principally induces a compensating rotation of the flexure hinge, almost without any internal load and no change in system behaviour.

This particular case study has been designed to demonstrate the difference between the overconstrained and exactly constrained case. Owing to the specific location of the flexure hinge, the system's first parasitic eigenfrequency (corresponding with the second eigenfrequency) is higher by a factor of approximately two in the overconstrained case. Since this frequency typically limits the attainable bandwidth or vibration isolation, it shows that the overconstrained system exhibits higher dynamic performance.

In the new dynamically stiffened exactly constrained case (viscoelastically constrained case), a custom elastomer is placed in parallel to the flexure hinge. It allows misalignments (by providing only low stiffness) while increasing the first parasitic eigenfrequency (by providing high stiffness), on the basis of a clear distinction in the frequency range in which these two seemingly conflicting attributes are desired.

**Table 1**

Elastomer compound formulation (PHR is parts per hundred rubber).

Component	PHR
SBR	137.5
Carbon black N339	50
Zinc oxide	4
Stearic acid	1
TMQ <sup>1</sup>	1.5
CBS <sup>2</sup>	2
Sulphur	15

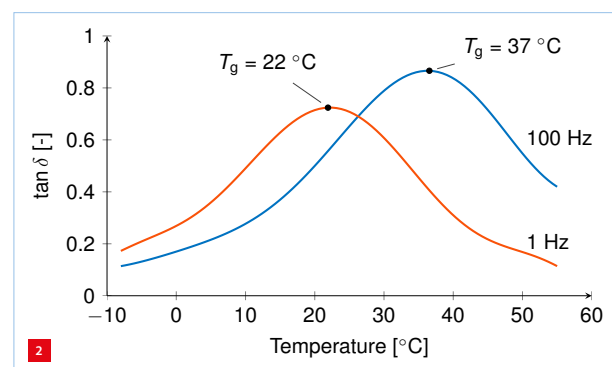
<sup>1</sup> TMQ is polymerised 2,2,4-trimethyl-1,2-dihydroquinoline.

<sup>2</sup> CBS is N-cyclohexyl benzothiazole sulfenamide.

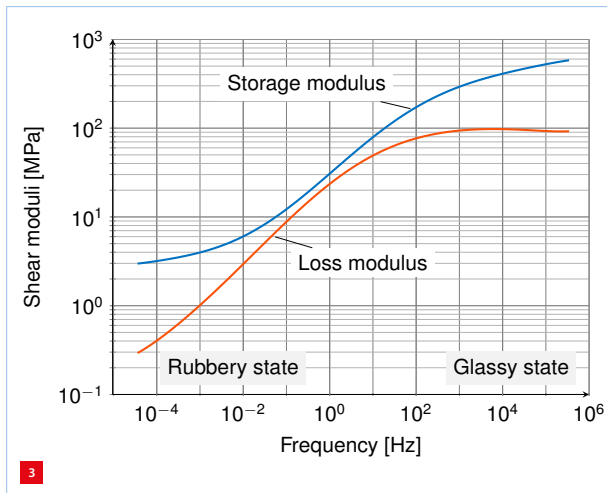
### Elastomer compound formulation

The viscoelastic behaviour of polymers is used to apply high stiffness in only a limited frequency range. The temperature- and frequency-dependent glass transition that polymers exhibit is exploited: the rubbery state is used for misalignment compensation at low frequencies and the glassy state for a stiffness increase at high frequencies. For this application, it means that at operating temperature (20 °C), the transition from rubber to glass should occur just before the first parasitic eigenfrequency. The formulation of a custom-synthesised elastomer compound satisfying these requirements is presented in this work.

Solution-polymerised styrene-butadiene rubber (S-SBR SE6233 from Sumitomo Industries, 37.5 parts per hundred rubber (PHR) oil extended) is used as the base polymer in the formulation. It is a synthetic rubber with a high styrene content (40% by mass) resulting in a glass transition temperature of -2 °C. The material is compounded according to the formulation given in Table 1. With a relatively high sulphur content and long vulcanisation time of 50 minutes (increasing the cross-linking density), a higher glass transition temperature is obtained.



Glass transition temperature as indicated by the maximum of  $\tan(\delta)$ .



Shear moduli (storage and loss) of the elastomer compound at 20 °C.

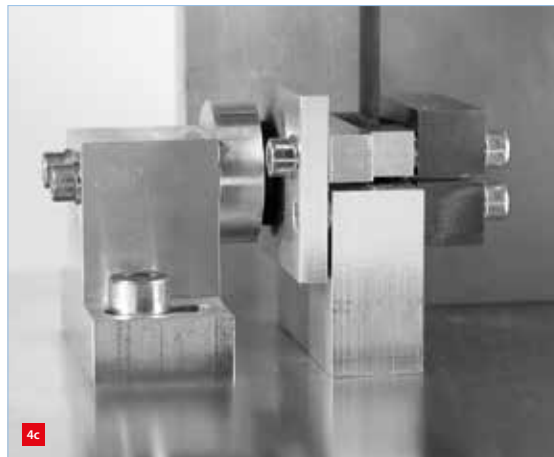
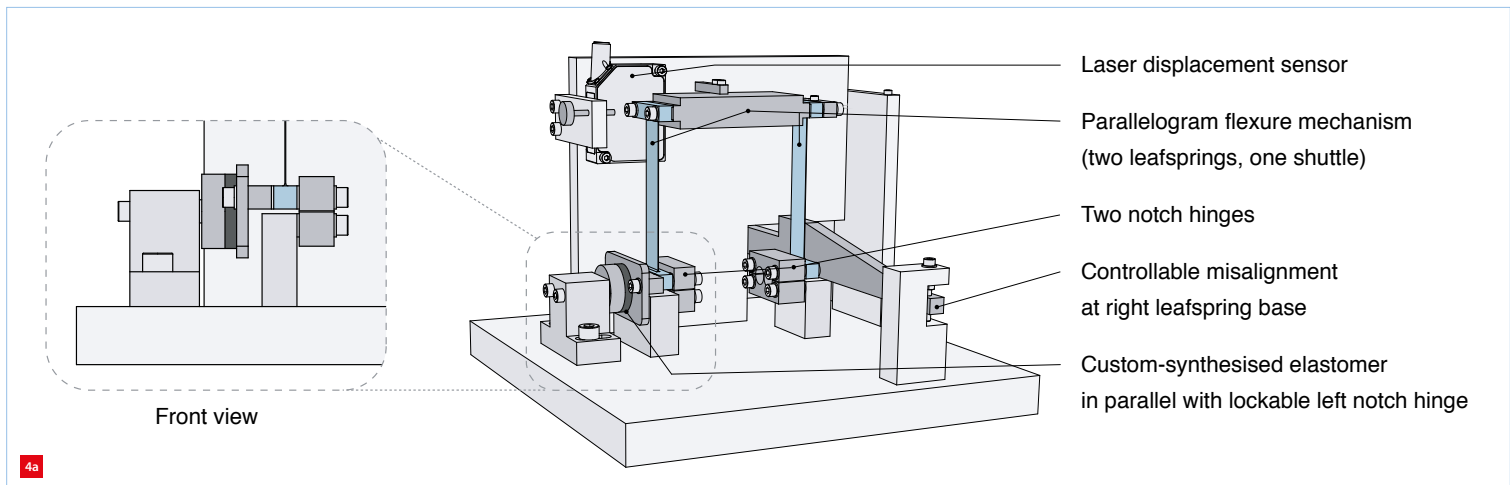
The compound is characterised by means of the results from dynamic mechanical analysis (DMA), in terms of shear moduli and  $\tan(\delta)$ . The latter is the so-called loss factor, representing the ratio between the loss (viscous) and the storage (elastic) modulus of the material. Here, the storage modulus measures the stored energy,

representing the elastic characteristic of the material; and the loss modulus measures the dissipated energy, representing the viscous portion of the material.

Figure 2 shows the glass transition temperature for frequencies of 1 Hz and 100 Hz, as the maximum of the  $\tan(\delta)$  curve. It follows that at operating temperature, the compound is in the transition state at 1 Hz and in the glassy state at 100 Hz. Figure 3 shows the master curves of both shear moduli (storage and loss) as a function of frequency for a single reference temperature of 20 °C. These curves were obtained from measurements over a limited frequency range at various temperatures, in accordance with the time-temperature equivalence by using the closed-form t-T-P shifting algorithm [11].

#### Experimental set-up

Figure 4 shows the measurement set-up. It has a screw for controlling the misalignment angle and a dial gauge on the back (not visible) for measuring the misalignment. The base plate, misalignment arm and other frame parts that carry loads are dimensioned such that parasitic compliances are

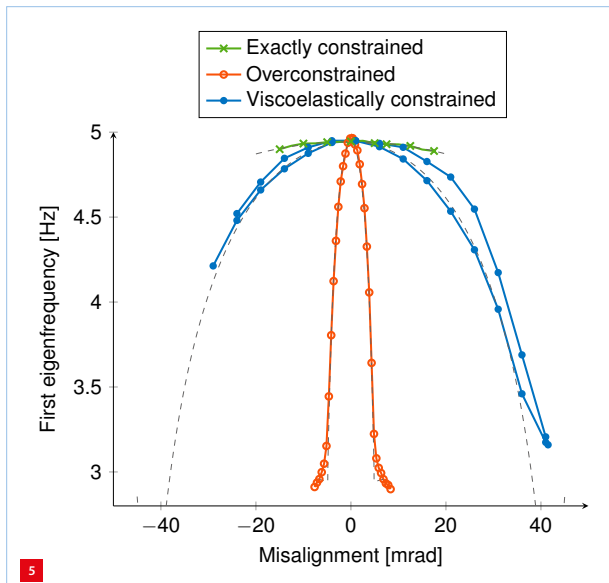


Experimental set-up of the parallel flexure mechanism.

(a) Schematic.

(b) Realisation, overview.

(c) Realisation, close-up of front view.



Measurement (solid lines) and simulation (dashed lines, without symbols) of the first eigenfrequency.

negligible. The leafsprings with support fillets at the ends are made of a single piece of material (Stavax stainless steel, AISI 420) by wire-EDM to avoid clamping of the leafsprings and the associated micro-slip hysteresis. The leafsprings have a nominal length of 100 mm, width of 20 mm, thickness of 0.35 mm. Young's modulus is 200 GPa, the Poisson ratio is 0.29, and the density is 7,700 kg/m<sup>3</sup>. Optimisation of the dimensioning and fastening of the elastomer element is outside the scope of this investigation, as is ageing. The left notch hinge in Figure 4 serves as the flexure hinge that can remove the redundant constraint; the right notch hinge serves to guide the misalignment arm.

The first eigenfrequency of the system, corresponding to a mode in which the shuttle moves in its DoF, serves as a measure of the misalignment sensitivity of the system, since it is affected strongly by the internal load that develops in the overconstrained case. The first eigenfrequency is measured by a laser displacement sensor.

The second eigenfrequency of the system, corresponding to a mode in which the shuttle moves in the  $y$ -direction of Figure 1, is the performance-limiting first parasitic eigenfrequency. It is measured by accelerometers (not visible) on the shuttle. For measurement of the second eigenfrequency by means of modal impact testing using a cabled sensor, excessive motion of the shuttle in its DoF has to be avoided. Therefore, an additional wire constraint is imposed, which does not introduce any significant stiffness in the measurement direction.

#### Numerical model

Simulations of the system are carried out in the flexible multibody software program SPACAR [12]. Each leafspring

is modelled by eight flexible three-dimensional beam elements that capture the linear and geometrically nonlinear effects associated with bending, shear, torsion, elongation, and warping [13]. The material characterisation from the DMA test is used as the constitutive relation for the elastomer compound model. A standard Kelvin-Voigt model is used with coefficients given by the measured storage and loss modulus as functions of frequency from Figure 3.

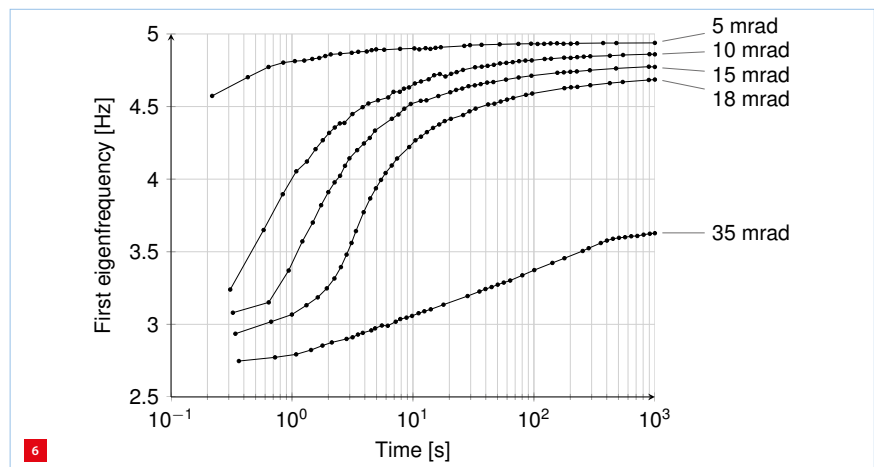
#### Results

Figure 5 shows the first eigenfrequency as a function of the misalignment angle. For all three cases, the measurement and simulation results match well. As has been reported before for the conventionally overconstrained case [5], it can be seen that the first eigenfrequency decreases strongly with misalignment. At only 5 mrad, the internal load exceeds the critical load, indicating that stiffness is lost and the mechanism has buckled.

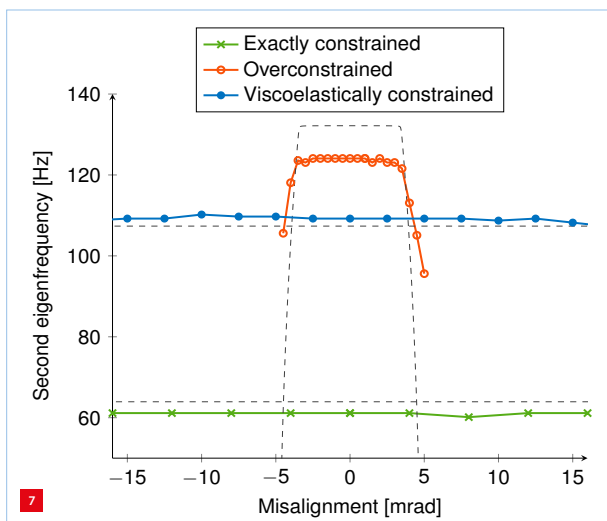
In the exactly constrained case, the first eigenfrequency hardly decreases with misalignment. The small decrease that is observed in both the experiment and the simulation is due to the small but finite stiffness of the notch hinge in the set-up causing just a small internal load.

In the new viscoelastically constrained case, a minor decrease in eigenfrequency is observed, indicating the desired low sensitivity to misalignment. In the experiment, the system behaviour at a maximum possible misalignment angle of 15 mrad (three times the overconstrained value) is largely unaffected. Measurements have been taken up to a positive misalignment value of 42 mrad without bifurcation, suggesting that the new viscoelastically constrained case has a critical misalignment that is at least eight times larger than the overconstrained case.

The eigenfrequencies are measured going from the stress-free state of zero misalignment to maximum positive misalignment,



Measurement (for various values of the misalignment angle) of the change in the first eigenfrequency over time, indicating stress relaxation.



Measurement (solid lines) and simulation (dashed lines, without symbols) of the second eigenfrequency.

then to maximum negative misalignment, and back to zero. Successive measurements are performed every two minutes. At the first maximum positive and negative misalignment measurement, the wait time is ten minutes; due to stress relaxation, the frequency then increases slightly and a loop in the frequency plot is observed, as witnessed by the two solid blue lines in Figure 5.

To measure the time scale at which internal stresses (caused by misalignment) decrease in the viscoelastically constrained case, a large misalignment of 15 mrad (three times the critical value of the overconstrained case) is applied quickly. Initially, this causes buckling of the mechanism. In this state, the free vibration of the shuttle, due to an excitation in the first natural mode, is recorded. The change of the first eigenfrequency over time, due to stress relaxation of the elastomer compound, is shown in Figure 6. It can be seen that 60% of the decrease in eigenfrequency is recovered within 10 seconds.

Figure 7 shows the second eigenfrequency as a function of the misalignment. For all three cases, the measurement and simulation results match within 6%. It is observed that the second eigenfrequency (the first parasitic eigenfrequency) in the overconstrained case (124 Hz) is a factor of 2.0 higher than in the exactly constrained case (61.1 Hz). Compared to the exactly constrained case, the new viscoelastically constrained case has an eigenfrequency of 109 Hz, which is a factor of 1.8 higher than the exactly constrained case. This clearly shows the improvement in dynamic performance over the exactly constrained case.

Also, failure of the overconstrained mechanism due to excessive misalignment can be observed: at the critical misalignment angle of 5 mrad, the second eigenfrequency drops rapidly. The viscoelastically constrained case does not show any effect of misalignment in the entire measured range.

## Conclusion

Measurements and simulations of a demonstrator set-up of a parallel flexure mechanism with a custom-synthesised elastomer compound have shown that:

- the first parasitic eigenfrequency goes from 61.1 Hz, without the viscoelastic overconstraint, to 109 Hz, with the viscoelastic constraint; this is close to the high value that can be achieved with a conventionally overconstrained design (124 Hz);
- the critical misalignment angle, at which buckling occurs and the mechanism no longer functions, goes from only 5 mrad, for the conventional overconstraint, to at least 42 mrad, for the viscoelastic overconstraint.

The measurements have been corroborated by a numerical nonlinear multibody analysis combined with DMA (dynamic mechanical analysis) test results of the elastomer compound. The results show that viscoelastic material can be used to significantly increase the dynamic performance of (flexure) mechanisms, while being tolerant to misalignments. Full details, including a detailed explanation of the elastomer and an extensive mathematical model, can be found in [14].

## REFERENCES

- [1] Slocum, A.H., *Precision Machine Design*, Prentice-Hall, Englewood Cliffs, 1992.
- [2] Smith, S.T., *Flexures: Elements of Elastic Mechanisms*, CRC Press, 2000.
- [3] Koster, M.P., *Constructieprincipes voor het nauwkeurig bewegen en positioneren* (Dutch), Twente University Press, 2000.
- [4] Schellekens, P., Rosielle, N., Vermeulen, H., Vermeulen, M., Wetzels, S., and Pril, W., "Design for Precision: Current Status and Trends", *CIRP Annals*, 47, pp. 557-586, 1998.
- [5] Meijaard, J.P., Brouwer, D.M., and Jonker, J.B., "Analytical and experimental investigation of a parallel leaf spring guidance", *Multibody System Dynamics*, 23, pp. 77-97, 2010.
- [6] Van de Sande, W.W.P.J., Aarts, R.G.K.M., and Brouwer, D.M., "Effects of misalignments on the static and dynamic behaviour of a multiple overconstrained compliant 4-bar mechanism", *Precision Engineering*, 60, pp. 143-151, 2019.
- [7] Nijenhuis, M., Meijaard, J.P., and Brouwer, D.M., "Misalignments in an overconstrained flexure mechanism: A cross-hinge stiffness investigation", *Precision Engineering*, 62, pp. 181-195, 2020.
- [8] Awtar, S., Shimotsu, K., and Shiladitya, S., "Elastic Averaging in Flexure Mechanisms: A Three-Beam Parallelogram Flexure Case Study", *J. Mechanisms and Robotics*, 2, 041006, pp. 1-12, 2010.
- [9] Aangenent, W.H.T.M., Koorneef, L.F., Ruijl, Th.A.M., Van den Berg, S.C.J.M., Van der Meulen, S.H., van Eijk, J., Wullms, P.H.G., and Van Lieshout, R.H.A., "Stage positioning system and lithographic apparatus", US Patent no. 9,897,926 B2, 2018.
- [10] Ruijl, Th.A.M., and Wullms, P., "Polymer damper technology for improved system dynamics", *Proceedings of the 19th euspen International Conference*, pp. 538-541, 2019.
- [11] Gergesova, M., Zupančič, B., Saprunov, I., and Emri, I., "The closed form t-T-p shifting (CFS) algorithm", *J. Rheology*, 55, pp. 1-6, 2011.
- [12] Jonker, J.B., and Meijaard, J.P., "SPACAR – Computer Program for Dynamic Analysis of Flexible Spatial Mechanisms and Manipulators", pp. 123-143 in Schiehlen, W. (ed.), *Multibody Systems Handbook*, Springer-Verlag, Berlin, 1990.
- [13] Jonker, J.B., and Meijaard, J.P., "A geometrically non-linear formulation of a three-dimensional beam element for solving large deflection multibody system problems", *J. Non-Lin. Mechanics*, 53, pp. 63-74, 2013.
- [14] Nijenhuis, M., Klein Avink, S.T.B., Dierkes, W.K., Noordermeer, J.W.M., and Brouwer, D.M., "Improved dynamic performance in flexure mechanisms by overconstraining using viscoelastic material", *Precision Engineering*, 63, pp. 115-125, 2020.



# A LIGHT-GUIDED ACTUATOR

In actuators, many kinds of physical effects can help to create motion – and organic chemistry can contribute as well. This is what researchers from the Chemistry Engineering department at Eindhoven University of Technology (TU/e, NL) have done by using liquid crystalline polymers to construct small robots. The motion of the liquid crystalline networks can be controlled by visible light thanks to the integration of azobenzene molecules. These light-driven robots can walk and transport low-weight cargos.

FRANS ZUURVEEN

These days we are very familiar with liquid crystals, because the most widely used pixel material in our TV sets consists of an assembly of liquid crystalline molecules. Triggered by an on/off switchable electrical voltage they are able to transmit or block light. In our 'picture on the wall' TV set light from behind the display enters a colour filter first and then a tiny pixel, thus providing a coloured point-like TV image element.

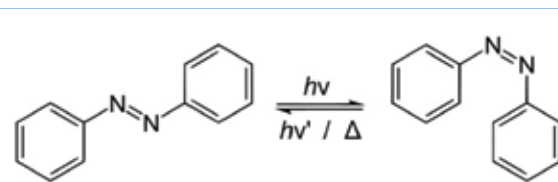
The liquid crystalline (LC) molecules in the soft actuator presented here function in a different way. In the applied material they have an elongated (rod-like) anisotropic shape. These molecular rods can be organised in oriented configurations, pointing parallel or perpendicular to the surface of thin actuator films. Figure 1 shows the 'splay' orientation, as applied by the TU/e chemists [1]. When organised in such a way, this anisotropic orientation can be 'frozen in' by polymerisation of the rod-like molecules, resulting in an aligned polymer film.

## Incorporating azobenzene

Azobenzene is a rather well-known base for many kinds of dyes, called chromophores, used to colour fabrics, for example. The reasons for incorporating azobenzene chromophores into the polymerised LC network, as according to Figure 1, is that they can exhibit light-induced chemical changes in their molecular structure. They can assume a different spatial configuration of atoms in two molecular structures, called isomers, which have the same chemical formula.



Side view of the 'splay' orientation of liquid crystal (LC) molecules in an LC network.



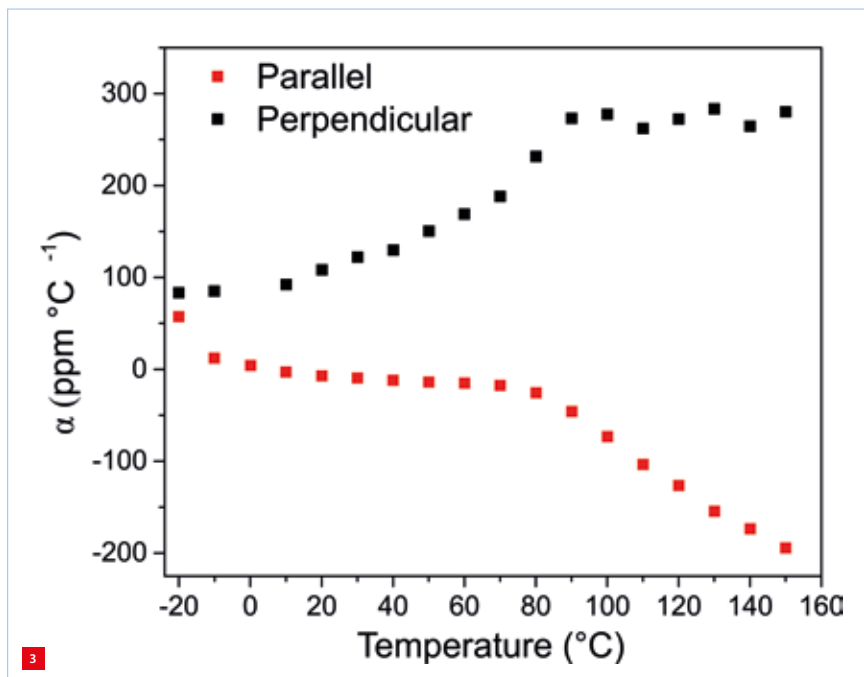
Isomerisation of azobenzene,  $C_{12}H_{10}N_2$ . Absorption of a light quantum  $h\nu$  induces the configuration of two phenyl groups connected by double-bonded nitrogen atoms to change from trans to cis. This isomeric conversion can be reversed by absorption of a lower-energy light quantum ( $h\nu' < h\nu$ ) or by slow thermal relaxation ( $\Delta$ ).

In azobenzene ( $C_{12}H_{10}N_2$ ) this effect originates from the connection of two phenyl groups by double-bonded nitrogen atoms (see Figure 2). With its structural formula  $C_6H_5-N=N-C_6H_5$  two spatial structures (isomers) of the azobenzene molecule are possible: a cis-configuration with the two phenyl group on one side of the  $N=N$  bond or a trans-configuration with these two group on opposite sides. Upon illumination with UV light, the azobenzene molecules will absorb the light and change their configuration from trans to cis. This isomeric conversion can be reversed, from cis back to trans, by absorption of (lower-energy) blue light – spontaneous (thermal) cis-to-trans relaxation is slow in azobenzene molecules.

However, some azobenzene chromophores exhibit fast thermal relaxation. In that case, illuminating the polymer film will result in the release of heat. Due to the molecular order of LC polymers, an increase in temperature leads to an overall contraction of the molecular volume parallel to the long axis of the rod-like LC molecules and a volumetric expansion in the perpendicular direction. By orienting the LC polymer in molecular alignments such as splay (Figure 1), these molecular volume changes can be magnified to macroscopic deformation. In a splay alignment, molecules are oriented either parallel or perpendicular to the polymer film surface. This then results in overall thermal expansion and contraction properties that are different on both sides, bottom and top, respectively (see Figure 3).

## AUTHOR'S NOTE

Frans Zuurveen, former editor of Philips Technical Review, is a freelance writer who lives in Vlissingen (NL).

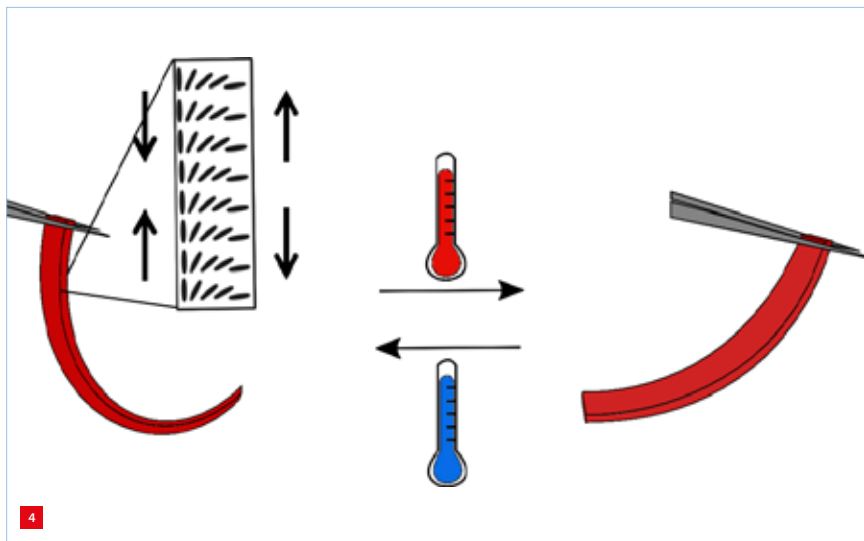


Measurement of different relative elongations as a function of temperature for the LC molecules' parallel and perpendicular orientation (with respect to the polymer film surface).

Figure 4 shows the resulting actuation of a splay-aligned LC polymer upon exposure to heat.

Note, for sake of completeness:

The mechanism underlying this phenomenon as described above is designated as photothermal. Depending on the properties of the chromophores applied, in other cases the dominant mechanism may be photomechanical by nature, originating from mechanical deformations due to the trans-cis conversion [2-3].



Opposite bending configurations of the chemical actuator with splay-oriented LC molecules under different illumination conditions (red = on, blue = off). The bending is actually caused by heat production, the arrows indicating either heat-induced contraction (left) or expansion (right) of the polymer film surface.

### Precision engineering

We will not go into the details of the chemical procedures involved in reaching an azobenzene-integrated LC network. Some aspects of this procedure do, however, involve a kind of precision technology, which we will describe briefly, with the omission of detailed chemical craftsmanship.

Two LC monomers act like 'building blocks' for the LC polymer network. Together with an azobenzene with fast cis-trans isomerisation, these monomers are mixed and dissolved in an organic fluid. Next, glass cells are prepared for the production of the actuator films. For that purpose, two glass slides are coated with polyimide alignment layers, one with parallel (planar) and the other with perpendicular alignment to produce the required splay configuration.

To achieve an accurately defined film thickness, glass bead spacers of 20 µm diameter are used. Thanks to capillary action the cells can be filled with the LC-azobenzene mixture. Then the mixture is polymerised to obtain the polymer film. After opening the cell, the film can be peeled off from the glass with the aid of razor blades.

### Designing an experimental robot

Figure 5 shows an experimental 10-mm sized robot with a mass of about 20 mg. It consists of a central hub of polypropylene plastic on which four legs with mutual angles of 90° are positioned at the bottom and two cargo handling arms at the top. The legs are about 12 mm long, the upper handling arms about 8 mm. The trick of the robot design is that the legs and upper arms are provided with two different azobenzene chromophores, depicted in Figure 5b in yellow and red. By addressing them with light of different wavelengths, legs and arms can be guided separately. Two collimated light sources are used to address the robot.

Without detailing the procedures for gripping, securing and transporting the load, the way in which the tiny robot is able to move will be explained by describing one complete stride of 4 mm that can be achieved with the aid of two different collimated-light sources of the same wavelength, as illustrated in Figure 6.

Firstly, one of the four legs is designated as the 'striding leg' (i). This leg is liberated from the walking surface by illuminating two legs on either side of the striding leg with low-intensity light (ii). This lifts the striding leg slightly, making it possible to stretch the striding leg by addressing it with the other light source (iii). Switching the light source off for the non-striding legs lowers the complete assembly again, bringing the striding leg back into contact with the surface (iv). Ceasing the illumination of the striding leg

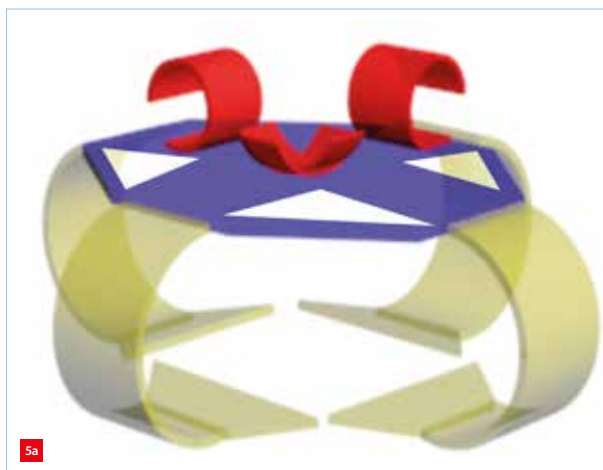
subsequently causes it to bend back into its previous position (v), dragging the complete device forward (vi): one finished step!

### To conclude

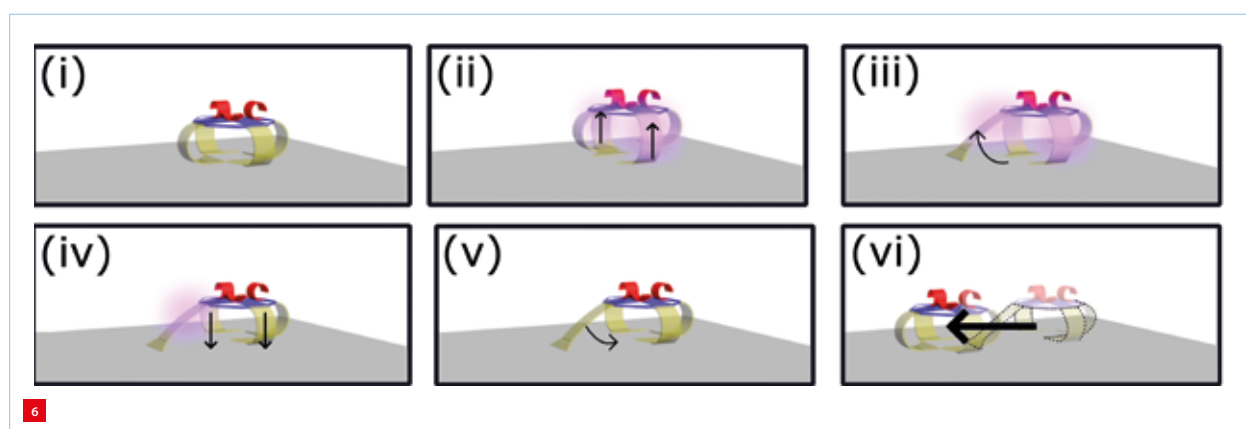
The integration of light-guided polymer actuators in a tiny robot proves the effectiveness of these devices. It will be clear that many more versatile applications may be easy to invent. Such robotic devices might be useful to transport and deliver medicines in the human body via blood vessels: therapeutics at the right time at the right place. Or they might be applicable for the repair of integrated circuits (ICs) or IC manufacturing machinery. In the near future the TU/e research group will try to miniaturise their robots, probably even into the sub-mm application area.

### REFERENCE

- [1] M. Pilz da Cunha, S. Ambergen, M.G. Debije, E.F.G.A. Homberg, J.M.J. den Toonder, and A.P.H.J. Schenning, "A soft transporter robot fuelled by light", *Advanced Science / Early View*, 20-02-2020.
- [2] M. Pilz da Cunha, E.A.J. van Thoor, M.G. Debije, D.J. Broer, and A.P.H.J. Schenning, "Unravelling the photothermal and photo-mechanical contributions to actuation of azobenzene-doped liquid crystal polymers in air and water", *J. Mater. Chem. C*, 7, 13502, 2019.
- [3] R. Verpaalen, M. Pilz da Cunha, T.A.P. Engels, M.G. Debije, and A.P.H.J. Schenning, "Liquid crystal networks on thermoplastics: reprogrammable photo-responsive actuators", *Angewandte Chemie - International Edition*, 59(11), pp. 4532-4536, (2020).



The experimental robot, 10 mm in size and about 20 mg in mass.  
 (a) A polypropylene hub (in blue) with four legs at the bottom and two cargo handling arms (in red) at the top. Legs and arms can be separately actuated by light because of their responses to different wavelengths.  
 (b) Realisation.



Accomplishing one striding step.  
 (i) Starting position with striding leg on the left.  
 (ii) Lifting the hub by illuminating two side legs.  
 (iii) Stretching the striding leg.  
 (iv) Lowering the hub by switching off illumination of side legs.  
 (v) Bending striding leg back to its starting position.  
 (vi) Dragging the complete device one step forward.

# THE ART OF MICROMACHINING

**The advent of ultrashort-pulsed lasers gave birth to the field of laser micromachining. In the Netherlands, Reith Laser has become one of the leaders in this field by devoting a lot of effort to mastering the laser machining process. The process is fundamentally instable, as it comprises a number of positive feedback mechanisms. This calls for adaptive control, which is still in its infancy, however.**

More than thirty years ago, in 1988, Reith Laser started as a laser machining workshop. Over the years it has grown into one of the leading companies in precision laser machining for industrial applications in the Netherlands. In 2018, founder Jan Reith sold his company to Veco, then part of SPGPrints. As of this year Reith Laser, located in Wijchen, NL (Figure 1), is part of the Muon Group (400 employees, turnover in excess of 80 million euros). The Muon group comprises companies in the fields of electroforming (Veco), chemical etching (UK-based Tecan) and laser material processing (Reith). It is headquartered in Eerbeek (NL), where Veco is located.

## Making holes

Building on their heritage in the fabrication of ultrafine sieves for milk, sugar and starch production and for textile printing, the Muon companies aim to capitalise on the synergy between their respective production technologies for microprecision engineering and manufacturing in markets that are driven by the ongoing miniaturisation. For example, sieves can be made by electroforming and then laser-welded into complete microfiltration modules. The same applies to cooling plates that are first etched and then

assembled with the aid of laser welding. On the other hand, when comparing the various production technologies, one of the advantages of laser drilling over etching is that it can achieve much larger length-to-diameter ratios for holes. Etching small holes in foil would require the foil to be very thin, making it very fragile. With laser machining small holes can be drilled in thicker, robust foils as well.

## Towards Reith Laser 2.0

Reith Laser, based in Wijchen (NL) with approximately fifty employees, has extensive metallurgical knowledge and covers five laser application areas; welding, cutting, drilling, marking and micromachining. It serves the semiconductor, medical, automotive, printing, display and other high-tech industries. Eric Hezemans, previously with NTS Systems Development, is the new managing director. His mission is to transform Reith Laser “from a laser engineering company with limited growth capacity into a focussed, medium and high added value 24/7 laser manufacturing company”.

“Reith Laser 2.0” strives to operate in a lean and highly digitalised and robotised fashion – towards one-piece flow – and offers its OEM customers application engineering

## EDITORIAL NOTE

This article is based on an interview with Eric Hezemans (managing director) and Walther Goethals (R&D manager) of Reith Laser, as well as on Goethals' presentation at the Precision Fair 2019.



Reith Laser is located in Wijchen (NL).



## Laser drilling

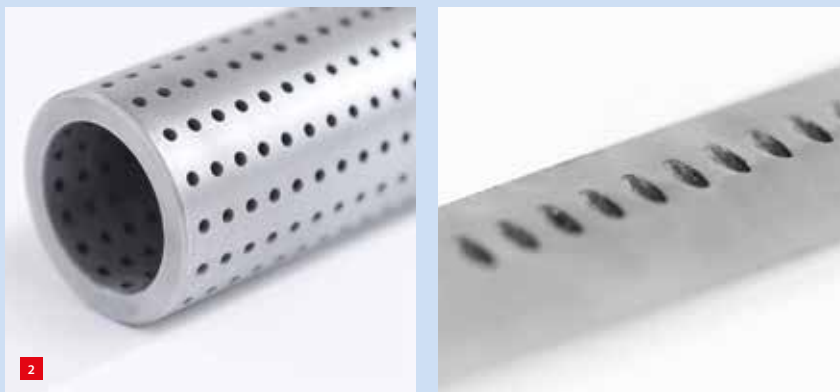
As an example, laser drilling is one of the laser machining processes that has developed rapidly over the past few years. At Reith Laser, it can be applied to a variety of materials, including metals, ranging from (stainless) steel and inconel to aluminium and titanium, and ceramics. Holes are burr-free and exhibit a small heat-affected zone. Additional advantages of the process are the small diameters and the high aspect ratios that are feasible. The tapering of holes, i.e. changing the diameter gradually as the 'digging' of the hole proceeds, is possible over a wide range of material thicknesses. Holes do not have to be round and they can be blind (Figure 2); their shape can be triangular, square, etc., when drilling becomes the cutting out of a 'pillar' of material in the desired cross-sectional shape.

Various drilling modes are available:

- Single-pulse drilling: The laser beam is stationary relative to the product, making this mode in particular suitable for very thin materials.
- Percussion drilling: The (pulsed) laser beam is pulsed with a secondary frequency (in the order of 1 Hz) at one specific spot of a material, with the beam diameter

changing during the process (approximately 0.1 to 1 mm), to achieve the final hole size.

- Trepanning: Once a single hole has been drilled in the material, the laser beam moves in an increasingly larger spiral ('orbital') diameter to further cut the hole towards its final size.
- Drilling on the fly: A laser pulse is constantly moving relative to the product and consecutively cutting holes in the product.



Examples of laser-drilled products.

support (Reith now employs over ten engineers), followed by first-tier supply. The company develops and builds customised machines for advanced laser processing applications.

Examples of high-end products include a ring in which thousands of holes have been drilled, under different angles and with tapering of the holes, i.e. their entrance and exit diameters differing by a few microns. Included in the challenge is the fact that no standard measurement procedure is available for the qualification of such products. Another example is a stage in which cooling channels have been machined; these have been covered by a metal sheet of only 200  $\mu\text{m}$  thickness that was laser welded, keeping it flat within 1  $\mu\text{m}$  and withstanding 10 bar of air pressure in leak testing. Here, Reith has provided engineering support for optimising the shape of the weld.

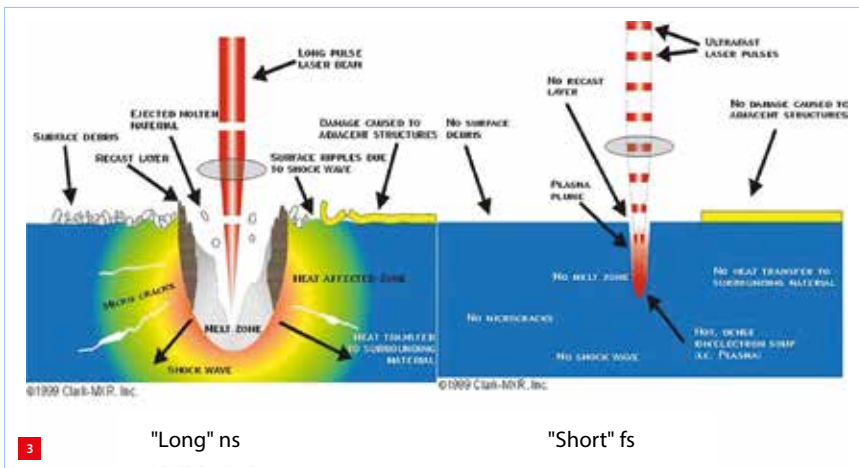
Currently, 95% of Reith's business is generated with conventional laser machining (18 machines in total), employing ms- and  $\mu\text{s}$ -pulsed laser beams with spot sizes from 20 to 600  $\mu\text{m}$ , achieving accuracies of 10 to 50  $\mu\text{m}$ . The remaining 5% of business comes from micromachining with ns- to fs-pulsed laser beams that generate a 10-30  $\mu\text{m}$  spot size and achieve machining accuracies of 1-2  $\mu\text{m}$ . Reith Laser now operates two tools for micromachining and the

ambition is to expand the share of this business line to 10-15%. Now is the right time, as the technology has matured over the years, partly due to Reith's extensive in-house R&D.

### Thermal process

The crux of laser machining is that it is a thermal process. A laser beam 'pumps' energy into a material, melting it to create a hole or a cut. This only works if more energy is supplied than is 'leaking away'; this is not straightforward, especially not for metals with a high heat conductivity. The second thermal challenge is that the heat supplied can change the structure and thus the properties of the material, creating a so-called heat-affected zone, which can exhibit both aesthetic and functional 'damage' (for example, internal stresses).

The solution for this is to refrain from a continuous energy supply (continuous wave laser), and use a pulsed laser beam instead. Each pulse can then have a higher power without increasing the total amount of energy injected. Over the years, the development of laser technology has resulted in increasingly shorter pulses, down to femtosecond pulses. The shorter the pulse, the less energy is supplied and the smaller the heat-affected zone (Figure 3). The reason for this is that the time during which this large power is



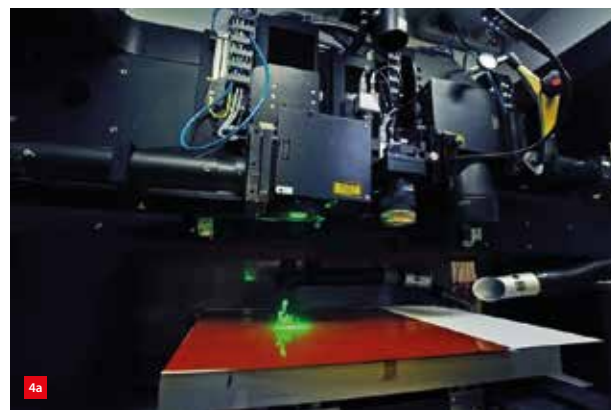
Impact of long- and short-pulse lasers. (Reproduced with permission from Clark-MXR, Inc.)

supplied is much shorter than the time constant of the heat leakage. In fact, the power is so large that the melting of the material is skipped; the atoms in the material are immediately ionised and the material is gasified right away. It is, so to speak, chipped off, taking with it all the laser energy, so that nothing can leak away into the surrounding zone.

### Micromachining

This 'cold' laser ablation process is denoted as micromachining (Figure 4), be it either cutting, drilling, patterning/structuring or polishing of a wide variety of materials, ranging from metals and ceramics to plastics, rubber and glass. There are a lot of parameters that influence this process and some of them are open-loop, i.e. they can have a positive feedback on the process, making it inherently unstable.

This can be compared to a child playing with a positive lens and trying to focus the sunlight on a white sheet of paper in order to burn a hole in the paper. Because of the white colour, a lot of light is reflected and it takes a lot of time to obtain any visible result. During this time the paper is gradually heated up by the focused light, causing it to discolour into black, upon which it will absorb the light much better and suddenly ignite.



Micromachining at Reith Laser.

(a) Set-up.

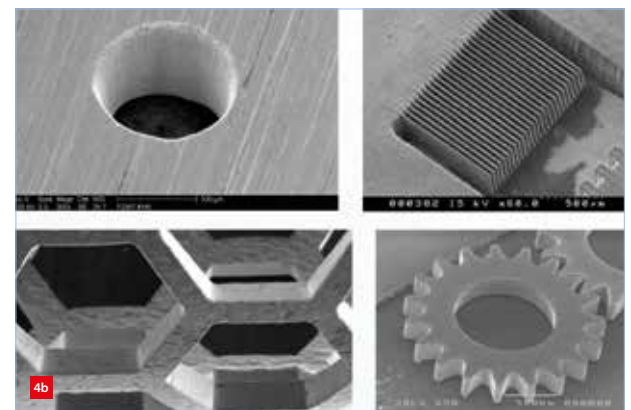
(b) Demo products.

The challenge for the child is to keep the sheet of paper 'in focus'. Exactly the same challenge is present in laser machining. The first question is what the optimal focus is. If the surface that is being processed is exactly in focus, the laser intensity is at its peak and that is an unstable situation; disturbances will lead to a slight 'out of focus' and any control action may result in an overshoot. Therefore, it is better to deliberately stay out of focus in a regime with a decent focus gradient that will guide control to maintain this situation. A second focus issue is concerned with the diameter of the hole that can be drilled. The diameter of a conventional drill equals the diameter of the hole that can be drilled using it. This is not the case for a laser beam, because of its 'hazy' cross-sectional intensity profile. In this profile there is a kind of threshold energy below which machining will not occur. This might define some kind of diameter, although the cross-sectional intensity profile generally is not rotation-symmetric.

Another process factor is the shielding gas that is often used to shield the 'melt pool' from the environment, to prevent the processed material from reacting with oxygen, nitrogen, etc., and the formation of recast layers. The gas flow in the processing zone can exhibit complex patterns, not dissimilar to those seen in the afterburner jet of a fighter plane. These patterns can influence the machining process.

### Removal rate

The primary objective of the laser machining process is to remove material, so the primary process output variable, and hence process control input variable, is the removal rate. A large number of parameters influences this removal rate, including the pulse energy, the material composition, the laser beam intensity profile and its focus, and the shielding gas flow pattern. These last two parameters, focus and flow, provide a nice example of the control challenge: when material is removed, focus as well as flow will change, which in turn may impact the removal rate – this creates a feedback loop which can be either negative or positive, potentially making the laser machining process unstable.



This fundamental conclusion was drawn by Reith Laser after years of experimenting. The stability of the laser beam had been improved, more granite had been added to the machining set-up in order to improve mechanical stability, environmental conditions had been kept strictly under control, etc. Elaborate simulations of the machining process had been set-up to predict the impact of parameter variations, damping had been introduced in the system, etc., etc. However, none of these measures provided a completely predictable and controllable process; optimal settings could still change from day to day.

This situation obviously calls for adaptive, real-time control. For example, optical sensors can monitor the process, to check the depth of a laser weld, the removal of material after drilling, or the occurrence of breakthrough when drilling through foil or sheet. Real inline process quality monitoring options are scarce to date, however. For example, optical coherence tomography, a kind of broadband interferometry, is still under development for laser machining applications. Reith Laser is currently working on these kinds of monitoring, in collaboration with large customers and laser manufacturers.

### Roadmap

This work is part of the roadmap for innovation in laser technology that Reith Laser is following. It comprises three

tracks; lasers, optics, and machines. The two main laser parameters, besides power, are pulse duration and wavelength, which are both decreasing. The pulse duration has been moving into the femtosecond domain for some time already and, as of recently, blue lasers have become available for machining purposes. This is advantageous, for example, for the machining of copper, as blue light reduces the reflection of laser power by a copper surface. At Reith Laser, initial experiments with laser welding of copper products have been performed.

Regarding the laser optics, after the adoption of scanning optics – it is easier and works much faster to move a 'lightweight' laser beam than the product on a heavy stage – the trend is now towards full optical metrology for adaptive control and the use of multi-beam configurations for the low-cost mass production of products with large numbers of holes. Combining this with the trends in the machine domain (automation, robotisation, big data), Reith's roadmap is proceeding towards ever more reliable, faster and more accurate laser machining.


#### INFORMATION

[WWW.REITHLASER.NL](http://WWW.REITHLASER.NL)  
[WWW.MUONGROUP.COM](http://WWW.MUONGROUP.COM)

## LESS Vibrations


## BETTER Results





### Solutions and products against vibrations:

- FAEBI® rubber air springs
- BiAir® membrane air springs
- Mechanical-pneumatic level control systems
- Electronic Pneumatic Position Control EPPC™
- Active Isolation System AIS™
- Customized laboratory tables
- and more...



**Your Bilz contact in the Netherlands:** **OUDE REIMER**

Willem Barentszweg 216 • NL-1212 BR Hilversum • phone: +31 35 6 46 08 20 • [info@oudereimer.nl](mailto:info@oudereimer.nl) • [www.oudereimer.nl](http://www.oudereimer.nl)

# FIRST MEASUREMENT TECHNOLOGY, THEN STANDARDS

Post-process metrology to validate the integrity of additive manufacturing (AM) builds is of vital importance for AM maturing as an industrial production technology. The nature and relative roughness of AM surfaces, whether analysing individual layers within a build or the surface of a finished part, render conventional metrology solutions somewhat impotent. ZYGO is working with Richard Leach, professor of Metrology at the University of Nottingham, UK, on various AM metrology projects. “You cannot develop standards if you don’t have the correct measurement technology in place to start with.”

The research of Richard Leach [1] in the area of advanced/ additive manufacturing includes information-rich surface metrology [2] and the calibration of optical surface and coordinate measuring instruments [3]. In his opinion, the issue of metrology is crucial to the success of AM as it begins to establish itself as a true production technology. “Basically, as we stand today, there is a lack of clarity as to the precise nature of defects that you get when undertaking an AM build, and you also have little idea how these may cause problems in terms of part functionality. We don’t have a detailed enough map of how the topography of the defects and the anomalies that you get during the AM process propagate through to the part in an end-use scenario.” “Essentially, we are working on — but still haven’t completely solved — the problem of understanding what

issues you get on the surface and under the surface when using AM, and how these relate to product functionality. Therefore, it is difficult to predict the mechanical properties, the thermal processes, the fatigue properties, etc..., from the types of structures we are seeing post-process. Defect-function analysis may allow us to move towards controlled AM by just stopping the process when things go wrong. Right now, we spend hours building a part that may in fact have a problem in layer one.”

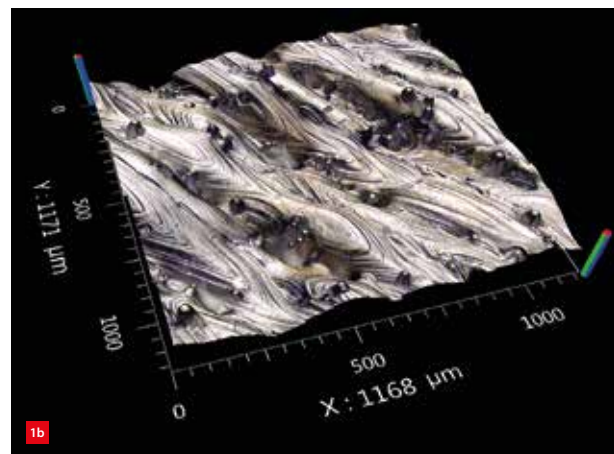
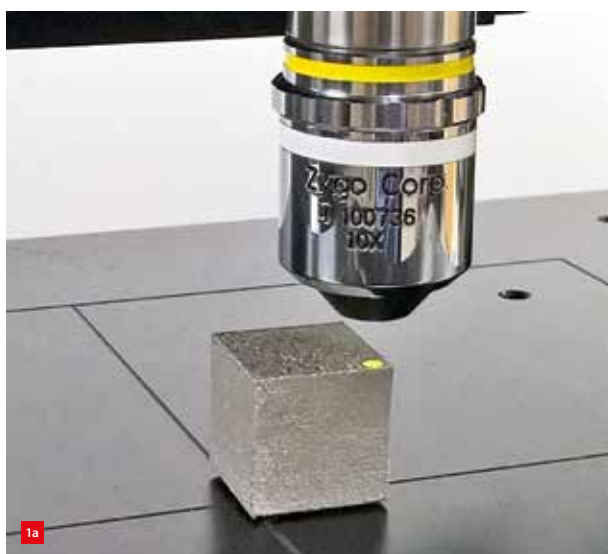
## Validation challenge

To ensure that AM-produced parts conform fully with design intent, part suppliers undertake far more mechanical testing and metrology verification than they would normally employ for conventional manufacturing processes. Necessarily, they are forced to focus on process development and throw in all the validation resources they can to ‘prove’ the integrity of the finished AM part. For example, they

## EDITORIAL NOTE

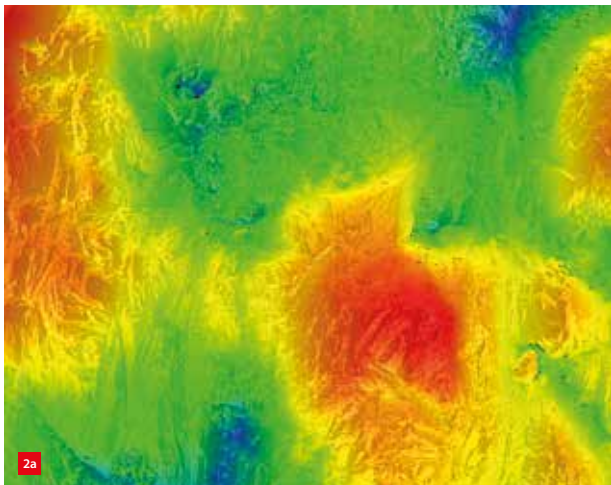
This article is based on an abridged contribution by Eric Felkel, product manager 3D optical profilers at Zygo Corporation in Middlefield, CT, USA. ZYGO, part of the Ultra Precision Technologies Division of Ametek, is a worldwide supplier of optical metrology instruments, high-precision optical components and complex electro-optical systems.

eric.felkel@ametech.com  
www.zygo.com



Measurement of a Ti6Al4V selective laser melting sample part at Nottingham University, using a ZYGO Nexview CSI microscope.  
(a) Set-up.  
(b) True-colour 3D image.





*AlSi10Mg sample fabricated at the University of Nottingham using laser powder bed fusion, measured by a ZYGO NewView CSI microscope.*  
 (a) Surface topography colour map.  
 (b) Surface structure in true-colour 3D.

have to rely on the statistical Gage R&R reproducibility and repeatability method as a stand-in for a more rigorous measurement uncertainty approach when evaluating the integrity and functional characteristics of AM parts. The current solution is what could be termed 'extreme-testing'.

Leach comments, "Everyone blames the confusion on a lack of standards for measuring AM parts, but this is not where attention should be focused. You cannot develop standards if you don't have the correct measurement technology in place to start with. That is why the emphasis with metrology instrument suppliers is on adapting metrology solutions to make them better aligned with the unique characteristics of the AM process and AM end-use parts. With respect to standards, our focus today is on producing a Good Practice Guide along with ASTM [4], showing OEMs what metrology solutions are in place today, and how to get the best results from these when applied to AM surfaces, and setting the instrument up in the best way to understand the data."

### Coherence scanning interferometry

So, the focus in the area of metrology for AM is to reduce today's time and cost inefficiencies of relying on a vast range of duplicate and often inadequate metrology steps to validate that an end-use part is fit for purpose. In this vital area, Leach is involved with a number of metrology instrument suppliers, including ZYGO.

"For post-process metrology, a number of alternatives exist, including confocal and focus variation, and ZYGO's coherence scanning interferometry (CSI [5]). Initially it was thought that CSI was not suitable to the vagaries of post-process AM parts, because it would fail to capture most of their highly irregular topographic features. But they enhanced their CSI instruments by introducing new ways of playing with the optical light source, illumination conditions, and also the company played with the detection conditions, which

led to the attainment of high-quality results for extremely rough and complex AM surfaces. I have to admit, initially even I thought that they probably wouldn't be able to be applied to AM parts, but they actually work extremely well."

### 'More Data'

ZYGO solved the problem with the introduction of its Nexview™ (Figure 1) instrument in 2014. This instrument and its sister product, the NewView™ (Figure 2), included innovative hardware and software upgrades, referred to as 'More Data Technology'. 'More Data' significantly improves the baseline sensitivity of CSI and enables high-dynamic range (HDR) operation making it valuable for a wide range of parts, from steeply-sloped smooth parts to exceptionally rough textures with poor reflectivity. Additionally, HDR is able to measure parts with a wide range of reflectance, often a struggle for other CSI instruments.

Leach concludes, "Our joint work is centred around understanding precisely how the CSI instrument works, and accurately modelling it for AM applications. At the moment, the issue is that AM surfaces are so different from what we are used to in terms of the raw surface and the post-processed surface that there is no standardised way of measuring and characterising these surfaces. Together we continue to optimise metrology solutions for the increasingly important area of AM for production scenarios."

### REFERENCES

- [1] [www.nottingham.ac.uk/research/manufacturing-metrology](http://www.nottingham.ac.uk/research/manufacturing-metrology)
- [2] N. Senin and R. Leach, "Smart measuring – Information-rich surface metrology", *Mikroniek*, 58 (6), pp. 18-23, 2018.
- [3] R. Leach, "Pleading for a complete framework – Calibration of optical surface and coordinate measuring instruments", *Mikroniek*, 59 (5), pp. 19-21.
- [4] [www.astm.org/industry/additive-manufacturing-overview.html](http://www.astm.org/industry/additive-manufacturing-overview.html)
- [5] M. Schmidt, "Advanced metrology for energy efficiency – Coherence scanning technology enabling reliable engine lightweighting", *Mikroniek*, 59 (6), pp. 10-13, 2019.

# ECP<sup>2</sup> COURSE CALENDAR



## COURSE (content partner)

ECP<sup>2</sup> points Provider Starting date

### FOUNDATION

Mechatronics System Design - part 1 (MA)	5	HTI	28 September 2020
Mechatronics System Design - part 2 (MA)	5	HTI	5 October 2020
Fundamentals of Metrology	4	NPL	to be planned
Design Principles	3	MC	13 October 2020
System Architecting (S&SA)	5	HTI	8 June 2020
Design Principles for Precision Engineering (MA)	5	HTI	to be planned (2021)
Motion Control Tuning (MA)	6	HTI	23 November 2020

### ADVANCED

Metrology and Calibration of Mechatronic Systems (MA)	3	HTI	27 October 2020
Surface Metrology; Instrumentation and Characterisation	3	HUD	to be planned
Actuation and Power Electronics (MA)	3	HTI	16 November 2020
Thermal Effects in Mechatronic Systems (MA)	3	HTI	1 December 2020
Dynamics and Modelling (MA)	3	HTI	23 November 2020
Manufacturability	5	LiS	to be planned
Green Belt Design for Six Sigma	4	HI	to be planned
RF1 Life Data Analysis and Reliability Testing	3	HI	to be planned
Ultra-Precision Manufacturing and Metrology	5	CRANF	to be planned

### SPECIFIC

Applied Optics (T2Prof)	6.5	HTI	to be planned (Q4 2020)
Advanced Optics	6.5	MC	17 September 2020
Machine Vision for Mechatronic Systems (MA)	2	HTI	upon request
Electronics for Non-Electronic Engineers – Analog (T2Prof)	6	HTI	to be planned
Electronics for Non-Electronic Engineers – Digital (T2Prof)	4	HTI	to be planned
Modern Optics for Optical Designers (T2Prof) - part 1	7.5	HTI	18 September 2020
Modern Optics for Optical Designers (T2Prof) - part 2	7.5	HTI	11 September 2020
Tribology	4	MC	27 October 2020
Basics & Design Principles for Ultra-Clean Vacuum (MA)	4	HTI	2 November 2020
Experimental Techniques in Mechatronics (MA)	3	HTI	30 November 2020
Advanced Motion Control (MA)	5	HTI	26 October 2020
Advanced Feedforward & Learning Control (MA)	2	HTI	30 September 2020
Advanced Mechatronic System Design (MA)	6	HTI	to be planned (2020)
Passive Damping for High Tech Systems (MA)	3	HTI	17 November 2020
Finite Element Method	2	MC	29 October 2020
Design for Manufacturing (Schout DfM)	3	HTI	1 September 2020

Please check for  
any rescheduling of  
courses due to the  
coronavirus crisis.

## ECP<sup>2</sup> program powered by euspen

The European Certified Precision Engineering Course Program (ECP<sup>2</sup>) has been developed to meet the demands in the market for continuous professional development and training of post-academic engineers (B.Sc. or M.Sc. with 2-10 years of work experience) within the fields of precision engineering and nanotechnology. They can earn certification points by following selected courses. Once participants have earned a total of 45 points, they will be certified. The ECP<sup>2</sup> certificate is an industrial standard for professional recognition and acknowledgement of precision engineering-related knowledge and skills, and allows the use of the ECP<sup>2</sup> title.

[WWW.ECP2.EU](http://WWW.ECP2.EU)

## Course providers

- High Tech Institute (HTI)  
[WWW.HIGHTECHINSTITUTE.NL](http://WWW.HIGHTECHINSTITUTE.NL)
- Mikrocentrum (MC)  
[WWW.MIKROCENTRUM.NL](http://WWW.MIKROCENTRUM.NL)
- LiS Academy (LiS)  
[WWW.LISACADEMY.NL](http://WWW.LISACADEMY.NL)
- Holland Innovative (HI)  
[WWW.HOLLANDINNOVATIVE.NL](http://WWW.HOLLANDINNOVATIVE.NL)
- Cranfield University (CRANF)  
[WWW.CRANFIELD.AC.UK](http://WWW.CRANFIELD.AC.UK)
- Univ. of Huddersfield (HUD)  
[WWW.HUD.AC.UK](http://WWW.HUD.AC.UK)
- National Physical Lab. (NPL)  
[WWW.NPL.CO.UK](http://WWW.NPL.CO.UK)

## Content partners

- DSPE  
[WWW.DSPE.NL](http://WWW.DSPE.NL)
- Mechatronics Academy (MA)  
[WWW.MECHATRONICS-ACADEMY.NL](http://WWW.MECHATRONICS-ACADEMY.NL)
- Technical Training for Prof. (T2Prof)  
[WWW.T2PROF.NL](http://WWW.T2PROF.NL)
- Schout DfM  
[WWW.SCHOUT.EU](http://WWW.SCHOUT.EU)
- Systems & Software Academy (S&SA)

## Extending the life of cam-operated automatic lathes

Tens of thousands of traditional cam-operated automatic lathes are still tirelessly mass-producing precision parts for the watch, automotive, dentistry and electronic industries globally. Though the official support for these machining tools is limited, quality spare parts and tools are still available thanks to UniParts. This Swiss company has manufactured and distributed precision spare parts and equipment for cam-operated automatic lathes on a global scale since 1997. It can produce a great variety of quality parts in short series in its main production facility in Poland.

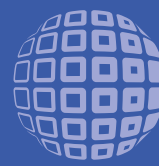
The old-school cam-operated automatic lathes, also named Swiss-type lathes, perhaps don't look like much to the outside world, but they keep on cutting, turning, tapping, knurling and drilling crucial parts for a wide array of products 24/7. "The tolerance of the small parts that are machined is in many cases in the region of one micron", says Per Borg, CEO of toolmaker UniParts. "For the industries using them, these workhorses are true gold mines that keep on spinning as long as spare parts are available. Because the original manufacturers only offer limited support for these machines, we saw a good after-sales business opportunity and a way for many industries to keep their production costs down without sacrificing quality."

"Modern CNC tooling machines are more versatile than a traditional Swiss-type lathe, so when the motors are worn out, it is often best to invest in a new CNC machine with state-of-the-art technology. Our job, however, is to maintain the old Swiss-type lathes." Most of UniParts' customers are end-users, with service workshops as the other main customer segment. The main markets are in Switzerland and Europe, but India, USA and Japan are growing markets. UniParts produces spare parts and attachments for most cam-operated automatic lathes made by Tornos, such as model MS7, and also for automatic lathes made by other producers, such as Bechler and Petermann.



The quality tools for the Swiss-type lathes are made in the same way they were produced by the original manufacturers.

[WWW.UNIPARTS.CH](http://WWW.UNIPARTS.CH)



# HIGH TECH INSTITUTE



### MECHATRONICS

## Basics & design principles for ultra-clean vacuum (UCV)

Engineering judgement obtained in the "normal atmospheric world" is often not valid under ultra-clean vacuum conditions. Moreover, any introduction of additional functionality introduces a source of gasses and contamination. Trainees will be introduced to the fundamentals of vacuum technique and will learn the essential design principles for modules operating in ultra-clean vacuum conditions. Key issue is to become aware of the fact that the whole chain of design, machining, cleaning and the assembly of the components is an integrated process which is as strong as the weakest link.

Data: 15 – 18 June 2020 + 2 – 5 November 2020

Location: Eindhoven

Investment: € 1,995.00 excl. VAT



[hightechinstitute.nl/UCV](http://hightechinstitute.nl/UCV)





## Integrated solution for deburring, cleaning and drying

As a cost-efficient answer to continually increasing demands on the absence of burrs and particulate cleanliness, Ecoclean has developed the EcoCvelox system. Its modular design allows a custom configuration and subsequent expansion, at any time, of equipment from a single source to provide a combined high-pressure water-jet deburring, cleaning and drying capability. Cycle times of only 15 seconds per pallet can thus be achieved. Other features of the EcoCvelox system include a CAD/CAM interface for rapid and easy offline programming of the high-pressure deburring function plus highly dynamic part handling technology. For part identification, a camera system can be integrated.

The modular design allows users to configure individual systems that merge high-pressure deburring, part cleaning and drying from a single source, and to expand them as needs evolve. A combination with other Ecoclean products, e.g. solvent cleaning prior to deburring in applications involving high oil drag-in, is also possible. The diverse standard modules of the EcoCvelox are rated for parts measuring 200 x 200 x 200 mm that are supplied on pallets.

Tooling configuration for the various processes is likewise adaptable to the specific parts. Thus, high-pressure deburring can be performed using the standard single spindle at up to 1,000 bar pressure. An optional high-pressure turret accommodating up to five different tools supports complex deburring operations. It provides a tool-to-tool changeover time of only 1.5 seconds. The tools for the spindle and the turret can be custom-designed to match the given part and can be made by 3D printing. For part cleaning, the processes of injection flood washing, spray cleaning and selective rinsing are available and can be combined. Drying can be achieved by high-velocity air blow-off and/or vacuum, with the air blowing solution being integrable into a cleaning module as well.

Part handling for the deburring process takes place in one Y-axis in the basic version. However, for high throughputs and the associated exacting



*High-pressure deburring can be performed using the standard single spindle or an optional high-pressure turret accommodating up to five different tools.*

cycle time requirements, the module can be fitted with a second Y-axis. This allows loading and unloading to proceed in parallel with deburring. The process time, at 14.5 seconds, thus becomes almost equivalent to the 15-second cycle duration. The same can be achieved for the cleaning and drying module by integrating a second, concurrently operating work chamber.

For process-inherent reasons, all tools used for deburring are subject to wear, which in turn results in a pressure drop. This means that tools need to be replaced after a certain number of operating hours. On the new EcoCvelox, a patented software and a VFD-controlled high-pressure pump ensure that the process pressure is readjusted for this effect. This smart solution, providing a continual adaptation of the high-pressure level, extends tool life by at least 50% and thus boosts plant availability at the same time.

[WWW.ECOCLEAN-GROUP.NET](http://WWW.ECOCLEAN-GROUP.NET)

## High-resolution encoder in compact housing

The Italian smart encoder and actuator manufacturer LIKA Electronic offers an extensive range of rotary miniature encoders with a housing of 28 to 40 mm for feedback applications, especially suitable for small installation spaces. The range includes an incremental as well as an absolute variant, with optical and magnetic technology and is designed to meet varied light and heavy industrial applications. A selection of very compact modular encoders for motor feedback is also available.

One of the latest innovations in the range is the new I30 universal incremental rotary encoder, which has been introduced in the Netherlands by Lika's official partner Tevel. The I30 has a robust miniature housing (up to IP65 protection) and provides a resolution of up to 2,048 pulses per revolution. It suits industrial applications in, e.g., production automation, electrical installations, packaging lines and textile machines.

[WWW.LIKA.IT](http://WWW.LIKA.IT)  
[WWW.TEVEL.NL](http://WWW.TEVEL.NL)





# Comparing AM component finishing methods

Additive manufacturing (AM) allows integration of precisely placed internal cooling channels into components. With a focus on automated post-processing – removal of residual powder and surface smoothing of these channels – the mechanical and chemical engineering departments of the Politecnico Milano (Italy) conducted a study together with Rösler Italiana. Rösler Oberflächentechnik (Germany) is a market leader in surface preparation and finishing and, under the brand name AM Solutions, offers AM equipment solutions and services. The study was concerned with the surface treatment methods mass finishing, shot blasting and chemically-supported mass finishing. It demonstrated that with all three methods a significant improvement of the overall surface quality could be achieved.

For the production of tooling components, selective laser melting (SLM) is the primary manufacturing method, yielding extremely dense workpieces. The downsides of this manufacturing method are that residual powder must be removed from the cooling channels and the high initial surface roughness of the components with  $R_a$  values between 10 and 20  $\mu\text{m}$ . These downsides negatively impact the functionality of the workpieces, resulting in reduced flow rates due to high friction, turbulence, pressure loss in the system and loose particles that can damage other equipment. Since the internal surface areas of complex components with integrated cavities cannot be

treated with conventional finishing technologies, innovative post-processing methods are required.

The choice of the most suitable surface finishing system is therefore critical for the service life of a component and the overall efficiency of a system. One option for smoothing the external and internal surface areas of AM components is mass finishing: workpieces are immersed into a circular work bowl filled with special processing media. In addition, dedicated compounds are added during the process. The vibration of the work bowl causes the media and workpieces to move around the bowl in a spiral movement. The constant 'rubbing' of the media against the workpieces produces a grinding/smoothing effect resulting in the desired surface quality.

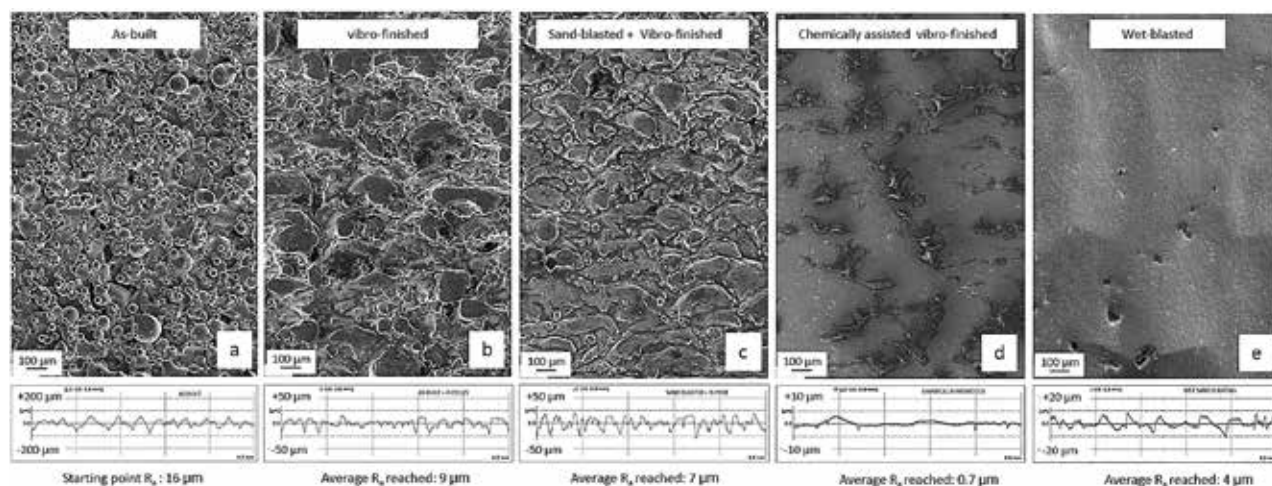
The evaluation study involved the treatment of parts with different shapes and internal passages with different diameters (3, 5, 7.5 and 10 mm) with mass finishing, shot blasting and chemically-supported mass finishing. Conventional mass finishing and shot blasting consistently removed the roughness peaks and produced similar surface roughness profiles. However, the best results were achieved with chemically-supported mass finishing. The workpieces had the smoothest surface, as shown in comparatively lower surface roughness readings, and displayed the typical chemically-accelerated finish. With  $R_a$  values of 0.7  $\mu\text{m}$  this method produced not only the lowest

surface roughness values, but it also required the shortest cycle time. It was also shown that the final roughness values were more or less identical in the vertical and horizontal internal passages.

The study also proved that mass finishing can create the required smoothing effect on the internal surface channel areas without affecting the channel geometry. The treated surface areas were free of powder 'splatters' and loose powder remnants. All three treatment methods improved the surface roughness readings on the internal channel areas.

The tests were conducted on a further development of an M3 machine from AM Solutions. This will not only allow the effective and targeted treatment of internal passages in the future, but it will also be a fully automated system for consistent finishing of 3D-printed components without any manual work requirements. Depending on the surface finish requirements several grinding and polishing processes can be run in sequence. After the automatic discharge of the media from the work bowl, the treated work pieces are removed from the clamping fixture. If required, a separate cleaning and drying stage can be added, of course, also fully automated. The same is true for the work piece handling including the transfer to subsequent manufacturing stages.

[WWW.ROSLER.COM](http://WWW.ROSLER.COM)



The finishing results:

- (a) As-built; starting point  $R_a$ : 16  $\mu\text{m}$ .
- (b) Vibro-finished (mass-finished); average  $R_a$  reached: 9  $\mu\text{m}$ .
- (c) Sand-blasted (shot-blasted) + vibro-finished; average  $R_a$  reached: 7  $\mu\text{m}$ .
- (d) Chemically-assisted vibro-finished; average  $R_a$  reached: 0.7  $\mu\text{m}$ .
- (e) Wet-blasted; average  $R_a$  reached: 4  $\mu\text{m}$ .

## AMSYSTEMS Center divided in three

After four years of innovation on next-generation 3D-printing/additive manufacturing (AM) equipment, AMSYSTEMS Center has entered a new phase. Having begun life as an initiative of TU/e High Tech Systems Center (HTSC) and TNO, aimed at bridging the gap between fundamental and applied research, the four market segments – Industrial Additive Manufacturing, Structural Electronics, Food, and Pharma – have gone through significant developments. As a result, and in view of the future focus and market opportunities, these segments have been split across three ventures.

The Digital Food Processing Initiative (DFPI), already established in 2018 by TNO, HTSC and Wageningen University & Research, will take over and accelerate AMSYSTEMS Center's food and pharma work, with a focus on propositions like sustainable food solutions and food experience. Secondly, AMSYSTEMS Center's Structural Electronics work has found

a new home in Holst Centre, a TNO entity with a prominent position in 2D- and 2.5D-printed electronics.

Finally, the new technology developer and supplier start-up AMSYSTEMS B.V. will promote the shift from prototyping to mass customisation in AM. On one hand, it will do contract development for OEMs and industrial users to generate AM solutions including new 3D-printing processes and dedicated production equipment. On the other hand, it positions itself as the supplier of next-generation additive manufacturing technologies by industrialising TNO's IP and patents (concerning, e.g., selective polymerisation and individual layer deposition) via sellable products.

[WWW.AMSYSTEMSCENTER.COM](http://WWW.AMSYSTEMSCENTER.COM)  
[WWW.DIGITALFOODPROCESSING.COM](http://WWW.DIGITALFOODPROCESSING.COM)  
[WWW.HOLSTCENTRE.COM](http://WWW.HOLSTCENTRE.COM)

## NTS CEO Marc Hendrikse resigns this summer

In 2005, Marc Hendrikse was part of the foundation that formed the current NTS, which develops, produces and assembles complex (opto-) mechatronic systems and modules for large, high-tech machine manufacturers. As director of Te Strake, he was one of the architects behind the merger with Nebato, which later became the NTS-Group. At the end of 2007, he was appointed the CEO of this company, which has seen significant growth over the recent years, achieving a turnover of roughly €280 million in 2019, partly due to the acquisition of high-tech company Norma in 2016. With approximately 1,700 employees around the globe, including about 1,050 in the Netherlands, NTS is one of the larger employers in the high-tech sector.

Recently, Marc Hendrikse announced his resignation as of 1 August: "In the years to come, achieving manageable growth will be vital for suppliers to the high-tech industry such as NTS. (...) The ongoing integration with Norma will continue to require attention from the management over the next two years. Given these




promising growth and development opportunities, I felt that, after 15 years of managing this wonderful company, it is now time to hand over the reins to a successor."

"Marc Hendrikse was a leading figure in helping NTS develop into the exceptional company we know today and achieve its unique market position", the NTS Supervisory Board commented. "He has also invested a great deal of energy into collaborations between companies in the Dutch high-tech industry, and into the worldwide prestige this sector enjoys – from which NTS has benefited."

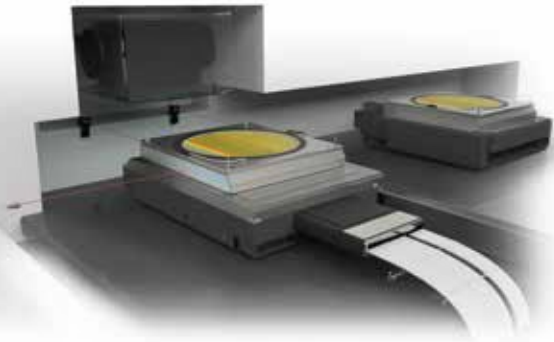
[WWW.NTS-GROUP.NL](http://WWW.NTS-GROUP.NL)

*NTS-Group CEO Marc Hendrikse will resign as of 1 August 2020. NTS expects to announce its new CEO soon.*




### Ultra Precise Positioning and Position Tracking

for precision technology applications, metrology,  
and quality control in semiconductor production




#### Nanopositioners

- UHV and clean room compatible
- 1 nm resolution
- 6 degrees of freedom



#### Interferometer

- UHV and clean room compatible
- 1 pm resolution
- Travel range 0 – 5000 mm (up to 2 m/s)



IDS3010

[www.attocube.com](http://www.attocube.com)

# Teachers of the Year

Susan van den Berg MSc. and Piet van Rens MSc. were announced as “Teachers of the Year” during High Tech Institute’s annual get-together early this year in Eindhoven (NL). Susan van den Berg teaches mechanical engineering at the Fontys University of Engineering and Piet van Rens has a distinguished history of working in the mechanical and industrial engineering industry and recently announced his retirement.

They are both part of the lecturing team for the mechatronics training “Design principles for precision engineering”. The 5-day course for all

engineers involved in mechanical, mechatronic and system design focuses on recognising and analysing mechanisms with a predictable and reproductive behaviour. In October 2019, the duo was asked to come to Wilton in the USA to deliver an in-company edition of the “Design principles for precision engineering” training to a group of 18 ASML employees. When asked if the course was recommended for others, participants responded with an emphatic 9.8 points out of a possible 10, and handed the lecturers a score of 9.4. Respondents also offered several praising comments.



“Teachers of the Year”; Susan van den Berg and Piet van Rens. (Photo: Martien Schouten)

[WWW.HIGHTECHINSTITUTE.NL](http://WWW.HIGHTECHINSTITUTE.NL)

## Saving energy on microfiltration

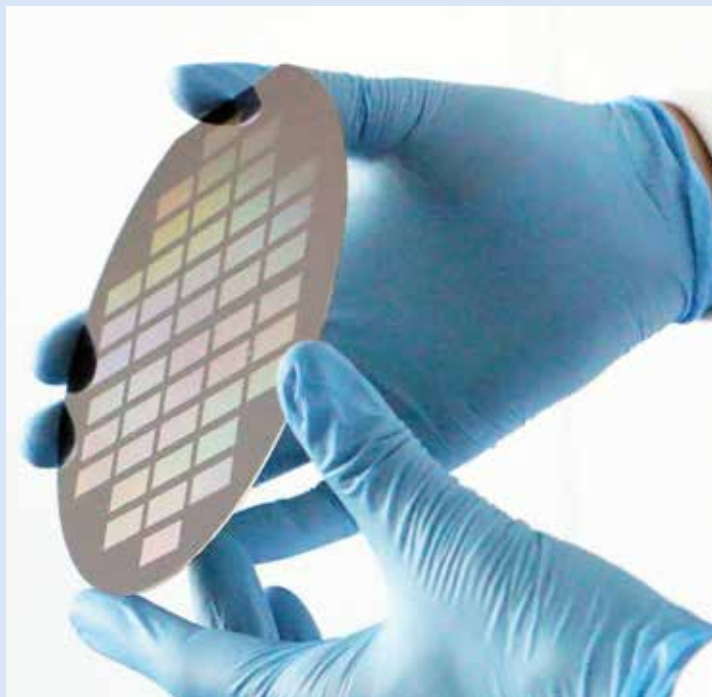
Microfiltration can be used to detect cancer cells in blood, purify food or detect contaminants in water. The ceramic microsieves by Dutch company Aquamarijn Micro Filtration contain extremely thin membranes that can filter very small particles from liquids such as water, milk or blood; examples include micro-organisms, such as bacteria, and other contaminants. Conventional membranes are relatively thick, which means that there must be continuous high fluid pressure on the filters for sufficient flow. This makes filtration a very energy-intensive process. Microsieves can quickly filter large quantities of fluid at low pressure and are therefore less energy-intensive. In the process, however, they silt up quickly. The challenge is therefore keeping the sieves clean.

Around 2015, Aquamarijn partnered with a Swiss company to develop a solution for the rapid contamination of microsieves. A type of vacuum cleaner aimed at a rotating filter cleans the membranes with every revolution of the disc. Energy is only required for rotating the disc, not for maintaining flow pressure. This reduces the energy consumption by almost 90%. To further develop this new type of microsieve, Aquamarijn collaborated with the Institute for Sustainable Process Technology (ISPT) and project partners DSM (for a business case demonstrator) and NIZO (concerning the model for energy and cost savings).

To support the launch of the new microsieve technology, Aquamarijn received a subsidy from the Netherlands Enterprise Agency (RVO). RVO has various subsidies for energy and climate innovation. These include VeKI (*Versnelde Klimaatinvesteringen Industrie* / Accelerated Climate Investments Industry), DEI+ (*Demonstratie Energie- en Klimaatinnovatie* – Circular Economy / Energy and Climate Innovation Demonstration – Circular Economy) and MOOI (*Missiegedreven Onderzoek Ontwikkeling*

*en Innovatie* / Mission-driven Research Development and Innovation). In a few years’ time, the new microsieve should enter the market. A forthcoming issue of Mikroniek will profile the technological innovation behind it.

[WWW.AQUAMARIJN.NL](http://WWW.AQUAMARIJN.NL)  
[WWW.RVO.NL](http://WWW.RVO.NL)



Aquamarijn’s microsieves can now operate with 90% less energy consumption.



## 8.0 release of SAM mechanism design software

The mechanism design software SAM, developed by Dutch company ARTAS-Engineering Software, is a tool for conceptual design, motion/force analysis and optimisation of mechanisms as applied in equipment, agricultural machines and automotive industry (roof mechanisms of convertibles) as well as in medical, lifestyle and domestic products. It is popular with occasional users, ARTAS claims, for its intuitive user interface and ease of use, with specialist users, for the advanced optimisation techniques, and with students and teachers, for making lectures and practical exercises more interesting. The figure below shows an example of delta robot design.

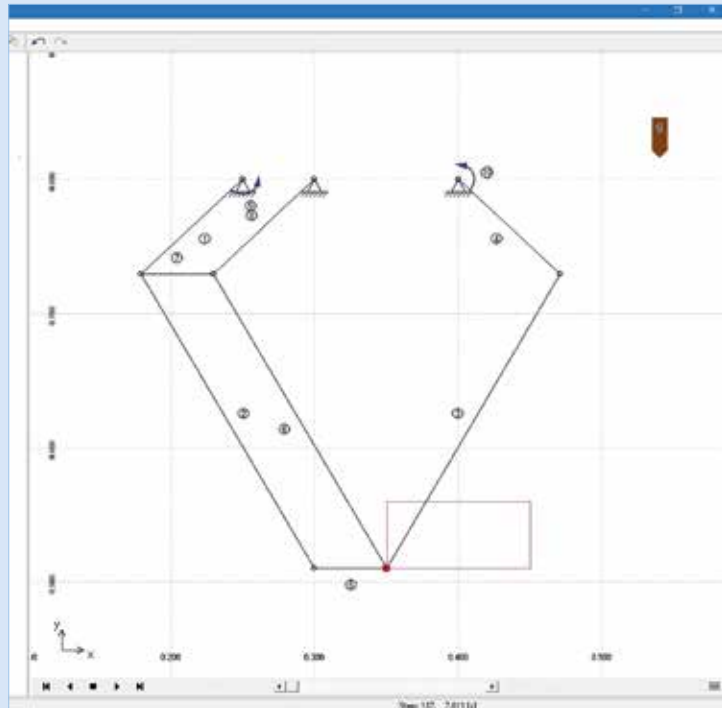
Recently, ARTAS introduced a new version, SAM 8.0, which features a number of enhancements:

- Curved slider:

A new slider element has been introduced that consists of two nodes and an arbitrarily curved shape, which is defined via Bezier points. This element can also be used to mimic a cam mechanism.

- Extended force/torque definition:

External force values and directions (or torque values) can be entered in



SAM-screenshot of a delta robot design: via an inverse kinematics analysis the desired motion of the end-effector has been first converted into the required motion setpoints of the two shoulder motors followed by a forward kinematics & kinetostatics analysis to determine the required driving torques (in the right side of the screenshot, not shown here), such that the correct motors could be selected.

a table of any size in which the argument can be time or any kinematics property of a node or an element. This feature can be used to define forces in a local moving coordinate system. It can also be used to model for example wind forces on a sports car spoiler that are a function of the vertical position of the spoiler.

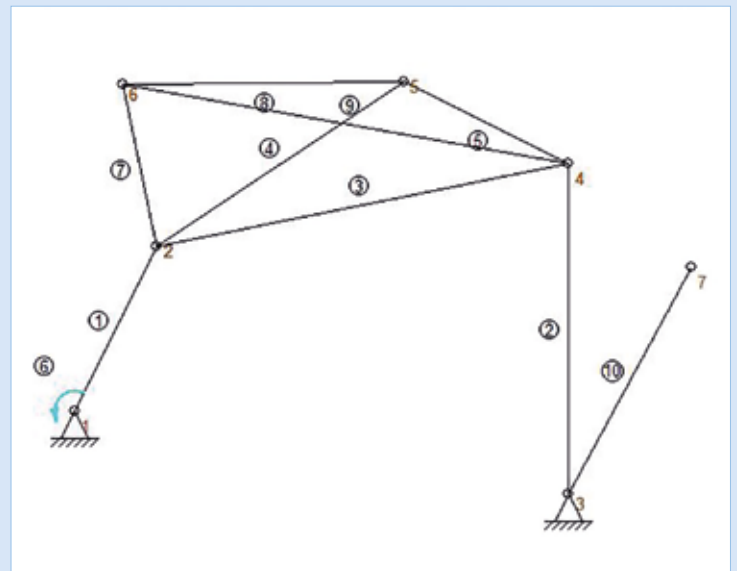
- New gas spring element:

A gas spring uses compressed air contained within a closed cylinder sealed by a sliding piston to pneumatically store potential energy and withstand external forces parallel to the direction of movement of the piston. The friction in the sealing means that the extension force differs from the compression force. To simplify the modelling of such a component a dedicated element was created with an intuitive user interface.

- SVD-based mobility analysis:

With some help from Prof. Dannis Brouwer (University of Twente), an SVD (Singular Value Decomposition) analysis has been introduced to determine whether the mechanism is kinematically indeterminate and/or statically indeterminate (overconstrained). In contrast to the analysis in the previous SAM release, based on the theory of Grübler, SVD analysis is able to give the right diagnosis in case the mechanism is simultaneously kinematically indeterminate (because on a global mechanism scale a constraint is missing) and overconstrained (because locally there is one constraint too many), as illustrated in the figure below.

WWW.ARTAS.NL



This mechanism is both kinematically indeterminate (element 10 is free to rotate) and overconstrained (only one diagonal allowed in the quadrilateral formed by nodes 2-6-5-4).

## Towards silicon lasers

Emitting light from silicon has been the 'Holy Grail' in the microelectronics industry for decades. Solving this puzzle would revolutionise computing, as chips will become faster than ever. Researchers from Eindhoven University of Technology (TU/e, NL) now have succeeded: they developed

an alloy with silicon that can emit light. The results have been published in Nature.

The energy consumption by data communication will be reduced dramatically by replacing electrical communication (via copper wires)



by optical communication (via glass fibres), and the speed of on-chip and chip-to-chip communication can be increased by a factor 1,000. In addition, photonic chips will also bring new applications within reach. Think of laser-based radar for self-driving cars and chemical sensors for medical diagnosis or for measuring air and food quality.

Using light in chips requires an integrated laser as light source. However, bulk silicon is extremely inefficient at emitting light. To create an all-silicon laser, scientists needed to produce a form of silicon that can emit light. That's what researchers from TU/e together with researchers from the universities of Jena, Linz and Munich now succeeded in. They combined silicon and germanium in a hexagonal structure, which has a direct band gap and therefore potentially could emit light.

Shaping silicon in a hexagonal structure, however, is not easy. The researchers created pure hexagonal silicon by first growing nanowires made from another material, with a hexagonal crystal structure. Then they grew a silicon-germanium shell on this template. Next, they managed to increase the quality of the hexagonal silicon-germanium shells by reducing their number of impurities and crystal defects to such extent that they emit light very efficiently.

This year, the researchers hope to create a silicon-based laser. This would enable a tight integration of optical functionality in the dominant

electronics platform, which would break open prospects for on-chip optical communication and affordable chemical sensors based on spectroscopy.

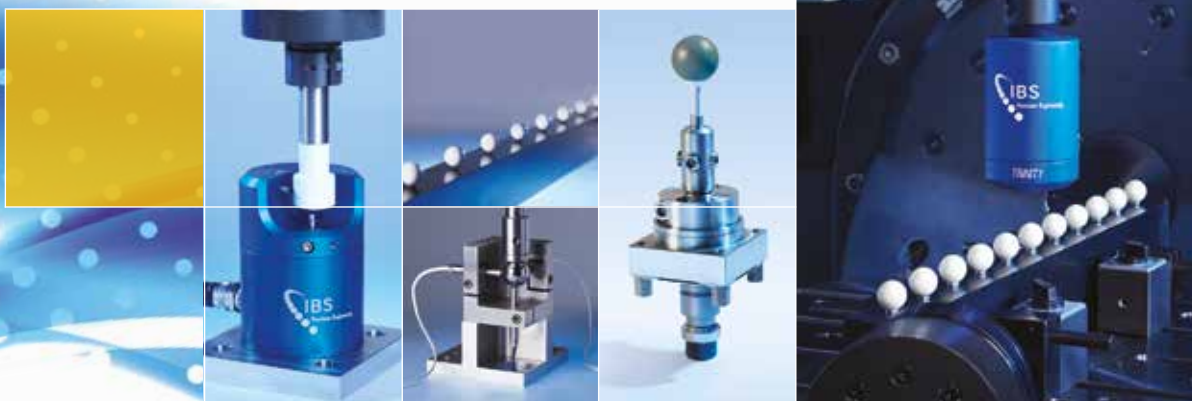
DOI: 10.1038/s41586-020-2150-y



*This Metal Organic Vapour Phase Epitaxy machine was used to grow the nanowires with hexagonal silicon-germanium shells. (Photo: Nando Harmsen, TU/e)*

## Machine Tool Qualification

Linear axis, rotary table & spindle accuracy



[www.ibspe.com](http://www.ibspe.com)

# UPCOMING EVENTS

Please check for any rescheduling,  
online reformatting  
or cancellation of events  
due to the coronavirus crisis.

## Virtual event

6-8 May 2020

### ASPE 2020 Spring Topical Meeting

ASPE's sixth topical meeting on the design and control of precision mechatronic systems.

[WWW.ASPE.NET](http://WWW.ASPE.NET)

## Virtual event

8-12 June 2020

### Euspen's 20th International Conference & Exhibition

The event features latest advances in traditional precision engineering fields such as metrology, ultra-precision machining, additive and replication processes, precision mechatronic systems & control, and precision cutting processes. This 20th edition was intended to be a landmark event at CERN, the largest particle physics laboratory in the world.

[WWW.EUSPEN.EU](http://WWW.EUSPEN.EU)

15-18 September, Geneva (CH)

### EPHJ Exhibition

Trade show presenting technological innovation and expertise in the watchmaking and jewellery, microtechnology and medical technology sectors.



[WWW.EPHJ.CH](http://WWW.EPHJ.CH)

23 September 2020, Den Bosch (NL)

### Dutch System Architecting Conference

The third edition of this conference features system architecting as a distinguishing discipline in the development and commercialisation of complex systems, products and machines.

[WWW.SYSARCH.NL](http://WWW.SYSARCH.NL)

7-11 September 2020, Porto (PT)

### European Optical Society Annual Meeting 2020

This event provides a platform for experts in the field of optics and photonics, bridging the gap between research, education and industry.



[WWW.MYEOS.ORG/EVENTS/EOS/EOSAM2020.HTML](http://WWW.MYEOS.ORG/EVENTS/EOS/EOSAM2020.HTML)

8-9 September 2020, Sint-Michielsgestel (NL)

### DSPE Conference on Precision Mechatronics 2020

Fifth edition of DSPE's conference on precision mechatronics, organised by DSPE. This year's theme is "Uncovering the Essence".



[WWW.DSPE-CONFERENCE.NL](http://WWW.DSPE-CONFERENCE.NL)

14-18 September 2020, Ilmenau (DE)

### 60th Ilmenau Scientific Colloquium

Flagship event of the Technische Universität Ilmenau, organised by the Dept. of Mechanical Engineering, reflecting the broadness and depth of modern engineering as well as the increasing integration of engineering disciplines.

[WWW.TU-ILMENAU.DE/60-IWK](http://WWW.TU-ILMENAU.DE/60-IWK)

29 September - 2 October 2020, Utrecht (NL)

### World Of Technology & Science 2020

Four 'worlds' (Automation, Laboratory, Motion & Drives and Electronics) and Industrial Processing will be exhibiting in the Jaarbeurs Utrecht.



[WWW.WOTS.NL](http://WWW.WOTS.NL)

6-8 October 2020, Braunschweig (DE)

### Special Interest Group Meeting: Structured & Freeform Surfaces

A special focus will be given to research fields in the following topics: replication techniques, structured surfaces to affect function, precision freeform surfaces, large-scale surface structuring, and surfaces for nanomanufacturing and metrology.

[WWW.EUSPEN.EU](http://WWW.EUSPEN.EU)

19-23 October 2020, Minneapolis (MN, USA)

### 35th ASPE Annual Meeting

Meeting of the American Society for Precision Engineering, introducing new concepts, processes, equipment, and products while highlighting recent advances in precision measurement, design, control, and fabrication.

[WWW.ASPE.NET](http://WWW.ASPE.NET)

4 November 2020, Bussum (NL)

### National Contamination Control Symposium

Event, organised by VCCN (Dutch Contamination Control Society), comprising a lecture programme, tutorials and an exhibition.

[WWW.VCCN.NL](http://WWW.VCCN.NL)

18-19 November 2020, Veldhoven (NL)

### Precision Fair 2020

Twentieth edition of the Benelux premier trade fair and conference on precision engineering, organised by Mikrocentrum.



[WWW.PRECISIEBEURS.NL](http://WWW.PRECISIEBEURS.NL)

## Additive Manufacturing / 3D metal printing



### Raytech

Dirk Martensstraat 3A  
8200 Brugge  
Belgium  
**T** +32 (0)50 45 44 05  
**E** info@raytech.be  
**W** www.raytech.be

Raytech offers 3D metal printing (titanium & aluminium) with a strong focus on small and accurate components. Optional treatments after 3D printing: laser welding – laser engraving – cleaning – polishing.

## Automation Technology



### Festo BV

Schieweg 62  
2627 AN DELFT  
The Netherlands  
**T** +31 (0)15-2518890  
**E** sales@festo.nl  
**W** www.festo.nl  
Contact person:  
Mr. Ing. Richard Huisman

Festo is a leading world-wide supplier of automation technology and the performance leader in industrial training and education programs.

member **DSPE**

## Cleanrooms



### Brecon Group

Droogdokkeneiland 7  
5026 SP Tilburg  
**T** +31 (0)76 504 70 80  
**E** brecon@brecon.nl  
**W** www.brecon.nl

Brecon Group can attribute a large proportion of its fame as an international cleanroom builder to continuity in the delivery of quality products within the semiconductor industry, with ASML as the most important associate in the past decades.

Brecon is active with cleanrooms in a high number of sectors on:  
\* Industrial and pharmaceutical  
\* Healthcare and medical devices

member **DSPE**



## Cleanrooms

### Connect 2 Cleanrooms BV

Newtonlaan 115  
Zen Building  
3584 BH Utrecht  
Nederland  
**T** +31 (0)30 210 60 51  
**E** info@connect2cleanrooms.com  
**W** www.connect2cleanrooms.nl

Developing the most appropriate cleanroom to transform your production is our passion. Our scalable and connected cleanrooms have been delivering regulatory compliance to our clients since 2002. We innovate to overcome your contamination control challenges – resulting in a new generation of scalable cleanrooms that set an unprecedented benchmark in the industry.

member **DSPE**

## Development



### TNO

**T** +31 (0)88-866 50 00  
**W** www.tno.nl

TNO is an independent innovation organisation that connects people and knowledge in order to create the innovations that sustainably boosts the competitiveness of industry and wellbeing of society.

member **DSPE**

## Development and Engineering



### Segula Technologies Nederland B.V.

De Witbogt 2  
5652 AG Eindhoven  
**T** +31 (0)40 8517 500  
**W** www.segula.nl

SEGULA Technologies Nederland BV develops advanced intelligent systems for the High Tech and Automotive industry. As a project organisation, we apply our (engineering) knowledge to non-linear systems. This knowledge is comprised of systems architecture and modelling, analysis, mechanics, mechatronics, electronics, software, system integration, calibration and validation.

member **DSPE**

## Education



### Leiden school for Instrumentmakers (LiS)

Einsteinweg 61  
2333 CC Leiden  
The Netherlands  
**T** +31 (0)71-5681168  
**E** info@lis.nl  
**W** www.lis.nl

The LiS is a modern level 4 MBO school with a long history of training Research instrumentmakers. The school establishes projects in cooperation with industry and scientific institutes thus allowing for professional work experience for our students. LiS TOP accepts contract work and organizes courses and summer school programs for those interested in precision engineering.

member **DSPE**

# YOUR COMPANY PROFILE IN THIS GUIDE?

**Please contact:**  
Sales & Services

Gerrit Kulsdom / +31 (0)229 211 211  
gerrit@salesandservices.nl

## Electrical Discharge Machining (EDM)



### CVT BV

Heiberg 29C  
5504 PA Veldhoven  
The Netherlands  
**T** +31 (0)497 54 10 40  
**E** info@cvtbv.nl  
**W** www.cvtbv.nl

Partner high tech industry for wire EDM precision parts. Flexible during day shifts for prototyping. Outside office hours low cost unmanned machining. Call and enjoy our expertise!

member **DSPE**



**Ter Hoek Vonkerosie**  
Propaanstraat 1  
7463 PN Rijssen  
**T** +31 (0)548 540807  
**F** +31 (0)548 540939  
**E** info@terhoek.com  
**W** www.terhoek.com

INNOVATION OF TOMORROW,  
INSPIRATION FOR TODAY  
Staying ahead by always going the extra mile. Based on that philosophy, Ter Hoek produces precision components for the high-tech manufacturing industry.

We support customers in developing high-quality, custom solutions that can then be series-produced with unparalleled accuracy. That is what makes us one of a kind.

It is in that combination of innovative customization and repeated precision that we find our passion. Inspired by tomorrow's innovation, each and every day.

member **DSPE**

## Lasers, Light and Nanomotion



### Laser 2000 Benelux C.V.

Voorbancken 13a  
3645 GV Vinkeveen  
Postbus 20, 3645 ZJ Vinkeveen  
**T** +31(0)297 266 191  
**F** +31(0)297 266 134  
**E** info@laser2000.nl  
**W** www.laser2000.nl

Laser 2000 Benelux considers it her mission to offer customers the latest photonics technologies available. Our areas of expertise are:

- Lasers, scanners and laser machines for industry and research
- Light metrology instruments for LED and luminaire industries
- Light sources for scientific applications
- Piezo- and stepper motion products for nano- and micro positioning
- Inspection and research grade high speed cameras
- Laser safety certified products



### Te Lintelo Systems B.V.

Mercurion 28A  
6903 PZ Zevenaar  
**T** +31 (0)316 340804  
**E** contact@tlsbv.nl  
**W** www.tlsbv.nl

Photonics is our passion! Our experienced team is fully equipped to assist you with finding your best optical business solution. For over 35 years TLS represent prominent suppliers in the photonics industry with well-educated engineers, experience and knowledge. Over the years we became the specialist in the field of:

- Lasers
- Light metrology,
- Opto-electronic equipment,
- Positioning equipment
- Laser beam characterization and positioning,
- Interferometry,
- (Special) Optical components,
- Fiber optics,
- Laser safety

Together with our high end suppliers we have the answer for you!

member **DSPE**

## Mechatronics Development



SOURCE OF YOUR TECHNOLOGY

### Sioux CCM

De Pinckart 24  
5674 CC Nuenen  
**T** +31 (0)40 2635000  
**F** info.ccm@sioux.eu  
**W** www.siox.eu

Sioux CCM is a technology partner with a strong focus on mechatronics.

We help leading companies with the high-tech development, industrialization and creation of their products, from concept stage to a prototype and/or delivery of series production. Commitment, motivation, education and skills of our employees are the solid basis for our business approach

Sioux CCM is part of the Sioux Group.

member **DSPE**



### MTA

Waterbeemd 8  
5705 DN Helmond  
**T** +31 (0)492 474992  
**E** info@m-t-a.nl  
**W** www.m-t-a.nl

MTA is an high-tech system supplier specialized in the development and manufacturing of mechatronic machines and systems.

Our clients are OEM s in the Packaging, Food, Graphics and High-tech industries.

member **DSPE**



## Mechatronics Development



**MI-Partners**  
Habraken 1199  
5507 TB Veldhoven  
The Netherlands  
**T** +31 (0)40 291 49 20  
**F** +31 (0)40 291 49 21  
**E** info@mi-partners.nl  
**W** www.mi-partners.nl

MI-Partners is active in R&D of high-end mechatronic products and systems. We are specialised in concept generation and validation for ultra-fast (>10g), extremely accurate (sub-nanometers) or complex positioning systems and breakthrough production equipment.

member **DSPE**

## Metal Precision Parts



**Etchform BV**  
Arendstraat 51  
1223 RE Hilversum  
**T** +31 (0)35 685 51 94  
**F** info@etchform.com  
**W** www.etchform.com

Etchform is a production and service company for etched and electroformed metal precision parts.

member **DSPE**

## Micro Drive Systems



**maxon benelux**  
Josink Kolkweg 38  
7545 PR Enschede  
The Netherlands  
**F** +31 53 744 0 713  
**E** info@maxongroup.nl  
**W** www.maxongroup.nl

maxon is a developer and manufacturer of brushed and brushless DC motors, as well as gearheads, encoders, controllers, and entire mechatronic systems. maxon drives are used wherever the requirements are particularly high: in NASA's Mars rovers, in surgical power tools, in humanoid robots, and in precision industrial applications, for example. To maintain its leadership in this demanding market, the company invests a considerable share of its annual revenue in research and development. Worldwide, maxon has more than 3000 employees at nine production sites and is represented by sales companies in more than 30 countries.

member **DSPE**

## Micro Drive Systems



**FAULHABER Benelux B.V.**  
**Drive Systems**  
High Tech Campus 9  
5656 AE Eindhoven  
The Netherlands  
**T** +31 (0)40 85155-40  
**E** info@faulhaber.be  
**E** info@faulhaber.nl  
**W** www.faulhaber.com

FAULHABER specializes in the development, production and deployment of high-precision small and miniaturized drive systems, servo components and drive electronics with output power of up to 200 watts. The product range includes brushless motors, DC micromotors, encoders and motion controllers. FAULHABER also provides customer-specific complete solutions for medical technology, automatic placement machines, precision optics, telecommunications, aerospace and robotics, among other things.



**Physik Instrumente (PI)**  
**Benelux BV**  
Hertog Hendrikstraat 7a  
5492 BA Sint-Oedenrode  
The Netherlands  
**T** +31 (0)499-375375  
**F** +31 (0)499 375373  
**E** benelux@pi.ws  
**W** www.pi.ws

Stay ahead with drive components, positioners and systems by PI. In-depth knowledge, extensive experience and the broadest and deepest portfolio in high-end nanopositioning components and systems provide leading companies with infinite possibilities in motion control.

member **DSPE**

## Motion Control Systems



**Aerotech United Kingdom**  
The Old Brick Kiln  
Ramsdell, Tadley  
Hampshire RG26 5PR  
UK  
**T** +44 (0)1256 855055  
**F** +44 (0)1256 855649  
**W** www.aerotech.co.uk

Aerotech's motion control solutions cater a wide range of applications, including medical technology and life science applications, semiconductor and flat panel display production, photonics, automotive, data storage, laser processing, electronics manufacturing and testing.

## Motion Control Systems



**Newport Spectra-Physics B.V.**  
Vechtensteinlaan 12 - 16  
3555 XS Utrecht  
**T** +31 (0)30 6592111  
**E** netherlands@newport.com  
**W** www.newport.com

Newport Spectra-Physics B.V. is a subsidiary of Newport, a leader in nano and micro positioning technologies with an extensive catalog of positioning and motion control products. Newport is part of MKS Instruments Inc., a global provider of instruments, subsystems and process control solutions that measure, control, power, monitor, and analyze critical parameters of advanced processes in manufacturing and research applications.

member **DSPE**



**Physik Instrumente (PI) Benelux BV**  
Hertog Hendrikstraat 7a  
5492 BA Sint-Oedenrode  
The Netherlands  
**T** +31 (0)499-375375  
**F** +31 (0)499 375373  
**E** benelux@pi.ws  
**W** www.pi.ws

Opt for state-of-the-art motion control systems from the world's leading provider PI. Developed, manufactured and qualified in-house by a dedicated and experienced team. Our portfolio includes a wide and deep range of components, drives, actuators and systems and offers infinite possibilities in motion control on a sub-micron and nanometer scale.

member **DSPE**

## Optical Components



**Molenaar Optics**  
Gerolaan 63A  
3707 SH Zeist  
**T** +31 (0)30 6951038  
**E** info@molenaar-optics.nl  
**W** www.molenaar-optics.eu

Molenaar Optics is offering optical engineering solutions and advanced products from world leading companies OptoSigma, Sill Optics and Pyser Optics.

member **DSPE**

## Piezo Systems



**HEINMADE BV**  
Heiberg 29C  
NL - 5504 PA Veldhoven  
**T** +31 (0)40 851 2180  
**E** info@heinmade.com  
**W** www.heinmade.com

As partner for piezo system solutions, HEINMADE serves market leaders in the high tech industry. Modules and systems are developed, produced and qualified in-house. HEINMADE distributes Noliac piezo components.

member **DSPE**

## Piezo Systems



**Physik Instrumente (PI) Benelux BV**  
Hertog Hendrikstraat 7a  
5492 BA Sint-Oedenrode  
The Netherlands  
**T** +31 (0)499-375375  
**F** +31 (0)499 375373  
**E** benelux@pi.ws  
**W** www.pi.ws

High-precision piezo systems and applications that perform on a sub-micron and nanometer scale: world leader PI develops, manufactures and qualifies these in-house. With a broad and deep portfolio with infinite possibilities in components, drives, actuators and systems at hand, our experienced team is dedicated to find the best solution for any motion control challenge.

member **DSPE**

## Precision Electro Chemical Machining



**Ter Hoek Applicatie Centrum B.V.**  
Propaanstraat 1  
7463 PN Rijssen  
**T** +31 (0)548 540807  
**F** +31 (0)548 540939  
**E** info@terhoek.com  
**W** www.terhoek.com

As Application Centre we possess the required knowledge to support our clients in every phase of development and process selection. With our own PEM800 machine we can also use PECM in-house for the benefit of our clients.

member **DSPE**

## Ultra-Precision Metrology & Engineering



**IBS Precision Engineering**  
Esp 201  
5633 AD Eindhoven  
**T** +31 (0)40 2901270  
**F** +31 (0)40 2901279  
**E** info@ibspe.com  
**W** www.ibspe.com

IBS Precision Engineering delivers world class measurement, positioning and motion systems where ultra-high precision is required. As a strategic engineering partner to the world's best manufacturing equipment and scientific instrument suppliers, IBS has a distinguished track record of proven and robust precision solutions. Leading edge metrology is at the core of all that IBS does. From complex carbon-fibre jet engine components to semiconductor chips accurate to tens of atoms; IBS has provided and engineered key enabling technologies.

member **DSPE**

## ADVERTISERS INDEX

■ Attocube systems AG	46
<a href="http://www.attocube.com">www.attocube.com</a>	
■ DSPE	Cover 2
<a href="http://www.dspe-conference.nl">www.dspe-conference.nl</a>	
■ Heidenhain Nederland BV	Cover 4
<a href="http://www.heidenhain.nl">www.heidenhain.nl</a>	
■ High Tech Institute	43
<a href="http://www.hightechinstitute.nl">www.hightechinstitute.nl</a>	
■ IBS Precision Engineering BV	49
<a href="http://www.ibspe.com">www.ibspe.com</a>	
■ Mikroniek Guide	51 - 54
■ NTS-Group	21
<a href="http://www.nts-group.nl">www.nts-group.nl</a>	
■ Oude Reimer BV	39
<a href="http://www.oudereimer.nl">www.oudereimer.nl</a>	

Dutch Society for Precision Engineering  
**DSPE**  
 YOUR PRECISION PORTAL

## Your button or banner on the website [www.DSPE.nl](http://www.DSPE.nl)?

The DSPE website is the meeting place for all who work in precision engineering.

The Dutch Society for Precision Engineering (DSPE) is a professional community for precision engineers: from scientists to craftsmen, employed from laboratories to workshops, from multinationals to small companies and universities.

If you are interested in a button or banner on the website [www.dspe.nl](http://www.dspe.nl), or in advertising in Mikroniek, please contact Gerrit Kulsdom at Sales & Services.



T: 00 31(0)229-211 211 ■ E: [gerrit@salesandservices.nl](mailto:gerrit@salesandservices.nl)

**DSPE**  
 YOUR PRECISION PORTAL



**MIKRONIEK**  
 PROFESSIONAL JOURNAL ON PRECISION ENGINEERING

**Mikroniek is the professional journal on precision engineering and the official organ of the DSPE, The Dutch Society for Precision Engineering.**

Mikroniek provides current information about technical developments in the fields of mechanics, optics and electronics and appears six times a year.

Subscribers are designers, engineers, scientists, researchers, entrepreneurs and managers in the area of precision engineering, precision mechanics, mechatronics and high tech industry. Mikroniek is the only professional journal in Europe that specifically focuses on technicians of all levels who are working in the field of precision technology.

### Publication dates 2020

nr.:	deadline:	publication:	theme (with reservation):
3.	22-05-2020	26-06-2020	Precision mechatronics (incl. DSPE Conference preview)
4.	31-07-2020	04-09-2020	Mechanisms & metamaterials
5.	18-09-2020	23-10-2020	Robotics (incl. Precision Fair preview)
6.	06-11-2020	11-12-2020	Systems engineering & design methodology

**For questions about advertising, please contact Gerrit Kulsdom**  
 T: 00 31(0)229-211 211 ■ E: [gerrit@salesandservices.nl](mailto:gerrit@salesandservices.nl) ■ I: [www.salesandservices.nl](http://www.salesandservices.nl)



# HEIDENHAIN



## Exposed Linear Encoders for Permanently Stable Measured Values

Machines in electronics manufacturing, in high-level automation, or medical technology need to position finely, quickly and exactly. Exposed linear encoders from HEIDENHAIN are used exactly wherever there is a need for positioning with extremely high accuracy or for precisely defined movements. Even if the encoder is subjected to contamination, the scanning signals stay lastingly stable. This is ensured by the new HEIDENHAIN signal processing ASIC, which almost completely compensates signal changes caused by contamination and maintains the encoder's original signal quality. And this without any significant increase in the noise component or interpolation error of the scanning signals, so the control loop receives highly accurate absolute or incremental position information permanently and reliably.

HEIDENHAIN NEDERLAND B.V.

6716 BM Ede, Netherlands

Telephone 0318-581800

[www.heidenhain.nl](http://www.heidenhain.nl)

Angle Encoders + Linear Encoders + Contouring Controls + Position Displays + Length Gauges + Rotary Encoders